Inhibition of IGA/SCC on Alloy 600 Surfaces Exposed to PWR Secondary Water

Volume 3: Precracking Model Boiler Tests

WARNING:
Please read the Export Control and License Agreement on the back cover before removing the Wrapping Material.

Technical Report

Inhibition of IGA/SCC on Alloy 600 Surfaces Exposed to PWR Secondary Water

Volume 3: Precracking Model Boiler Tests

TR-106212-V3

Final Report, November 1998

EPRI Project Manager
T. Gaudreau

EPRI • 3412 Hillview Avenue, Palo Alto, California 94304 • PO Box 10412, Palo Alto, California 94303 USA
800.313.3774 • 650.855.2121 • askepri@epri.com • www.epri.com

DISCLAIMER OF WARRANTIES AND LIMITATION OF LIABILITIES

ORGANIZATION(S) THAT PREPARED THIS PACKAGE

Commissarat a L'Energie Atomique
Dominion Engineering

ORDERING INFORMATION

Requests for copies of this package should be directed to the EPRI Distribution Center, 207 Coggins Drive, P.O. Box 23205, Pleasant Hill, CA 94523, (925) 934-4212.

CITATIONS

This report was prepared by

Commissarat a L'Energie Atomique
BP No. 6 92260 Fonenay-Aux-Roses
Paris, France

Principal Investigator
J. Daret

Dominion Engineering
6862 Elm Street
McLean, Virginia 22101

Principal Investigator
M. Partridge

This report describes research sponsored by EPRI.

The report is a corporate document that should be cited in the literature in the following manner:

Inhibition of IGA/SCC on Alloy 600 Surfaces Exposed to PWR Secondary Water: Precracking Model Boiler Tests, EPRI, Palo Alto, CA: 1998. Report TR-106212-V3.

REPORT SUMMARY

Intergranular attack/stress corrosion cracking (IGA/SCC) of Alloy 600 steam generator tubing in alkaline environments continues to be a serious problem. EPRI has an extensive program devoted to qualifying corrosion inhibitors for use in PWR steam generators. Researchers have identified several potential inhibitor materials in laboratory tests. This report documents testing of these potential inhibitors in model boilers contaminated with sodium hydroxide.

Background

PWR steam generator corrosion is a major contributor to lost availability and increased maintenance and repair costs. A number of EPRI reports (NP-3051, NP-3060, NP-4053, NP-4272, NP-4457, NP-4978, NP-5363, NP-6115, NP-6721) document corrosion under alkaline or caustic environments. Researchers have demonstrated the use of titanium and cerium based inhibitors to mitigate IGA/SCC in alkaline or caustic environments in static autoclave and CERT laboratory experiments. However, they have been unable to demonstrate inhibition of IGA/SCC in the more realistic heat transfer conditions of a steam generator.

Objectives

To evaluate the use of titanium dioxide and cerium acetate as inhibitors in a model boiler contaminated with continuous sodium hydroxide injection. To investigate and compare the growth of IGA/SCC in sodium hydroxide-contaminated model boilers with no inhibitor; with a boric acid buffer; and with titanium dioxide or cerium acetate inhibitors.

Approach

Investigators used a four loop model boiler operating with prototypic primary and secondary pressures, temperatures and heat flux. Tube support plate (TSP) intersections consisted of virgin and precracked tube materials with open, eccentric TSPs or sludge prepacked, concentric TSPs. Sodium hydroxide was continuously injected into the feedwater at a concentration of 1 to 4 mg-kg^{-1} (ppm) and simulated plant sludge was periodically injected into different boilers via individual auxiliary feedwater pumps. Plant managers operated the four boilers continuously until a through wall leak developed in one of the boilers. They replaced the leaking tube sections or continued operating the boiler with the leaking tube for a short time. After

completion of the test period, each boiler was hydro tested to identify leaking tubes followed by disassembly of the tube and destructive examination of each tube intersection. Investigators correlated secondary side environment and the degree of crack initiation and growth.

Results

Tube corrosion in the reference boiler with no inhibitor, and in the boiler with a boric acid buffer was consistent with previous tests. Through wall cracks can occur in as little as 6 days with just sodium hydroxide injection. No through wall cracks occurred in the model boiler tests when operators added boric acid to the makeup tank in quantities sufficient to neutralize the sodium hydroxide solution.

The addition of cerium acetate to the model boiler reduced crack growth rates but did not stop crack initiation and growth compared to the reference sodium hydroxide tests. The titanium dioxide inhibitors did demonstrate increased resistance of alloy 600 to IGSCC in caustic environments, but only under favorable conditions in which the titanium dioxide contacted the Alloy 600 surface. Since the solubility of titanium dioxide in steam generator secondary side water is low, the mechanism for transport of the titanium dioxide to the Alloy 600 surface is important. The success of IGSCC inhibition by titanium dioxide is a function of its ability to reach the Alloy 600 surface.

EPRI Perspective

The results of this series of model boiler tests show that titanium dioxide is effective in inhibiting IGSCC in alloy 600, if the titanium compound can reach the alloy 600 surface. Therefore, steam generators with clean tube support plate crevices are more likely to benefit from titanium dioxide treatment than those with packed crevices. The most beneficial time to apply titanium dioxide treatment is following a chemical cleaning. Several plant studies involving addition of titanium are currently underway. EPRI will continue to track and report the results of these studies.

TR-106212-V3

Interest Categories

Steam generators

Keywords

Steam generators
Stress corrosion
Inconel alloys
Inhibitors

ABSTRACT

EPRI has an extensive program devoted to qualifying corrosion inhibitors for use in PWR steam generators. A major effort in this qualification program is model boiler or heat flux testing under conditions that approach steam generator operating conditions. The work described in this report addresses one phase of this model boiler effort performed by C.E.A. The primary objectives of this project are to test the effectiveness of selected chemical additives (inhibitors) to inhibit intergranular attack/stress corrosion cracking (IGA/IGSCC) initiation and propagation in alloy 600. Four series of tests were performed, three with inhibitors (titanium dioxide and cerium acetate) and one with a boric acid environment.

Cerium acetate inhibitor was not completely effective in increasing the resistance of alloy 600 to IGSCC in caustic environments. The titanium dioxide inhibitors did demonstrate increased resistance of alloy 600 to IGSCC in caustic environments, but primarily when the tube support plate crevice was open. Exposure to an environment of boric acid was used as a reference condition and was effective in inhibiting significant IGSCC. This report describes the experimental procedure used to perform the tests, the results from the tests and conclusions based on the test results.

ACKNOWLEDGMENTS

These tests were performed in LA HAGUE by the Laboratoire d'Essais Technologiques de Corrosion (principal investigator Jacques Daret) in collaboration with the Laboratoire de Controle par Methodes Electromagnetiques (eddy current examination, principal investigator Remy Besnard) and the Laboratoire de Controle par Ultrasons (ultrasonic examination, principal investigator Christian Gondard), two laboratories of C.E.A. Saclay Center. The contributions of M. J. Partridge, Dominion Engineering, in the preparation of this report is gratefully appreciated.

We express our gratitude to J.P.N. Paine for his helpful suggestions and discussions of this work.

CONTENTS

LIST OF FIGURES

LIST OF TABLES

EXECUTIVE SUMMARY

Background

PWR steam generator secondary side corrosion has been a major contributor to lost availability and increased maintenance and repair costs. EPRI has had an extensive program devoted to qualifying corrosion inhibitors for use in PWR steam generators. Work had proceeded at several laboratories under EPRI contract to screen various compounds for use in controlling crevice corrosion. A major effort in this qualification program was model boiler or heat flux testing under conditions that approach steam generator operating conditions. The work described in this report addresses one phase of this model boiler effort.

Test Program

The C.E.A program involved testing the effectiveness of selected chemical additives (inhibitors) to inhibit intergranular attack/stress corrosion cracking (IGA/IGSCC) initiation and propagation in mill annealed alloy 600. This test program utilized the AJAX model boilers to perform each task. The first series of model boiler tests performed under Task 2a of the contract are reported in Volume 2 of this report. This volume reports on the Task 3 results, conclusions and recommendation for the tests that are a continuation of Task 2a. The specific features of the Task 3 test program were:

- Precrack alloy 600 in a caustic faulted environment so that the inhibition tests carried out in this program can have a mixture of precracked and new (virgin) tube-to-tube support plate intersections in each test.
- Perform model boiler tests using a mixture of precracked and virgin tube-to-tube support plate intersections with the following environments:
  - — Caustic faulted environment with no inhibitor; used as a reference condition.
  - — Caustic faulted environment with titanium dioxide added as an inhibitor.
  - — Caustic faulted environment with titanium dioxide with a zeta potential modifier (sodium aluminate) added as an inhibitor.

— Caustic faulted environment with cerium acetate added as an inhibitor.

— Caustic faulted environment with boric acid added, as a comparison with past model boiler tests.

- Perform eddy current and ultrasonic examination of tube-to-tube support plate intersections after the precracking test phase.

- Perform destructive examinations to define the corrosion that occurred.

Elimination of Previous Experimental Problems

Two significant experimental problems affected the results of the previous inhibitor testing of Task 2a: (1) inhibitors were not injected continuously as was the sodium hydroxide, and (2) the set screws on the tube support plate (TSP) simulator were overtightened in a number of cases causing preferential cracking at the contact point between the set screw and the tube. The Task 3 tests completely corrected the first problem by injecting the inhibitors and boric acid continuously.

The second problem was addressed during the test program by switching the TSP set screw configuration from one internal screw to two external screws and a strongback. All the precracking tests were performed with the internal set screw configuration. Subsequent tests used a combination of virgin tube material with external set screws and precracked tubes with internal set screws. In one test using titanium dioxide plus sodium aluminate inhibitor, Test 16-16, six of the precracked intersections had their set screws moved from the interior (where they had been during the precracking test) to the exterior for the inhibitor test. Unfortunately, two of the six intersections cracked with the characteristic of an overtightened set screw.

Conclusions

The overall conclusions of the Task 3 test program follow.

Cracking in Caustic

- Mill annealed alloy 600 tubing will crack through wall in model boiler tests with pure caustic pollution in as little as 6 days with a Na^+ concentration of about 2.3 $mg\text{-}kg^{-1}$ (ppm) in the make-up tank or 13 days with a Na^+ concentration of about 0.58 $mg\text{-}kg^{-1}$ (ppm).

- The time to initiate cracking in a pure caustic environment could not be determined from the model boiler tests. However, the maximum crack initiation and propagation rate is about 7 μm per hour.

- Residual pollutants in the model boiler shell from previous tests can significantly effect the time to obtain initial through wall cracks in a pure caustic environment.

- Nondestructive test results correlated with the results of the destructive examinations.

Titanium Dioxide Inhibitor Testing

- Under favorable conditions titanium dioxide can inhibit IGSCC of alloy 600.

- IGSCC of virgin alloy 600 tube material in open, eccentric TSP crevices was completely inhibited by titanium dioxide with and without the sodium aluminate zeta potential modifier. None of the five intersections tested had any IGSCC identified at the completion of the two tests.

- The inhibition of IGSCC for precracked alloy 600 tube material in open, eccentric TSP crevices was mixed. Five of twelve intersections experienced through wall leaks. The IGSCC of two of the five 100% through wall cracked tubes was associated with overtightened TSP set screws. IGSCC in the remaining seven intersections either grew slowly or not at all. Since the initial crack depths were not accurately known, the rate of crack growth could not be calculated.

- Titanium dioxide did not inhibit the IGSCC of intersections that had been packed with simulated plant sludge.

- Titanium dioxide can incorporate itself in the oxide film of alloy 600, if the surface is exposed to water containing titanium dioxide.

- Titanium dioxide can react with magnetite to form ilmenite and precipitate on heat transfer surfaces.

- Since titanium dioxide does not penetrate sludge deposits it is probably in the form of a fine or colloidal size solid as opposed to being dissolved.

Cerium Acetate Inhibitor Testing

- Cerium acetate did not completely inhibit IGSCC of alloy 600 in any TSP configuration.

- 100% through wall IGSCC of alloy 600 tube material was experienced by: (1) open, eccentric TSPs with virgin tube material, (2) open, eccentric TSPs with precracked tube material, (3) prepacked, concentric TSPs with virgin tube material, and (4) prepacked, concentric TSPs with precracked tube material.

- Significant quantities of cerium were able to penetrate prepacked TSP crevices, but did not provide IGSCC inhibition.

- While complete IGSCC inhibition was not accomplished with cerium acetate, the time to failure with cerium acetate injection was a factor of two or more greater than with just sodium hydroxide alone.

Cracking in Caustic With Addition of Boric Acid Buffer

- Boric acid can neutralize sodium hydroxide if present in sufficient quantity. By adding both the boric acid and sodium hydroxide to the feedwater makeup tank, sodium borate was actually being injected into the model boiler.

- Virgin tube material experienced shallow intergranular penetrations of about 4% of tube wall in both open crevice and packed crevice TSP configurations.

- Precracked tube intersections did not crack through wall. Since the initial crack depths were not accurately known, the rate of crack growth could not be calculated.

- These results are consistent with previous model boiler tests performed by C.E.A.

Recommendations

- For steam generators that are experiencing IGSCC with an environment that is believed to be caustic and the generators have open TSP crevices, then titanium hydroxide should be considered as an inhibitor.

- Soaking steam generators during shutdown periods with a soluble form of titanium, such as DuPont TYZOR, should be considered as a part of a titanium inhibitor program. Continuous injection of titanium compounds should also be a part of the program.

- The solubility of titanium dioxide in near neutral water is low, therefore the use of colloidal size particles for injection will yield the greatest benefit.

- Ilmenite can form in the steam generator in a reaction with iron, therefore, overloading the steam generators with large quantities of titanium compounds is not recommended.

- For steam generators that are experiencing IGSCC with an environment that is believed to be caustic, then boric acid should be considered as a buffer whether TSP crevices are open or packed with deposits.

- There is no inherent reason identified why both titanium dioxide and boric acid cannot be used concurrently.

1

INTRODUCTION

Background

EPRI has an extensive program devoted to qualifying corrosion inhibitors for use in PWR steam generators. Work is proceeding at several laboratories under EPRI contract to screen various compounds for use in controlling crevice corrosion. A major effort in this qualification program is model boiler or heat flux testing under conditions that approach steam generator operating conditions. The work described in this interim report addresses one phase of this model boiler effort.

Objectives

The primary objective of this phase of the project was to test the effectiveness of selected chemical additives (inhibitors) to inhibit intergranular attack/stress corrosion cracking (IGA/IGSCC) initiation and propagation in alloy 600. Model boiler tests were performed using a mixture of precracked and virgin tube-to-tube support plate intersections with the following environments:

- Caustic faulted environment with no inhibitor; used as a reference condition.
- Caustic faulted environment with titanium dioxide added as an inhibitor.
- Caustic faulted environment with titanium dioxide with a zeta potential modifier (sodium aluminate) added as an inhibitor.
- Caustic faulted environment with cerium acetate added as an inhibitor.
- Caustic faulted environment with boric acid added as a buffer, as a comparison with past model boiler tests.

To assist in the assessment of the effectiveness of each potential inhibitor the following were performed:

- Perform nondestructive examinations of the reference intersections to define the depth and degree of IGSCC so that intersections could be used for future model boiler tests with inhibitors.

- Perform destructive examinations to define the corrosion observed.

- In the nondestructive and destructive examinations carried out as part of the task, search for all forms of corrosion or damage that may be initiated or aggravated by the presence of the inhibitor, especially wastage and pitting.

Investigations Performed

Task 3 was a follow-on to Task 2, Subtask 2a, which involved inhibitor testing. Four model boilers were operated for Task 3: Boilers 13, 14, 15 and 16. The model boiler were operated at prototypic primary and secondary temperatures and pressures with typical all volatile treatment (AVT) secondary side water chemistry. Sodium hydroxide was added continuously to each boiler via its makeup system. Inhibitors were added continuously via each boiler's auxiliary makeup system. Twelve tube-to-tube support plate (TSP) intersections were installed in each boiler. The tube material was either virgin material or "precracked" material that had been previously exposed to a caustic environment or other means to induce cracking. The TSPs were either eccentrically mounted on the tube with set screws and open crevices, or they were concentrically mounted and packed with simulated plant sludge. The boiler number and test sequence number for each test are listed in Table 1-1. A detailed description of each test is given in Section 2.

Following the precracking tests all intersections were nondestructively examined to identify those intersections that could be used as "precracked" intersections for subsequent tests. Some intersections were also destructively examined to serve as a baseline for interpreting the nondestructive examination results.

At the completion of all tests the intersections were disassembled and destructively examined. Microanalyses, such as EDS, Auger and XPS, were performed on a number of tube intersections to determine the composition of the surface oxides and deposits. The results of the nondestructive and destructive examinations are described in Section 3.

Section 4 identifies the conclusions from the Task 3 test program.

Table 1-1
Model Boiler, Sequence Numbers and Run Numbers for Task 3 Tests

Model Boiler No.	Test Sequence No.	Run No.	Test Description
13	16	-	Precracking with 4 ppm NaOH Makeup
13	17	-	Reference with 1 ppm NaOH Makeup
13	18	-	Reference with 1 ppm NaOH Makeup
14	16	-	Precracking with 4 ppm NaOH Makeup
14	17	1	Boric Acid with 1 ppm NaOH Makeup
14	17	2	Boric Acid with 1 ppm NaOH Makeup
14	17	3	Boric Acid with 1 ppm NaOH Makeup
15	15	-	Precracking with 4 ppm NaOH Makeup
15	15	1	Cerium Acetate with 1 ppm NaOH Makeup
15	15	2	Cerium Acetate with 1 ppm NaOH Makeup
16	14	-	Precracking with 4 ppm NaOH Makeup
16	15	-	Titanium Hydroxide with 1 ppm NaOH Makeup
16	16	1	Titanium Hydroxide plus Sodium Aluminate with 1 ppm NaOH Makeup
16	16	2	Titanium Hydroxide plus Sodium Aluminate with 1 ppm NaOH Makeup

2

EXPERIMENTAL DESCRIPTION

Test Facility Description

The test facility used in this program is one of the AJAX loops existing in the Laboratoire d'Essais Technologiques de Corrosion of the French C.E.A., at La Hague. Figure 2-1 presents a schematic flow sheet of an AJAX loop. These experimental facilities were specially designed for corrosion studies in PWR steam generators. They are used as refreshed autoclave systems with U-bend tubes being internally heated with circulating hot pressurized water. Their basic technical characteristics can be summarized as follows:

Primary Circuit

- Pump and pipes material: 316 stainless steel.
- Electric heater power: 192 kW (655,000 Btu-h^{-1}).
- Maximum temperature and pressure: 350°C (662°F) and 20 MPa (2900 psi).
- Maximum flow rate at hot temperature: 28 m^3-h^{-1} (990 ft^3-h^{-1}), 0.1 % of flow is regenerated by ion exchange resins.

Secondary Circuit

- Shell and tube sheet material: carbon steel.
- Steam pipes, condenser material: alloy 800.
- Maximum temperature and pressure: 300°C (572°F) and 10 MPa (1450 psi).
- Average heat flux density: 300 kW-m^{-2} (97,000 Btu-h^{-1}-ft^{-2}).
- Model boiler volume: 10 dm^3 (2.6 gallons).
- Continuous feed and blowdown rate ≤ 1.5 dm^3-h^{-1} (0.4 gal-h^{-1}).

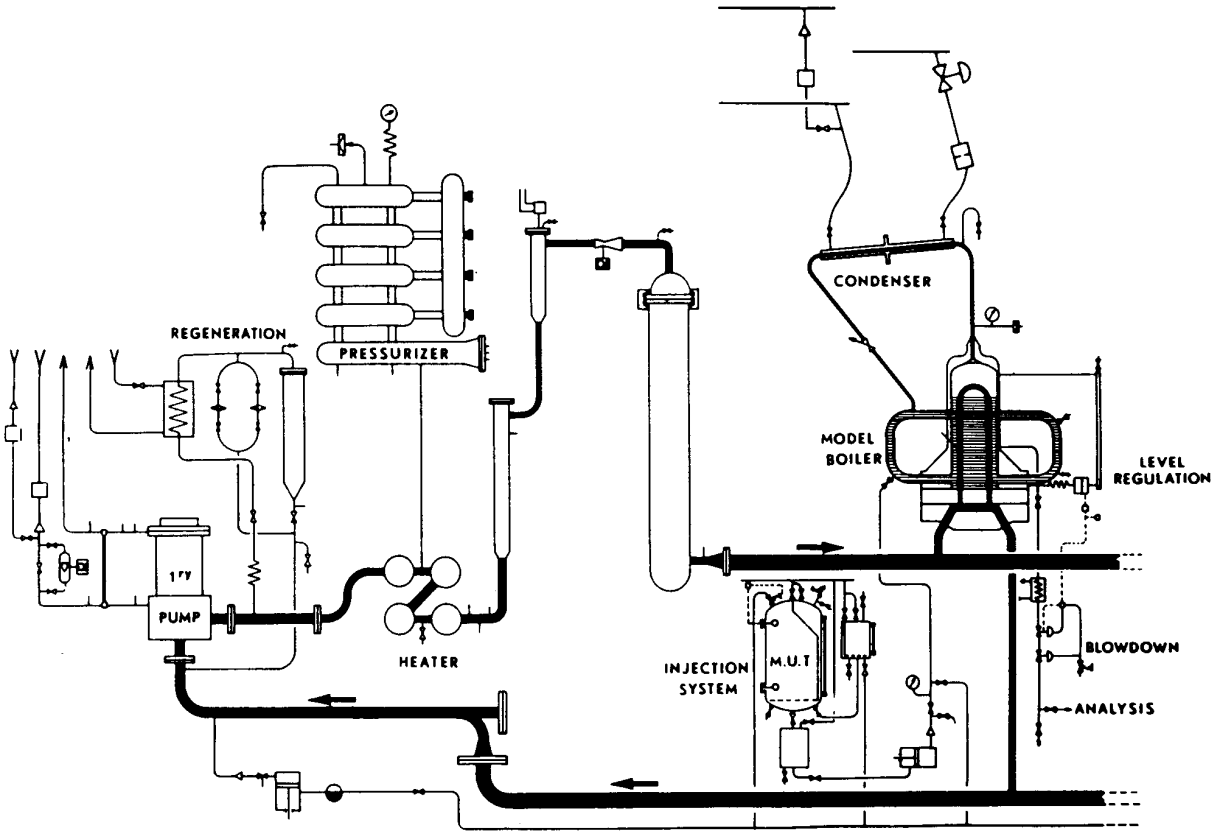

Figure 2-1
Schematic Flow Sheet of an AJAX Loop

There is no significant difference, i.e., about 2 to 3°C (3.6 to 5.4 °F), between the "hot leg" and the "cold leg", so that all parts of the tube bundle can be considered as operating under hot leg conditions with an average heat flux density of 300 kW-m^{-2}.

Model Boiler Arrangement

Figure 2-2 shows a photograph of a fully equipped mock-up of a typical tube bundle prior to testing. The tube-to-tube sheet joint is full depth mechanical roll plus a KISS roll. The nomenclature used to identify specific tests and specific tube-to-tube support plate (TSP) intersections is: the number sequence 14-17 refers to Boiler No. 14 - Test Sequence No. 17, and the number sequence 14-17-3-2 refers to Boiler No. 14 - Test Sequence No. 17 - straight section of Tube No. 3 - TSP No. 2. TSPs are numbered from the tube sheet up. Thus, the TSP closest to the tube sheet is No. 1 for each tube in the bundle. In some cases a portion of a tube, with its tube support plate simulator, was removed after one testing phase and replaced with another tube. The first tube is identified by the letter "a" and the replacement tube is identified by the letter "b."

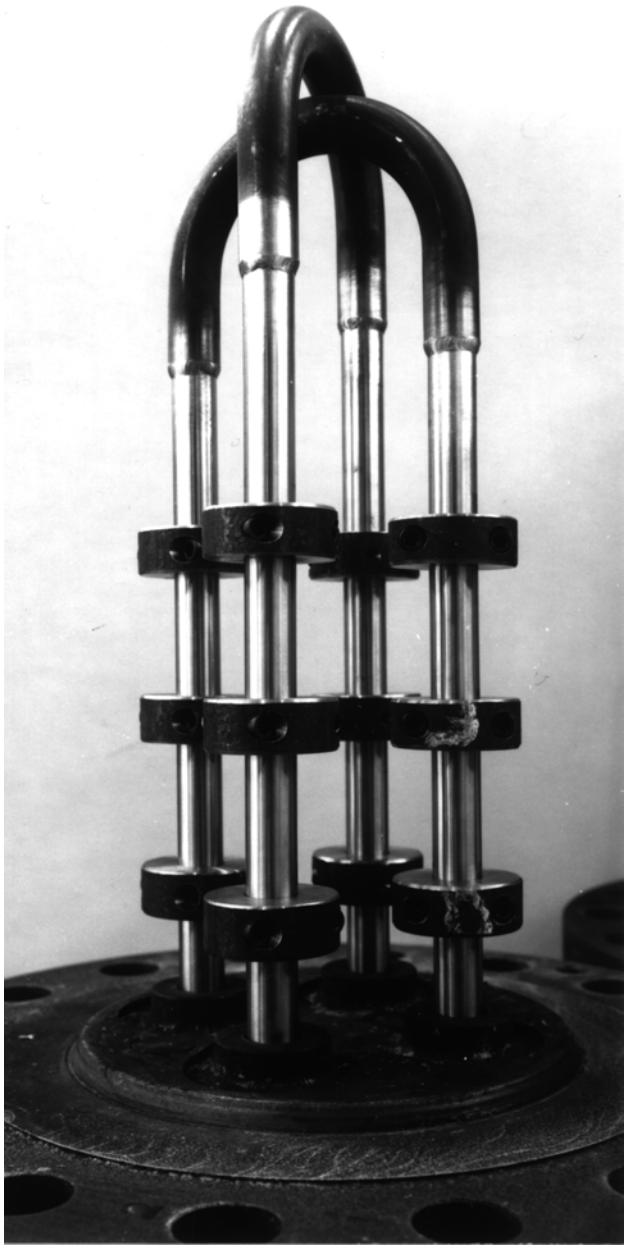

Figure 2-2
Photograph of a Fully Equipped Mock-Up Prior to Testing

This continuation of Task 2a involved the use of both eccentric open and concentric prepacked tube support plate simulators, as shown in Figures 2-3 and 2-4, for tube support plate (TSP) intersections. Three TSP simulators were used for each of the four tubes. All TSP simulators were made of A-285 carbon steel with drilled holes and open or prepacked crevices. The TSPs were held to the tube by set screws; initial tests used a single set screw through the TSP and later tests used two set screws through a strong back welded to the TSP.

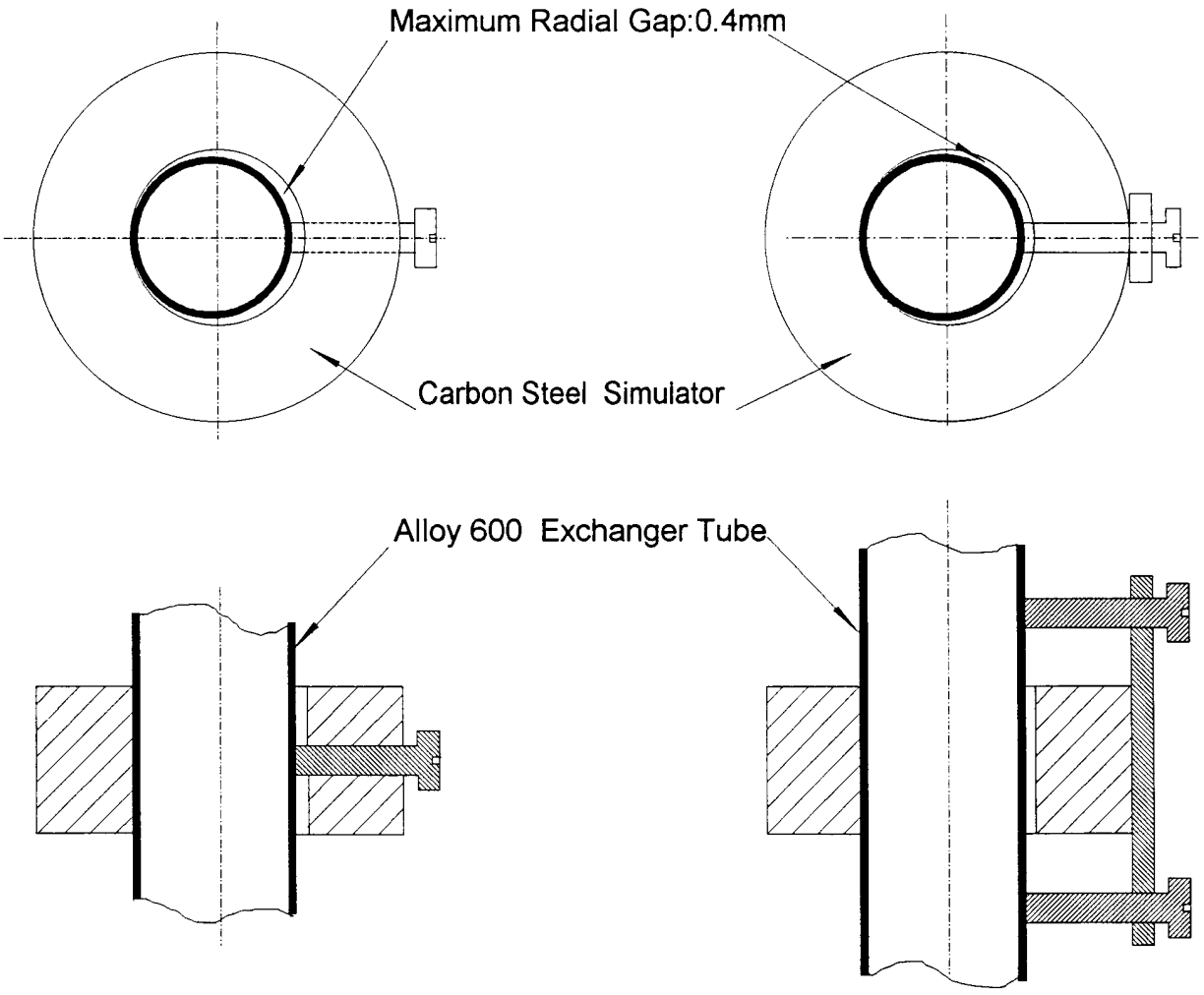

Figure 2-3
Schematic of a Drilled Hole Tube Support Plate Simulator Eccentrically Mounted

An internal set screw arrangement is shown on the left and an external set screw arrangement is shown on the right.

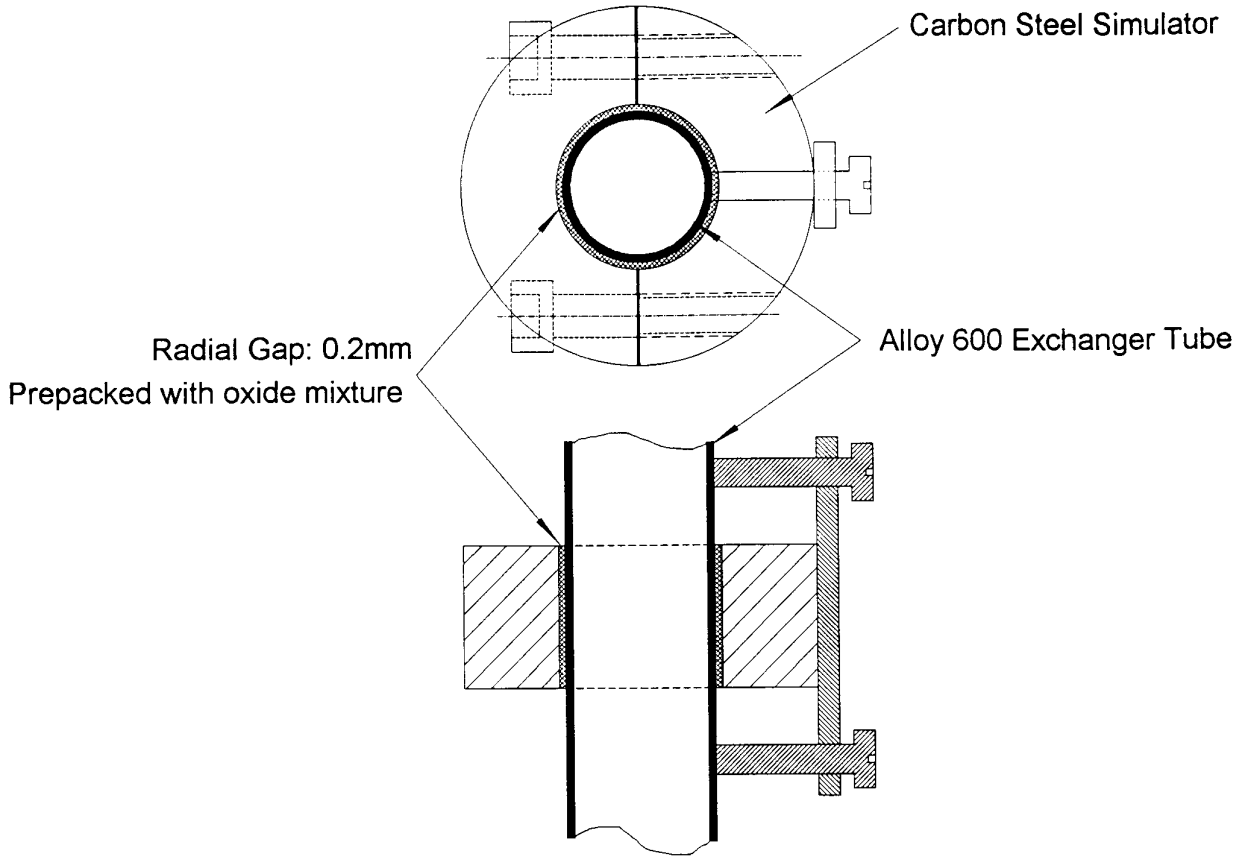

Figure 2-4
Schematic of a Drilled Hole Tube Support Plate Simulator Concentrically Mounted and Prepacked

Materials Description

The tubing material used for this task is typical of tubing used in operating steam generators and was low temperature mill annealed alloy 600, 3/4 inch in diameter manufactured by Babcock & Wilcox, Heat No. 96834.

Appendix A fully describes the material's characteristics. The chemical composition of the material heat is listed in Table A-1. The heat treatment parameters for the mill anneal treatment is identified in Table A-2. The average carbide decorations in the exterior surface and bulk material grains are summarized in Tables A-3 and A-4, respectively, and are compared in Table A-5. The mechanical properties of this heat of material are given in Table A-6.

Test Conditions

This task involved a precrack period of operation during which time NaOH was continuously injected into the boilers via the makeup tank and system. Precracking was performed for Tests 13-16, 14-16, 15-15 and 16-14. Following reconfiguration of the boiler tube bundles with a mixture of precracked and new (i.e., virgin) tube material, operation resumed with a short period of AVT plus candidate inhibitor operation and then continuous injection of NaOH and the candidate inhibitor or boric acid via the makeup system. In addition, daily or weekly batch mode injections of simulated plant sludge were made in each test. Operation of each boiler continued until primary-to-secondary leakage was considered to represent tube through wall cracks.

Primary Circuit

The test conditions for the primary circuit were kept constant for all secondary side environments. The significant parameters were:

- Temperature: 335°C (635°F)
- Pressure: 16 MPa (2320 psi)
- Flow rate at hot temperature: 20 to 25 m^3-h^{-1} (710 to 880 ft^3-h^{-1}) with 0.1 % of the flow regenerated/purified by ion exchange resins.
- Chemistry during the precracking and candidate inhibitor testing periods:
  15 mg-kg^{-1} (ppm) Li (LiOH)
  30 to 50 cm^3 H_2/kg H_2O (STP)

Secondary Circuit

The operating parameters during the precracking and inhibitor periods were:

- Temperature: 295°C (563°F)
- Pressure: 8 MPa (1160 psi)

Simulated plant sludge was added to tests by three different methods. During some tests, each working day 1 gram of simulated plant sludge was added to the boiler via a sample bomb (i.e., there was no injection on Saturdays, Sundays or holidays). Other tests injected 0.35 g of simulated plant sludge once per week. In addition, some tube support plates were prepacked with simulated plant sludge and concentrically mounted on the tubes. Each test description identifies the methods used for that particular test. The composition of the simulated plant sludge is identified in Table 2-1.

This sludge was formulated by Westinghouse Electric Company and is considered to be more oxidizing than the French simulated plant sludge used in the first series of tests in Task 2a (see Volume 2 of this report for composition of the French sludge).

Table 2-1
Composition of the Westinghouse Simulated Steam Generator Sludge

Constituent	Weight Percent
Fe_3O_4	93.0%
CuO	2.0%
NiO	3.0%
Cr_2O_3	2.0%

During the precracking period of operation the following conditions applied:

- AVT Chemistry: NH_4^+ = 0.25 mg-kg^{-1} (ppm)
  N_2H_4 = 50 µg-kg^{-1} (ppb)

- The makeup water contained either 1.0 or 4.0 mg-kg^{-1} (ppm) NaOH which resulted in 15 or 60 µg-kg^{-1} (ppb) of Na^+ in the feedwater entering the boiler. Only precracking Tests 13-16, 14-16, 15-15 and 16-14 used 4 mg-kg^{-1} (ppm) NaOH; all other tests used 1 mg-kg^{-1} (ppm) NaOH.

- The makeup and blowdown rates were 1.5 kg-h^{-1}

During the inhibitor testing period the following modified conditions applied:

- AVT Chemistry: NH_4^+ = 0.25 mg-kg^{-1} (ppm)
  N_2H_4 = 50 µg-kg^{-1} (ppb)

- The makeup water contained 1.0 mg-kg^{-1} (ppm) NaOH which resulted in 15 µg-kg^{-1} (ppb) of Na^+ in the feedwater entering the boiler.

- The makeup rate was 1.5 kg-h^{-1} and the blowdown rate was 1.4 kg-h^{-1} with a steam bleed of 0.1 kg-h^{-1}.

- Candidate inhibitors or boric acid were also added continuously via the makeup system. This is different from the batch mode method used to add candidate inhibitors in the first series of Task 2a model boiler tests described in Volume 2 of

this report. Continuous addition of candidate inhibitors was considered an important change to the test procedure. The composition of the candidate inhibitors are identified in Appendix B, Tables B-1 and B-2.

Four series of tests were performed on an AJAX test loop, which can accommodate four test boilers in operation simultaneously. The test parameters for the four precracking tests of the first series are given in Table 2-2. The 24 days of exposure to NaOH were preceded by 13 days of operation with an AVT environment.

Prior to the performance of the precracking tests, the four boiler shells were grit blasted with alumina and washed with dilute acetic acid to try to remove any residual materials resulting from the shell's previous test environment. Following the completion of the precracking tests, a sample of each shell's interior surface film was analyzed by EDS to evaluate the possible influence each shell's residual film could have on its precracking results.

Table 2-2
Test Parameters for Boiler Tests 13-16, 14-16, 15-15 and 16-14

Test No.	NaOH Conc mg-kg^{-1}	Simulated Plant Sludge When Added	Simulated Plant Sludge Amount Added	Simulated Plant Sludge Total Added	Total Test Time With NaOH	Previous Test Environment
13-16	4	Daily[1]	1 g	16 g	24 days	Resins (No Phosphates)
14-16	4	Daily[1]	1 g	16 g	24 days	Resins + Phosphates
15-15	4	Daily[1]	1 g	16 g	24 days	Cerous Acetate
16-14	4	Daily[1]	1 g	16 g	24 days	AVT for 20,000 h

[1] Daily except for weekends and holidays

Tube intersections from the four above precracking tests were used, together with virgin tube sections, to make up the reference, boric acid and candidate inhibitor test assemblies. The test parameters for the next three series of tests are given in Table 2-3. Those three series of tests were carried out on the same AJAX loop using the same boiler shells. Tests 13-17, 14-17 Run 1, 15-15 Run 1 and 16-15 were all run simultaneously on the loop. Likewise, Tests 13-18, 14-17 Run 2, 15-15 Run 2 and 16-16 Run 1 were run at the same time. Finally, Tests 14-17 Run 3 and 16-16 Run 2 were run simultaneously.

Exposure to NaOH in Tests 13-17, 14-17 Run 1 and 15-15 Run 1 was preceded by 12 days of operation with an AVT environment. Exposure to NaOH in Test 16-15 was preceded by 19 days of operation with an AVT environment followed by a 150°C soak with 1.2% DuPont TYZOR LA. Tests 16-16 Run 1 and 16-16 Run 2 were preceded by a two day soak period with 1.2% DuPont TYZOR LA. All other tests immediately started

operation with a NaOH environment and did not have a period of operation with only an AVT environment.

Table 2-3
Test Parameters for Boiler Tests 13-17, 13-18, 14-17, 15-15, 16-15 and 16-16

Test No.	Run No.	Type of Test	NaOH Conc $mg\text{-}kg^{-1}$	Simulated Plant Sludge When Added	Simulated Plant Sludge Amount Added	Simulated Plant Sludge Total Added	Test/Run Time With NaOH
13-17	-	Reference	1	Daily[1]	1 g	21 g	28 days
13-18	-	Reference	1	Weekly	0.35 g	1.05 g	19 days
14-17	1	Boric Acid	1	Daily[1]	1 g	21 g	28 days
14-17	2	Boric Acid	1	Weekly	0.35 g	1.05 g	19 days
14-17	3	Boric Acid	1	Weekly	0.35 g	1.05 g	27 days
15-15	1	Cerous Acetate	1	Daily[1]	1 g	21 g	28 days
15-15	2	Cerous Acetate	1	Weekly	0.35 g	1.05 g	19 days
16-15	-	Titanium Dioxide	1	Daily[1]	1 g	15 g	21 days
16-16	1	Titanium Dioxide[2]	1	Weekly	0.35 g	1.05 g	19 days
16-16	2	Titanium Dioxide[2]	1	Weekly	0.35 g	1.05 g	27 days

[1] Daily except for weekends and holidays

[2] Sodium aluminate was added as a zeta potential modifier

Target values were established for the addition of boric acid, cerous acetate, titanium dioxide and sodium aluminate to the makeup tanks of their respective tests. For boric acid the target boron to sodium molar ratio was 18:1. For 1 $mg\text{-}kg^{-1}$ of NaOH in the makeup tank there is 0.575 $mg\text{-}kg^{-1}$ of Na^+. Thus, a boron concentration of 5 $mg\text{-}kg^{-1}$ will yield a molar ratio of 18.5:1.

For cerous acetate the target sodium to cerium molar ratio was 6:1. A 1 $mg\text{-}kg^{-1}$ solution of NaOH and a 0.56 $mg\text{-}kg^{-1}$ solution of cerium in the combined makeup will yield a molar ratio of 6.3. For Test 15-15, cerous acetate was added to the auxiliary makeup tank in the amount of 55 mg per 10 liters of water; thus the concentration of cerium in the auxiliary feedwater tank was 5.5 $mg\text{-}kg^{-1}$. The flow from the makeup tank was 1.5 $l\text{-}hr^{-1}$ and the flow from the auxiliary makeup tank was 0.5 $l\text{-}hr^{-1}$. Accordingly, the concentration of cerium acetate in the combined makeup was 1.38 $mg\text{-}kg^{-1}$. The cerium acetate was purchased as having 1.5 waters of hydration, but was later believed to have 6 waters of hydration based on analysis. Accordingly, the concentration of cerium in the combined makeup flow would have been:

- Ce in combined makeup = 0.56 mg-kg^{-1} (ppm) if 1.5 waters of hydration (sodium to cerium molar ratio = 6.3), or

- Ce in combined makeup = 0.45 mg-kg^{-1} (ppm) if 6 waters of hydration (sodium to cerium molar ratio = 5.1).

Likewise, the target sodium to titanium molar ratio was 6:1. A 1 mg-kg^{-1} solution of NaOH and a 0.19 mg-kg^{-1} solution of titanium in the combined makeup will yield a molar ratio of 6.3. These values are summarized in Table 2-4. For Tests 16-15 and 16-16 TiO_2 was added to the auxiliary makeup tank in the amount of 12.6 mg per 10 liters of water; thus the concentration of TiO_2 in the auxiliary makeup tank was 1.26 mg-kg^{-1}. The flow from the makeup tank was 1.5 l-hr^{-1} and the flow from the auxiliary makeup tank was 0.4 l-hr^{-1}. Accordingly, the concentration of TiO_2 in the combined makeup was 0.26 mg-kg^{-1} resulting in the titanium concentration being 0.16 mg-kg^{-1}, which is 16% less than the target amount of 0.19 mg-kg^{-1}. Titanium in the combined makeup or feedwater was not directly measured.

The target weight ratio for addition of sodium aluminate to the titanium dioxide for Test 16-16 was 0.365 g $NaAlO_2$/10 g TiO_2. This results in a weight ratio based on titanium of 0.061 g $NaAlO_2$/1 g Ti. These values are summarized in Table 2-5. For Test 16-16, TiO_2 and sodium aluminate were added to the auxiliary makeup tank in the amounts of 12.6 mg and 0.46 mg per 10 liters of water, respectively. This yields a weight ratio of 0.0365 g $NaAlO_2$/1 g TiO_2, which is equal to the target value.

DuPont TYZOR LA, a water soluble titanium lactate solution, was added to boiler 16-15 during a 150°C soak period following 19 days of operation of Test 16-15 with an AVT environment. TYZOR LA was also added to the boiler 16-16 several times during the test when the AJAX loop was shut down for other reasons. The DuPont product is a 50% solution of TYZOR LA in water having a nominal titanium concentration of 81 g-kg^{-1}. The target value of TYZOR LA solution was 1.2%, resulting in a titanium concentration of about 1950 mg-kg^{-1} in the 16-15 and 16-16 boilers during their soak periods.

For the time periods that NaOH was added to the feedwater of each boiler test, the resultant average makeup and blowdown conditions and chemical concentrations are identified in Tables 2-6 through 2-9 for the precracking tests and in Tables 2-10 through 2-19 for the reference tests, boric acid tests and candidate inhibitor tests.

Table 2-4
Target Molar and Weight Ratios for Additives and 0.575 mg-kg^{-1} Na^+ Makeup

Additive	Target Molar Ratio	Target Weight Ratio	Actual Makeup Concentration	Weight Ratio
Boric Acid	18 [B]:1 [Na]	8.47 g B: 1 g Na	5 mg-kg^{-1} B	8.70
Cerous Acetate	6 [Na]:1 [Ce]	0.98 g Na: 1 g Ce	0.45 mg-kg^{-1} Ce	1.28
Cerous Acetate	6 [Na]:3 [Ac*]	0.78 g Na: 1 g Ac*	0.58 mg-kg^{-1} Ac*	1.00
Titanium Dioxide	6 [Na]:1 [Ti]	2.88 g Na: 1 g Ti	0.16 mg-kg^{-1} Ti	3.59

* Ac = Acetate; In cerous acetate there are 3 acetate ions for each cerium ion. Weight ratios are based on $Ce(Ac)_3 \bullet 6.0\ H_2O$

Table 2-5
Target Weight Ratio Value for Sodium Aluminate Addition to Titanium Dioxide

Additive	Target Weight Ratio	Target Makeup Tank Additive Concentration for 0.19 mg-kg^{-1} Ti	Resulting Weight Ratio
Sodium Aluminate	0.061 g $NaAlO_2$:1 g Ti	0.0116 mg-kg^{-1} $NaAlO_2$	0.061

Table 2-6
Average Chemical Composition of Makeup and Blowdown for Boiler Test 13-16 (Precracking Test)

Parameter	**Makeup Tank Av. Value (Std Dev)**	**Blowdown Av. Value (Std Dev)**
pH @ 25°C	10.1 (0.2)	9.8 (0.3)
Total Conductivity, µS-cm^{-1}	24.0 (1.2)	22.2 (1.1)
Na^+, mg-kg^{-1}	2.56 (0.15)	2.50 (0.11)
NH_4^+, mg-kg^{-1}	0.26 (0.02)	0.27 (0.03)

Table 2-7
Average Chemical Composition of Makeup and Blowdown for Boiler Test 14-16 (Precracking Test)

Parameter	Makeup Tank Av. Value (Std Dev)	Blowdown Av. Value (Std Dev)
pH @ 25°C	9.5 (0.2)	9.4 (0.2)
Total Conductivity, $\mu S\text{-}cm^{-1}$	22.1 (1.7)	20.2 (1.1)
Na^+, $mg\text{-}kg^{-1}$	2.39 (0.19)	2.24 (0.09)
$NH4^+$, $mg\text{-}kg^{-1}$	0.26 (0.01)	0.27 (0.02)

Table 2-8
Average Chemical Composition of Makeup and Blowdown for Boiler Test 15-15 (Precracking Test)

Parameter	Makeup Tank Av. Value (Std Dev)	Blowdown Av. Value (Std Dev)
pH @ 25°C	9.5 (0.2)	9.5 (0.3)
Total Conductivity, $\mu S\text{-}cm^{-1}$	23.0 (1.0)	20.2 (1.4)
Na^+, $mg\text{-}kg^{-1}$	2.26 (0.20)	2.13 (0.20)
$NH4^+$, $mg\text{-}kg^{-1}$	0.25 (0.04)	0.26 (0.03)

Table 2-9
Average Chemical Composition of Makeup and Blowdown for Boiler Test 16-14 (Precracking Test)

Parameter	Makeup Tank Av. Value (Std Dev)	Blowdown Av. Value (Std Dev)
pH @ 25°C	9.7 (0.1)	9.7 (0.1)
Total Conductivity, $\mu S\text{-}cm^{-1}$	23.0 (0.8)	20.6 (1.8)
Na^+, $mg\text{-}kg^{-1}$	2.23 (0.13)	2.18 (0.24)
$NH4^+$, $mg\text{-}kg^{-1}$	0.25 (0.02)	0.27 (0.03)

Table 2-10
Average Chemical Composition of Makeup and Blowdown for Boiler Test 13-17 (Reference Test)

Parameter	Makeup Tank Av. Value (Std Dev)	Blowdown Av. Value (Std Dev)
pH @ 25°C	9.13 (0.05)	9.00 (0.08)
Total Conductivity, $\mu S\text{-}cm^{-1}$	7.4 (0.5)	5.8 (0.9)
Na^+, $mg\text{-}kg^{-1}$	0.82 (0.09)	0.61 (0.25)
$NH4^+$, $mg\text{-}kg^{-1}$	0.36 (0.06)	0.33 (0.07)

Table 2-11
Average Chemical Composition of Makeup and Blowdown for Boiler Test 13-18 (Reference Test)

Parameter	Makeup Tank Av. Value (Std Dev)	Blowdown Av. Value (Std Dev)
pH @ 25°C	9.5 (0.2)	9.1 (0.1)
Total Conductivity, $\mu S\text{-}cm^{-1}$	6.4 (0.3)	8.0 (3.9)
Na^+, $mg\text{-}kg^{-1}$	0.64 (0.09)	0.54 (0.12)
$NH4^+$, $mg\text{-}kg^{-1}$	0.30 (0.01)	0.32 (0.04)

Table 2-12
Average Chemical Composition of Combined Makeup and Blowdown for Boiler Test 14-17-1 (Boric Acid Test Run 1)

Parameter	Combined Makeup Av. Value (Std Dev)	Blowdown Av. Value (Std Dev)
pH @ 25°C	7.6 (0.04)	7.5 (0.2)
Total Conductivity, $\mu S\text{-}cm^{-1}$	3.7 (0.1)	2.9 (0.6)
Na^+, $mg\text{-}kg^{-1}$	0.62 (0.09)	0.32 (.11)
$NH4^+$, $mg\text{-}kg^{-1}$	0.26 (0.03)	0.27 (0.06)
B, $mg\text{-}kg^{-1}$	4.0 (0.8)	3.9 (0.7)
B:Na Weight Ratio (Target = 8.5)	6.4	12.2

Table 2-13
Average Chemical Composition of Combined Makeup and Blowdown for Boiler Test 14-17-2 (Boric Acid Test Run 2)

Parameter	Combined Makeup Av. Value (Std Dev)	Blowdown Av. Value (Std Dev)
pH @ 25°C	8.0 (0.2)	7.6 (0.1)
Total Conductivity, $\mu S\text{-}cm^{-1}$	4.2 (0.3)	2.8 (0.2)
Na^+, $mg\text{-}kg^{-1}$	0.61 (0.09)	0.30 (0.07)
NH_4^+, $mg\text{-}kg^{-1}$	0.31 (0.04)	0.30 (0.04)
B, $mg\text{-}kg^{-1}$	4.8 (0.4)	4.4 (0.3)
B:Na Weight Ratio (Target = 8.5)	7.9	14.7

Table 2-14
Average Chemical Composition of Combined Makeup and Blowdown for Boiler Test 14-17-3 (Boric Acid Test Run 3)

Parameter	Combined Makeup Av. Value (Std Dev)	Blowdown Av. Value (Std Dev)
pH @ 25°C	7.9 (0.1)	7.9 (0.3)
Total Conductivity, $\mu S\text{-}cm^{-1}$	3.5 (0.2)	3.1 (0.9)
Na^+, $mg\text{-}kg^{-1}$	0.50 (0.03)	0.47 (0.38)
NH_4^+, $mg\text{-}kg^{-1}$	0.25 (0.01)	0.25 (0.01)
B, $mg\text{-}kg^{-1}$	4.1 (0.9)	4.1 (0.5)
B:Na Weight Ratio (Target = 8.5)	8.2	8.7

Table 2-15
Average Chemical Composition of Combined Makeup and Blowdown for Boiler Test 15-15-1 (Cerous Acetate Test Run 1)

Parameter	Combined Makeup Av. Value	Blowdown Av. Value (Std Dev)
pH @ 25°C	9.0	9.1(0.2)
Total Conductivity, µS-cm^{-1}	7.0	5.4 (0.9)
Na^+, mg-kg^{-1}	0.69	0.51 (0.21)
$NH4^+$, mg-kg^{-1}	0.29	0.28 (0.06)
Acetate, mg-kg^{-1}	0.56	0.40 (0.27)
Ce, mg-kg^{-1}	0.128	<0.01
Na:Ce Weight Ratio (Target = 0.98)	5.4	(Based on measured Ce value)
Na:Ce Weight Ratio (Target = 0.98)	1.5	(Based on Aux. Makeup Tank conc.)
Na:Acetate Weight Ratio (Target = 0.78)	1.2	(Based on measured acetate value)
Na:Acetate Weight Ratio (Target = 0.78)	1.2	(Based on Aux. Makeup Tank conc.)

Table 2-16
Average Chemical Composition of Combined Makeup and Blowdown for Boiler Test 15-15-2 (Cerous Acetate Test Run 2)

Parameter	Combined Makeup Av. Value	Blowdown Av. Value (Std Dev)
pH @ 25°C	9.1	8.6 (0.7)
Total Conductivity, µS-cm^{-1}	6.1	5.7 (0.9)
Na^+, mg-kg^{-1}	0.64	0.55 (0.26)
$NH4^+$, mg-kg^{-1}	0.32	0.21 (0.11)
Acetate, mg-kg^{-1}	0.50	0.47 (0.13)
Ce, mg-kg^{-1}	0.075	<0.05
Na:Ce Weight Ratio (Target = 0.98)	8.5	(Based on measured Ce value)
Na:Ce Weight Ratio (Target = 0.98)	1.4	(Based on Aux. Makeup Tank conc.)
Na:Acetate Weight Ratio (Target = 0.78)	1.3	(Based on measured acetate value)
Na:Acetate Weight Ratio (Target = 0.78)	1.1	(Based on Aux. Makeup Tank conc.)

Table 2-17
Average Chemical Composition of Combined Makeup and Blowdown for Boiler Test 16-15 (Titanium Dioxide Test)

Parameter	Combined Makeup Av. Value	Blowdown Av. Value (Std Dev)
pH @ 25°C	9.1	8.8 (0.1)
Total Conductivity, µS-cm^{-1}	6.5	4.2 (0.5)
Na^+, mg-kg^{-1}	0.64	0.43 (0.14)
$NH4^+$, mg-kg^{-1}	0.38	0.29 (0.06)
Na:Ti Weight Ratio (Target = 2.9)	4.0	(Based on Aux. Makeup Tank conc.)

Table 2-18
Average Chemical Composition of Combined Makeup and Blowdown for Boiler Test 16-16-1 (Titanium Dioxide with Sodium Aluminate Test Run 1)

Parameter	Combined Makeup Av. Value	Blowdown Av. Value (Std Dev)
pH @ 25°C	9.2	8.9 (0.2)
Total Conductivity, µS-cm^{-1}	5.8	5.2 (0.8)
Na^+, mg-kg^{-1}	0.68	0.39 (0.13)
$NH4^+$, mg-kg^{-1}	0.37	0.36 (0.05)
Na:Ti Weight Ratio (Target = 2.9)	4.2	(Based on Aux. Makeup Tank conc.)

Table 2-19
Average Chemical Composition of Combined Makeup and Blowdown for Boiler Test 16-16-2 (Titanium Dioxide with Sodium Aluminate Test Run 2)

Parameter	Combined Makeup Av. Value	Blowdown Av. Value (Std Dev)
pH @ 25°C	8.7	8.1 (0.3)
Total Conductivity, µS-cm^{-1}	5.9	5.5 (1.7)
Na^+, mg-kg^{-1}	0.61	0.34 (0.07)
$NH4^+$, mg-kg^{-1}	0.31	0.30 (0.08)
Na:Ti Weight Ratio (Target = 2.9)	3.8	(Based on Aux. Makeup Tank conc.)

Test Bundle Configuration

The test bundles for the precracking tests, Tests 13-16, 14-16, 15-15 and 16-14, were all assembled with virgin tube material. All TSPs were attached eccentrically with internal set screws. Following completion of the precracking tests, each tube-to-TSP intersection was nondestructively examined to determine which intersections could be used for subsequent tests. The results of those nondestructive examinations are given in Appendix C. Some intersections were destructively examined to assess the correlation between the nondestructive and destructive examination results. Test assemblies for Tests 13-17 (Reference), 14-17-1 (Boric Acid Run 1), 15-15-1 (Cerous Acetate Run 1) and 16-15 (Titanium Dioxide) were then configured using selected intersections from the precracking tests and virgin material. The configuration of these four assemblies are given in Tables 2-20 through 2-23.

Table 2-20
Test Assembly Configuration for Test 13-17 (Reference)

		Leg #1	Leg #2	Leg #3	Leg #4
3rd Elevation	Intersection	13-17-1-3	13-17-2-3	13-17-3-3	13-17-4-3
	Tube	Virgin	Virgin	Virgin	Virgin
	Set Screw	External	External	External	External
	TSP	Concentric	Concentric	Eccentric	Eccentric
2nd Elevation	Intersection	13-17-1-2	13-17-2-2	13-17-3-2	13-17-4-2
	Tube	Virgin	Virgin	Virgin	Virgin
	Set Screw	External	External	External	External
	TSP	Concentric	Concentric	Eccentric	Eccentric
1st Elevation	Intersection	13-17-1-1	13-17-2-1	13-17-3-1	13-17-4-1
	Tube	Virgin	Virgin	Virgin	Virgin
	Set Screw	External	External	External	External
	TSP	Concentric	Concentric	Eccentric	Eccentric

All concentric TSPs are also prepacked with sludge.

Table 2-21
Test Assembly Configuration for Test 14-17-1 (Boric Acid Run 1)

		Leg #1	Leg #2	Leg #3	Leg #4
	Intersection	14-16-1-3	14-17-2-3	14-17-3-3	14-17-4-3
3rd	Tube	Precrack<15%	Virgin	Virgin	Virgin
Elevation	Set Screw	Internal	External	External	External
	TSP	Eccentric	Eccentric	Concentric	Concentric
	Intersection	16-14-1-1	14-17-2-2	14-17-3-2	14-17-4-2
2nd	Tube	Precrack<15%	Virgin	Virgin	Virgin
Elevation	Set Screw	Internal	External	External	External
	TSP	Eccentric	Eccentric	Concentric	Concentric
	Intersection	14-16-1-1	14-17-2-1	14-17-3-1	14-17-4-1
1st	Tube	Precrack<15%	Virgin	Virgin	Virgin
Elevation	Set Screw	Internal	External	External	External
	TSP	Eccentric	Eccentric	Concentric	Concentric

All concentric TSPs are also prepacked with sludge.

Table 2-22
Test Assembly Configuration for Test 15-15-1 (Cerous Acetate Run 1)

		Leg #1	Leg #2	Leg #3	Leg #4
	Intersection	15-15-1-3b	15-15-2-3b	15-15-3-3	15-15-4-3b
3rd	Tube	Virgin	Virgin	Precrack<15%	Virgin
Elevation	Set Screw	External	External	Internal	External
TSP	Concentric	Eccentric	Eccentric	Eccentric	
	Intersection	15-15-1-2b	15-15-2-2	15-15-3-2	15-15-4-2
2nd	Tube	Virgin	Precrack<15%	Precrack<15%	Precrack<15%
Elevation	Set Screw	External	Internal	Internal	Internal
	TSP	Concentric	Eccentric	Eccentric	Eccentric
	Intersection	15-15-1-1b	15-15-2-1	15-15-3-1	15-15-4-1
1st	Tube	Virgin	Precrack<15%	Precrack<15%	Precrack<15%
Elevation	Set Screw	External	Internal	Internal	Internal
	TSP	Concentric	Eccentric	Eccentric	Eccentric

All concentric TSPs are also prepacked with sludge.

Table 2-23
Test Assembly Configuration for Test 16-15 (Titanium Dioxide)

		Leg #1	Leg #2	Leg #3	Leg #4
	Intersection	16-15-1-3	16-15-2-3	13-16-3-3	13-16-4-3
3rd	Tube	Virgin	Virgin	Precrack<30%	Precrack<15%
Elevation	Set Screw	External	External	Internal	Internal
	TSP	Eccentric	Concentric	Eccentric	Eccentric
	Intersection	16-15-1-2	16-15-2-2	16-14-2-3	13-16-4-2
2nd	Tube	Virgin	Virgin	Precrack<30%	Precrack<15%
Elevation	Set Screw	External	External	Internal	Internal
	TSP	Eccentric	Concentric	Eccentric	Eccentric
	Intersection	16-15-1-1	16-15-2-1	16-14-2-1	13-16-4-1
1st	Tube	Virgin	Virgin	Precrack<15%	Precrack<15%
Elevation	Set Screw	External	External	Internal	Internal
	TSP	Eccentric	Concentric	Eccentric	Eccentric

All concentric TSPs are also prepacked with sludge.

The first series of candidate inhibitor tests was followed by a second series. Test 13-17 was replaced by 13-18 (Reference), Test 14-17-1 continued as 14-17-2 (Boric Acid Run 2), 15-15-1 continued as 15-15-2 (Cerous Acetate Run 2), and 16-15 was replaced by 16-16-1 (Titanium Dioxide with Sodium Aluminate Run 1). The assemblies for Tests 13-18 and 16-16-1 were new; the assemblies for Tests 14-17-2 and 15-15-2 were essentially unchanged, except for two intersections in each assembly which were replaced by intersections made from precracked tubes received from ENSA. The configuration of these four assemblies are given in Tables 2-24 through 2-27.

Table 2-24
Test Assembly Configuration for Test 13-18 (Reference)

		Leg #1	Leg #2	Leg #3	Leg #4
	Intersection	13-16-1-3	E7-F	13-18-3-3	13-18-4-3
3rd	Tube	Precrack<15%	ENSA 54-55%	Virgin	Virgin
Elevation	Set Screw	Internal	External	External	External
	TSP	Eccentric	Free Span	Concentric	Concentric
	Intersection	13-16-1-2	E7-C, D, E	13-18-3-2	13-18-4-2
2nd	Tube	Precrack<15%	ENSA 30-54%	Virgin	Virgin
Elevation	Set Screw	Internal	External	External	External
	TSP	Eccentric	Concentric	Concentric	Eccentric
	Intersection	13-16-1-1	E7-A	13-18-3-1	E2-A
1st	Tube	Precrack<15%	ENSA 50-64%	Virgin	ENSA 47%
Elevation	Set Screw	Internal	External	External	External
	TSP	Eccentric	Concentric	Concentric	Concentric

All concentric TSPs are also prepacked with sludge.

Table 2-25
Test Assembly Configuration for Tests 14-17-2 and 14-17-3 (Boric Acid Runs 2 and 3)

		Leg #1	Leg #2	Leg #3	Leg #4
	Intersection	14-16-1-3	14-17-2-3	E9-C	14-17-4-3
3rd	Tube	Precrack<15%	Virgin	ENSA 42-48%	Virgin
Elevation	Set Screw	Internal	External	External	External
	TSP	Eccentric	Eccentric	Concentric	Concentric
	Intersection	16-14-1-1	14-17-2-2	E9-B	14-17-4-2
2nd	Tube	Precrack<15%	Virgin	ENSA 45-77%	Virgin
Elevation	Set Screw	Internal	External	External	External
	TSP	Eccentric	Eccentric	Free Span	Concentric
	Intersection	14-16-1-1	14-17-2-1	14-17-3-1	14-17-4-1
1st	Tube	Precrack<15%	Virgin	Virgin	Virgin
Elevation	Set Screw	Internal	External	External	External
	TSP	Eccentric	Eccentric	Concentric	Concentric

All concentric TSPs are also prepacked with sludge.

Table 2-26
Test Assembly Configuration for Test 15-15-2 (Cerous Acetate Run 2)

		Leg #1	Leg #2	Leg #3	Leg #4
	Intersection	E9-E	15-15-2-3b	15-15-3-3	15-15-4-3b
3rd	Tube	ENSA 59%	Virgin	Precrack<15%	Virgin
Elevation	Set Screw	External	External	Internal	External
	TSP	Concentric	Eccentric	Eccentric	Eccentric
	Intersection	E9-D	15-15-2-2	15-15-3-2	15-15-4-2
2nd	Tube	ENSA 59-72%	Precrack<15%	Precrack<15%	Precrack<15%
Elevation	Set Screw	External	Internal	Internal	Internal
	TSP	Free Span	Eccentric	Eccentric	Eccentric
	Intersection	15-15-1-1b	15-15-2-1	15-15-3-1	15-15-4-1
1st	Tube	Virgin	Precrack<15%	Precrack<15%	Precrack<15%
Elevation	Set Screw	External	Internal	Internal	Internal
	TSP	Concentric	Eccentric	Eccentric	Eccentric

All concentric TSPs are also prepacked with sludge.

Table 2-27
Test Assembly Configuration for Test 16-16-1 (Titanium Dioxide with Sodium Aluminate Run 1)

		Leg #1	Leg #2	Leg #3	Leg #4
	Intersection	E1-F	E5-D	14-16-3-3	14-16-4-3
3rd	Tube	ENSA 49-54%	ENSA 53-59%	Precrack<15%	Precrack<15%
Elevation	Set Screw	External	External	Internal	Internal
	TSP	Concentric	Free Span	Eccentric	Eccentric
	Intersection	E12-B	16-16-2-2	14-16-3-2	14-16-4-2
2nd	Tube	ENSA 48-51%	Virgin	Precrack<15%	Precrack<15%
Elevation	Set Screw	External	External	Internal	Internal
	TSP	Concentric	Concentric	Eccentric	Eccentric
	Intersection	E12-A	16-16-2-1	14-16-3-1	14-16-4-1
1st	Tube	ENSA 17-31%	Virgin	Precrack<15%	Precrack<15%
Elevation	Set Screw	External	External	Internal	Internal
	TSP	Concentric	Eccentric	Eccentric	Eccentric

All concentric TSPs are also prepacked with sludge.

After the second series of candidate inhibitor tests two boilers were operated for one more test period. Boiler 14-17 was operated for a third run with boric acid (14-17-3) and boiler 16-16 was operated for a second run with titanium dioxide with sodium aluminate (16-16-2). The test assembly configuration for Test 14-17-3 was identical to that for Test 14-17-2 and is given in Table 2-25, above. One change was made to the assembly for Test 16-16-2; tube intersection 14-16-4-3 located at the third elevation of leg #4 in the 16-16 boiler was leaking after Run 2 and removed and not replaced by another intersection. The assembly configuration for Test 16-16-2 is given in Table 2-28.

Table 2-28
Test Assembly Configuration for Test 16-16-2 (Titanium Dioxide with Sodium Aluminate Run 2)

		Leg #1	Leg #2	Leg #3	Leg #4
3rd Elevation	Intersection	E1-F	E5-D	14-16-3-3	
	Tube	ENSA 49-54%	ENSA 53-59%	Precrack<15%	No TSP
	Set Screw	External	External	Internal	Simulator
	TSP	Concentric	Free Span	Eccentric	Installed
2nd Elevation	Intersection	E12-B	16-16-2-2	14-16-3-2	14-16-4-2
	Tube	ENSA 48-51%	Virgin	Precrack<15%	Precrack<15%
	Set Screw	External	External	Internal	Internal
	TSP	Concentric	Concentric	Eccentric	Eccentric
1st Elevation	Intersection	E12-A	16-16-2-1	14-16-3-1	14-16-4-1
	Tube	ENSA 17-31%	Virgin	Precrack<15%	Precrack<15%
	Set Screw	External	External	Internal	Internal
	TSP	Concentric	Eccentric	Eccentric	Eccentric

All concentric TSPs are also prepacked with sludge.

Test Chronology

The chronology of the test sequence during the precracking period of operation for Tests 13-16, 14-16, 15-15 and 16-14 is identified in Table 2-29.

Table 2-29
Chronology of Test Conditions During the Precracking Period for Tests 13-16, 14-16, 15-15 and 16-14

Time Period, Days	Test Condition	Comments
0 to 13	AVT	
13 to 34	AVT + NaOH	
Day 34	AVT + NaOH	Leaks occur in Boilers 13, 14 & 16
34 to 37	AVT + NaOH	Continued operation with leaks
Day 37	Cold Shutdown and Drain	

Following reconfiguration of the four boiler assemblies, each of the boilers resumed operation as Tests 13-17 (Reference), 14-17 (Boric Acid Run 1), 15-15 (Cerous Acetate Run 1), and 16-15 (Titanium Dioxide). The chronology of the test sequence for each boiler during this period of operation is identified in Tables 2-30 through 2-33.

Table 2-30
Chronology of Test Conditions for Test 13-17 (Reference)

Time Period, Days	Test Condition	Comments
0 to 12	AVT	
12 to 19	AVT + NaOH	
20 to 23	150°C Shutdown	TYZOR soak in Test 16-15
23 to 30	AVT + NaOH	
Day 30	AVT + NaOH	Leak occurred
30 to 44	AVT + NaOH	Continued operation with leak
Day 44	Cold Shutdown and Drain	Total of 28 days exposure to NaOH

Table 2-31
Chronology of Test Conditions for Test 14-17-1 (Boric Acid Run 1)

Time Period, Days	Test Condition	Comments
0 to 12	AVT	
12 to 19	AVT + NaOH + Boric Acid	
20 to 23	150°C Shutdown	TYZOR soak in Test 16-15
23 to 44	AVT + NaOH + Boric Acid	
Day 44	Cold Shutdown and Drain	Total of 28 days exposure to NaOH

Table 2-32
Chronology of Test Conditions for Test 15-15-1 (Cerous Acetate Run 1)

Time Period, Days	Test Condition	Comments
0 to 12	AVT	
12 to 19	AVT + NaOH + CeAcetate	
20 to 23	150°C Shutdown	TYZOR soak in Test 16-15
23 to 44	AVT + NaOH + CeAcetate	
Day 44	Cold Shutdown and Drain	Total of 28 days exposure to NaOH

Table 2-33
Chronology of Test Conditions for Test 16-15 (Titanium Dioxide)

Time Period, Days	Test Condition	Comments
0 to 19	AVT + TiO_2	
20 to 23	150°C Shutdown	1.2 % TYZOR soak
24 to 41-42	AVT + NaOH + TiO_2	
Day 41 or 42*	AVT + NaOH + TiO_2	Leak occurred
41-42 to 44	AVT + NaOH + TiO_2	Continued operation with leak
Day 44	Cold Shutdown and Drain	Total of 21 days exposure to NaOH

* Leak occurred sometime on the 41st or 42nd day.

The second series of candidate inhibitor tests involved four boilers on the loop: Test 13-18 (Reference), 14-17-2 (Boric Acid Run 2), 15-15-2 (Cerous Acetate Run 2), and 16-16-1 (Titanium Dioxide with Sodium Aluminate Run 1). The chronology of the test sequence for each boiler during this period of operation is identified in Tables 2-34 through 2-37. Note that there was not an initial period of operation with only AVT water chemistry for these four tests.

Table 2-34
Chronology of Test Conditions for Test 13-18 (Reference)

Time Period, Days	Test Condition	Comments
0 to 9	AVT + NaOH	
Day 9	AVT + NaOH	Leak occurred
9 to 19	AVT + NaOH	Continued operation with leak
Day 19	Cold Shutdown and Drain	Total of 19 days exposure to NaOH

Table 2-35
Chronology of Test Conditions for Test 14-17-2 (Boric Acid Run 2)

Time Period, Days	Test Condition	Comments
0 to 19	AVT + NaOH + Boric Acid	
Day 19	Cold Shutdown and Drain	Total of 19 days exposure to NaOH. Original intersections have a total of 47 days exposure to NaOH.

Table 2-36
Chronology of Test Conditions for Test 15-15-2 (Cerous Acetate Run 2)

Time Period, Days	Test Condition	Comments
0 to 11	AVT + NaOH + CeAcetate	
Day 11	AVT + NaOH + CeAcetate	Leak occurred
11 to 19	AVT + NaOH + CeAcetate	Continued operation with leak
Day 19	Cold Shutdown and Drain	Total of 19 days exposure to NaOH. Original intersections have a total of 47 days exposure to NaOH.

Table 2-37
Chronology of Test Conditions for Test 16-16-1 (Titanium Dioxide with Sodium Aluminate Run 1)

Time Period, Days	Test Condition	Comments
0 to 19	AVT + NaOH + TiO_2	
Day 19	AVT + NaOH + TiO_2	Leak occurred
Day 19	Cold Shutdown and Drain	Total of 19 days exposure to NaOH

After the leaking intersection was removed from Test 16-16, Tests 14-17 (Boric Acid Run 3) and 16-16 (Titanium Dioxide with Sodium Aluminate Run 2) were reinstalled on the loop and operated for another 27 days. The chronology of the test sequence for each boiler during this period of operation is identified in Tables 2-38 and 2-39. Again, note that there was not an initial period of operation with only AVT water chemistry for these two test continuations.

Table 2-38
Chronology of Test Conditions for Test 14-17-3 (Boric Acid Run 3)

Time Period, Days	Test Condition	Comments
0 to 27	AVT + NaOH + Boric Acid	
Day 27	Cold Shutdown and Drain	Total of 27 days exposure to NaOH. Original intersections have a total of 74 days exposure to NaOH.

Table 2-39
Chronology of Test Conditions for Test 16-16-2 (Titanium Dioxide with Sodium Aluminate Run 2)

Time Period, Days	Test Condition	Comments
0 to 26	AVT + NaOH + TiO_2	
Day 26	AVT + NaOH + TiO_2	Leak occurred
26 to 27	AVT + NaOH + TiO_2	Continued operation with leak
Day 27	Cold Shutdown and Drain	Total of 27 days exposure to NaOH. Original intersections have a total of 46 days exposure to NaOH.

Test Evaluations

The model boiler tests were evaluated using a combination of nondestructive examinations, destructive examinations and microanalyses of tube surfaces and deposits.

Nondestructive Examination Methods

Nondestructive examinations, eddy current and ultrasonic examinations, were performed only on the tube intersections from the four precracking tests (i.e., 13-16, 14-16, 15-15 and 16-14) in order to try to quantify the degree of cracking for each intersection. Intersections with significant cracking were not used in subsequent tests. Descriptions of the nondestructive examination methods are found in Appendix C.

Destructive Examination Methods

The section of the tube including the TSP was cut from the tube bundle and the TSP simulator was removed from the tube section. A plastic replica was made of the exterior surface of most tube sections in the area of the TSP. The replica was viewed under a microscope and a complete detailed mapping of cracks on the exterior surface of each tube-to-TSP intersection was made. In order to make the cracks of most tubes more visible most were bulged (expanded) by inserting a flexible plug inside the tube and compressing the plug hydraulically. Tubes so expanded are noted on their respective map. These maps are useful in identifying axial cracks with transverse components or circumferential cracks. Also included on some maps were the general areas of discoloration indicating the extent of the region where surface films formed due to boiling. In tube intersections where no cracking was found after bulging the tube, no surface maps were produced. Exterior surface micrographs were made of selected areas.

Following the crack mapping, tubes with cracking were sectioned, mounted, and viewed for crack categorization and percent through wall determination. Cracks were generally determined to be either IGA or IGSCC. Sectioning was performed at one or more axial positions of each specimen.

Microanalysis Methods

EDS was performed on deposits taken from the inside of AJAX shells SG 13 through SG 16 after the precracking tests and prior to the start of all other tests. The purpose of these analyses was to characterize the shell deposits prior to performing the scheduled reference, boric acid and candidate inhibitor tests to identify possible contamination of

the tests by residual material on the shells. Also, the analysis could help identify differences in the degree of IGSCC observed in the four precracking tests.

A number of tube-to-TSP intersections were analyzed by EDS when the tubes were removed from service and destructively examined. Several areas of each intersection were analyzed and a range of values (i.e., maximum and minimum) were recorded for the elements expected. Areas typically analyzed were: (1) deposits found in the areas of maximum cracking and deposition (generally about ±90° from the line of contact), (2) at the line of contact with the TSP, (3) at the maximum gap (i.e., at the set screw), and (4) at the tube free span above the TSP. Several points along the depth of cracks in Intersections 14-16-4-3 (from Test 16-16) and 15-15-1-1 (Test 15-15) were analyzed by EDS. Several intersections were sent to other laboratories for other microanalysis methods, such as Auger, XRD and XPS. The microanalysis method used for each tube-to-TSP intersection and tube free span are identified below in Table 2-40.

XRD analysis was performed by NWT (CAMET) on samples of solids to identify the weight percent of TiO_2 (Anatase), TiO_2 (Rutile), $FeTiO_3$ (Ilmenite), Fe_3O_4 (Magnetite) and Fe_2O_3 (Hematite) contained in each. The solids were taken from:

- Filtrate of drain from Test 13-17 by CEA (NaOH only) - Membrane #1898-1
- Filtrate of drain from Test 16-15 by CEA (NaOH + TiO_2) - Membrane #1898-2
- Filtrate of W sludge in pure water by NWT - Membrane #1898-3
- Filtrate of drain from Test 13-17 by NWT (NaOH only) - Membrane #1898-4
- Filtrate of drain from Test 16-15 by NWT (NaOH + TiO_2) - Membrane #1898-5

XRD analysis was also performed by NWT (CAMET) on samples of filtered solids from the drains from Test 16-15 (i.e., TiO_2) and Test 16-16 (i.e., TiO_2 with $NaAlO_2$) to identify possible differences in weight percent of TiO_2 (Anatase), TiO_2 (Rutile), $FeTiO_3$ (Ilmenite), Fe_3O_4 (Magnetite) and Fe_2O_3 (Hematite) contained in each. Significant differences could be the result of the sodium aluminate zeta potential modifier used in Test 16-16.

Table 2-40
Microanalysis Methods Used

Free Span Tube No. or Intersection No.	Exposure Tests†	Analysis Method	No. at Each Location		
			Crevice	Free Span	Crack Face
13-16-4-3	13-16P, 16-15	EDS	1	1	0
14-16-1-2	14-16P	EDS	2	1	0
14-16-1-3	14-16P, 14-17-1 & 2	EDS	3	1	0
14-16-4-3	14-16P, 16-16-1 & 2	EDS	0	0	1
15-15-1-1b	15-15-1 & 2	EDS	0	1	1
15-15-2-2	15-15P, 15-15-1 & 2	EDS	2	1	0
15-15-2-3b	15-15-1 & 2	EDS	2	1	0
15-15-4-3b	15-15-1 & 2	EDS	2	1	0
16-15-2-3	16-15	EDS	0	1	0
13-16-1	13-16P, 13-18	Auger/XPS	0	1	0
13-16-3	13-16P, 16-15	Auger/XPS	0	1	0
14-17-3	14-17-1	Auger/XPS	0	1	0
15-15	15-15P, 15-15-1 & 2	Auger/XPS	0	1	0
13-16-1	13-16P, 13-18	XRD	0	1	0
13-16-3	13-16P, 16-15	XRD	0	1	0
14-17-3	14-17-1	XRD	0	1	0
15-15	15-15P, 15-15-1 & 2	XRD	0	1	0
15-15-1-3b	15-15-1	Auger/SEM	1	0	0
14-16-3-1	14-16P, 16-16-1 & 2	XRD	1	1	0
14-16-3-1 TSP*	14-16P, 16-16-1 & 2	XRD	2 (ID)	1(Top)	0

† "P" indicates that the test is a precracking test.
* XRD performed on the TSP carbon steel ring surfaces.

3

RESULTS AND DISCUSSION

As identified in Section 2, four series of tests were performed on an AJAX test loop, which can accommodate four test boilers in operation simultaneously. The first test series consisted of four precracking tests: 13-16, 14-16, 15-15 and 16-14. Table 3-1 shows the test configuration for the following three series of tests and the time each test series was subject to a sodium hydroxide environment.

Table 3-1
AJAX Test Configurations

Test Series	Reference Test	Boric Acid Test/Run	CeAcetate Test/Run	TiO_2 Test/Run	Test Time With NaOH
2	13-17	14-17/1	15-15/1	16-15	28 days*
3	13-18	14-17/2	15-15/2	16-16/1	19 days
4	None	14-17/3	None	16-16/2	27 days

* 16-15 had 7 additional days of exposure to only an AVT environment; therefore its test time with NaOH was limited to 21 days.

Surface replica maps are presented in Appendix D for all intersections examined.

Precracking Tests 13-16, 14-16, 15-15 and 16-14

Boiler Tests 13-16, 14-16, 15-15 and 16-14 were precracking tests. NaOH was added to the boiler feedwater via the make-up tank and system at a concentration of 4 ppm sodium hydroxide in the make-up tank (2.3 ppm Na^+). Experience at C.E.A. with model boiler precracking has shown that mill annealed alloy 600 commercial tubing will typically crack through wall in 6 to 27 days of exposure to NaOH. Once a through wall leak is detected in one tube, then it is expected that the other tube intersections will have a distribution of crack depths. After shutting down the boiler, all nonleaking intersections are normally nondestructively examined to detect and size all cracks in order to determine which intersections are suitable for continued use in the model boiler test. A few nonleaking intersections are destructively examined to confirm the nondestructive examination results.

Leaks were detected in Tests 13-16, 14-16 and 16-14 after 21 days exposure to caustic. All four boilers continued operation until the 24th day to try to develop an acceptable distribution of crack depths among all the tubes.

Nondestructive Examinations

Eddy Current Examination. A summary of the maximum signals for the bobbin coil and rotating probe eddy current examinations of Tests 13-16, 14-16, 15-15 and 16-14 is shown in Table 3-2.

- Five of the 12 intersections in Test 13-16 had crack indications of about 50% through wall or greater. Seven intersections had no quantifiable signals. The seven intersections with no signals were used in Test 13-18 (3) or Test 16-15 (4).

- Two of the 12 intersections in Test 14-16 had crack indications of about 50% through wall or greater. Ten intersections had no quantifiable signals. Eight of the those ten intersections were used in Test 14-17 (2) or Test 16-16 (6). The two remaining intersections with no signals were destructively examined.

- None of the 12 intersections in Test 15-15 had a quantifiable crack indication by eddy current examination. Seven intersections were used in Test 15-15 (7), and the other five intersections were destructively examined.

- Eight of the 12 intersections in Test 16-14 had crack indications of about 70% through wall or greater. Four intersections had no quantifiable signals. Three of those intersections were used in Test 14-17 (1) or Test 16-15 (2), and intersection 16-14-2-2 was destructively examined.

- Essentially all significant eddy current signals were located ± 70° to 110° from the set screw contact point on the tube.

Table 3-2
Eddy Current Examination Results for Boiler Tests 13-16, 14-16, 15-15 and 16-14

Intersection Number	Maximum Crack Depth, % Through Wall*			
	Test 13-16	Test 14-16	Test 15-15	Test 16-14
1-1	<40%	<40%	<40%	<40%
1-2	<40%	100%	<40%	100%
1-3	<40%	<40%	<40%	90%
2-1	100%	<40%	<40%	<40%
2-2	70%	50%	<40%	<40%
2-3	90%	<40%	<40%	<40%
3-1	50%	<40%	<40%	100%
3-2	90%	<40%	<40%	90%
3-3	<40%	<40%	<40%	100%
4-1	<40%	<40%	<40%	80%
4-2	<40%	<40%	<40%	70%
4-3	<40%	<40%	<40%	100%

* An eddy current result value of <40% indicates that no significant signal was found and the actual crack depth can be from zero to 40%.

Ultrasonic Examination. A summary of the maximum signals for the ultrasonic longitudinal and circumferential examinations of Tests 13-16, 14-16, 15-15 and 16-14 is shown in Table 3-3.

- Five of the 12 intersections in Test 13-16 had crack indications of about 75% through wall or greater. One intersection had a crack indication of about 30%. Six intersections had no quantifiable signals.

- One of the 12 intersections in Test 14-16 had a crack indications of about 100% through wall. Eleven intersections had no quantifiable signals.

- Only one of the 12 intersections in Test 15-15 had a quantifiable crack indication and it only indicated a depth of 30% through wall. All other intersections had no quantifiable signals.

- Nine of the 12 intersections in Test 16-14 had crack indications of about 75% through wall or greater. One intersection had a crack indication of about 30%. Two intersections had no quantifiable signals.

- Essentially all significant ultrasonic signals were located ± 70° to 110° from the set screw contact point on the tube.

Table 3-3
Ultrasonic Examination Results for Boiler Tests 13-16, 14-16, 15-15 and 16-14

Intersection Number	Maximum Crack Depth, % Through Wall*			
	Test 13-16	Test 14-16	Test 15-15	Test 16-14
1-1	<15%	<15%	30%	<15%
1-2	<15%	100%	<15%	100%
1-3	<15%	<15%	<15%	100%
2-1	100%	<15%	<15%	<15%
2-2	75%	<15%	<15%	75%
2-3	100%	<15%	<15%	30%
3-1	75%	<15%	<15%	100%
3-2	100%	<15%	<15%	90%
3-3	30%	<15%	<15%	100%
4-1	<15%	<15%	<15%	90%
4-2	<15%	<15%	<15%	75%
4-3	<15%	<15%	<15%	90%

* An ultrasonic result value of <15% indicates that no significant signal was found and the actual crack depth can be from zero to 15%.

Destructive Examination

A number of tube intersections were destructively examined following the precracking phase in order to confirm the nondestructive examination results. Tube intersections that were found leaking during hydrostatic testing were not always destructively examined. Those intersections that were destructively examined are identified in Table 3-4 with a comparison between their maximum nondestructive examination results and their destructive examination results. In general, there is excellent correlation between the eddy current (ECT) and ultrasonic (UT) nondestructive examination results and the destructive examination results.

Table 3-4
Intersections Destructively Examined Following the Precracking Phase

	Maximum Percent Through Wall			
Intersection No.	Eddy Current	Ultrasonic	Destructive	Comment
13-16-2-1	100%	100%	100%	Tube leaked
13-16-2-2	70%	75%	SCC*	
13-16-2-3	90%	100%	100%	Tube leaked
13-16-3-1	50%	75%	SCC*	
13-16-3-2	90%	100%	100%	Tube leaked
14-16-1-2	100%	100%	100%	Tube leaked
14-16-2-1	<40%	<15%	SCC*	
14-16-2-2	50%	<15%	Zero	
14-16-2-3	<40%	<15%	SCC*	
15-15-1-1a	<40%	30%	40%	
15-15-1-2a	<40%	<15%	Zero	
15-15-1-3a	<40%	<15%	SCC*	
15-15-2-3a	<40%	<15%	65%	
15-15-4-3a	<40%	<15%	Zero	
16-14-1-2	100%	100%	100%	Tube leaked
16-14-1-3	90%	100%	100%	
16-14-2-2	<40%	75%	65%	
16-14-3-1	100%	100%	100%	Tube leaked
16-14-3-2	90%	90%	90%	
16-14-3-3	100%	100%	100%	Tube leaked
16-14-4-1	80%	90%	90%	
16-14-4-2	70%	75%	90%	
16-14-4-3	100%	90%	90%	

* SCC was found, but the maximum depth of SCC was not determined.

Figure 3-1 shows a cracked area on intersection 16-14-2-2 following the precracking Test 16-14. The tube was bulged prior to taking the micrograph, which could have affected the maximum depth. Eddy current examination called the maximum crack depth as <40% and the ultrasonic examination called the maximum crack depth as 75%. Destructive examination of the bulged tube shows a crack depth of 65% in Figure 3-1, which is in reasonable agreement with the ultrasonic examination, but not with the eddy current examination. Another area of Intersection 16-14-2-2 has a spot of shallow IGA/IGP, as shown in Figure 3-2.

A few exceptions to the generally good agreement between the nondestructive and destructive examinations were tube intersections 14-16-2-2 (ECT overcall) and 15-15-2-3a (ECT and UT undercall). Figures 3-3 and 3-4 show areas of significant IGSCC in Intersection 15-15-2-3a. Eddy current examination called the maximum crack depth as <40% and the ultrasonic examination called the maximum crack depth as <15%. The crack depth (after bulging) shown in Figure 3-3 is 65% and is 15% in Figure 3-4.

Based on the generally acceptable correlation between nondestructive and destructive examination results, intersections were selected from the remaining intersections for use in the reference, boric acid and candidate inhibitor tests that followed. See Table 2-20 through Table 2-28 for the configuration of those test assemblies.

Figure 3-5 shows IGSCC in test section ENSA E9-D which was installed in the free span region of Tube #1 of the Run 2 of the cerium Test 15-15. The estimated initial crack depth was 59 to 72% through wall. The measured depth of the crack shown in Figure 3-5 is 87%. Thus, even in the tube free span region existing cracks continued to grow.

Figure 3-6 is a typical surface replica map for precracked tube Intersection 13-16-3-1 that shows the location of all outside surface cracks. Appendix D presents all surface replica maps that were produced.

Figure 3-1
Intersection 16-14-2-2 Following Precracking Test 16-14 With a 65% Through Wall Crack (After Tube Bulging) - No Etching

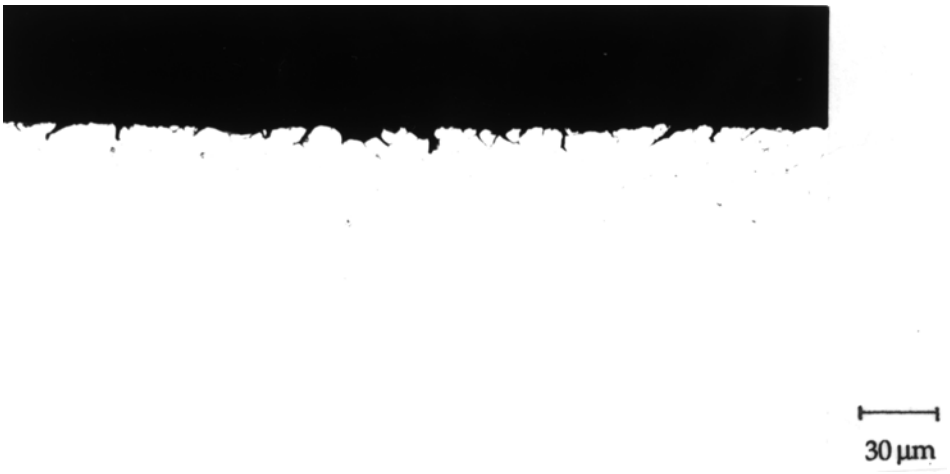

Figure 3-2
Intersection 16-14-2-2 Following Precracking Test 16-14 With an Area of Shallow IGA/IGP - No Etching

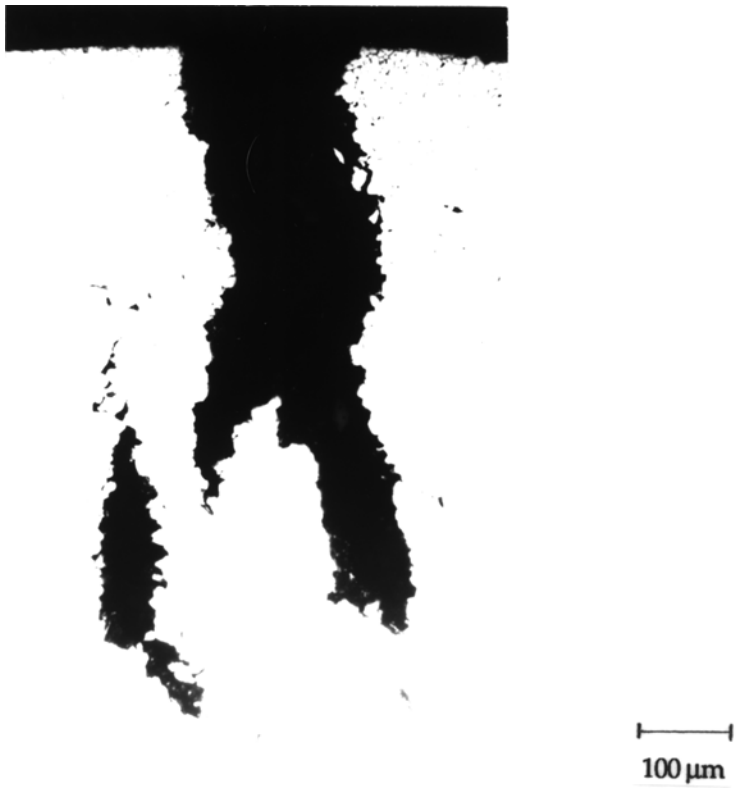

Figure 3-3
Intersection 15-15-2-3a Following Precracking Test 15-15 With a 65% Through Wall Crack (After Tube Bulging) - No Etching

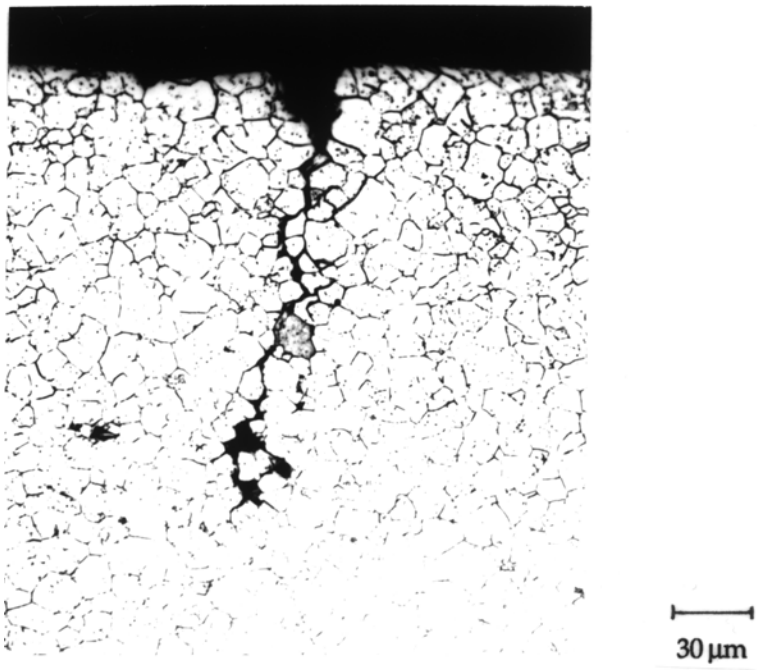

Figure 3-4
Intersection 15-15-2-3a Following Precracking Test 15-15 With a 15% Through Wall Crack (After Tube Bulging) - With Oxalic Acid Etching

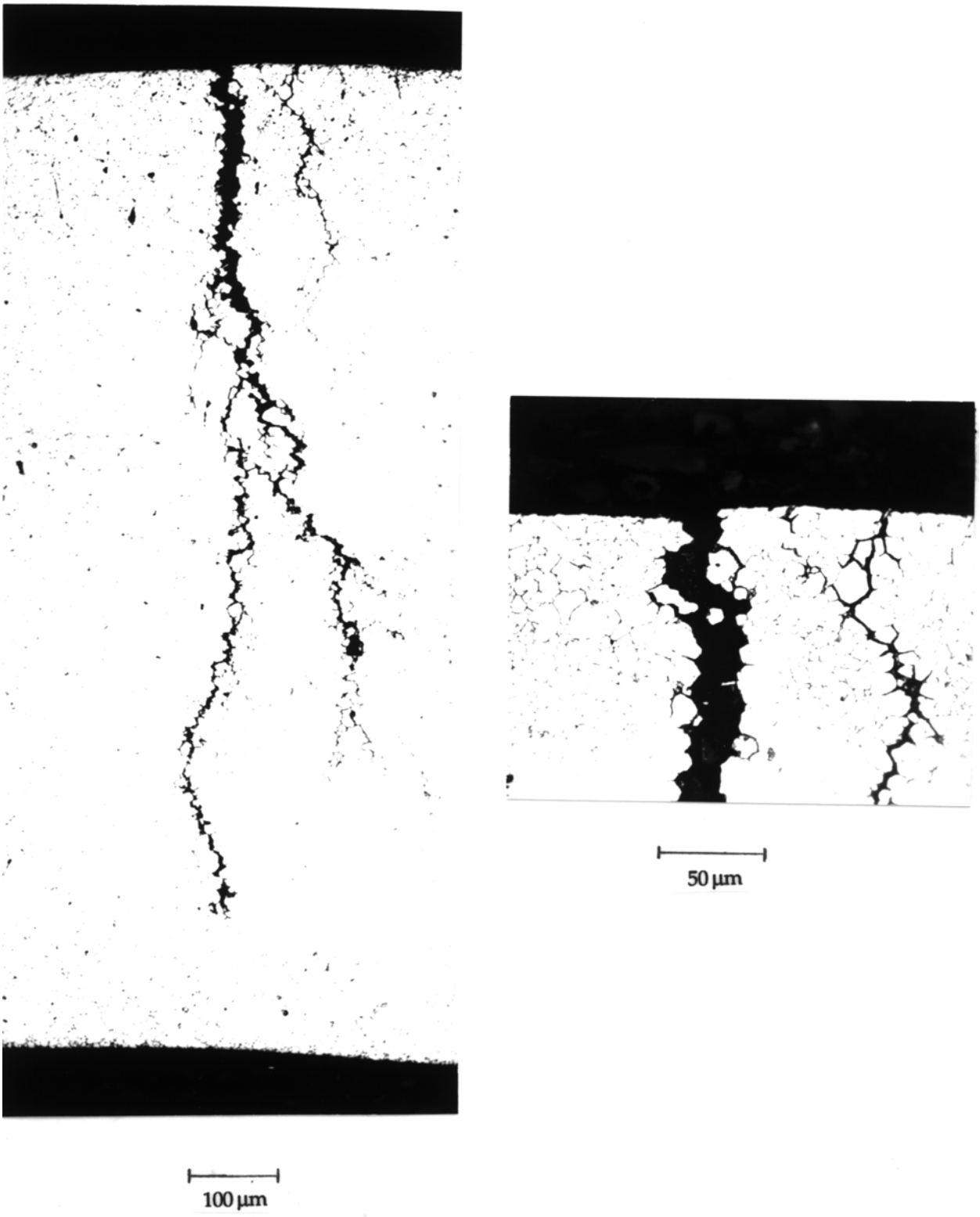

Figure 3-5
Test Section ENSA E9-D from the Tube Free Span Region of Test 15-15, Run 2 with Cerium Inhibitor

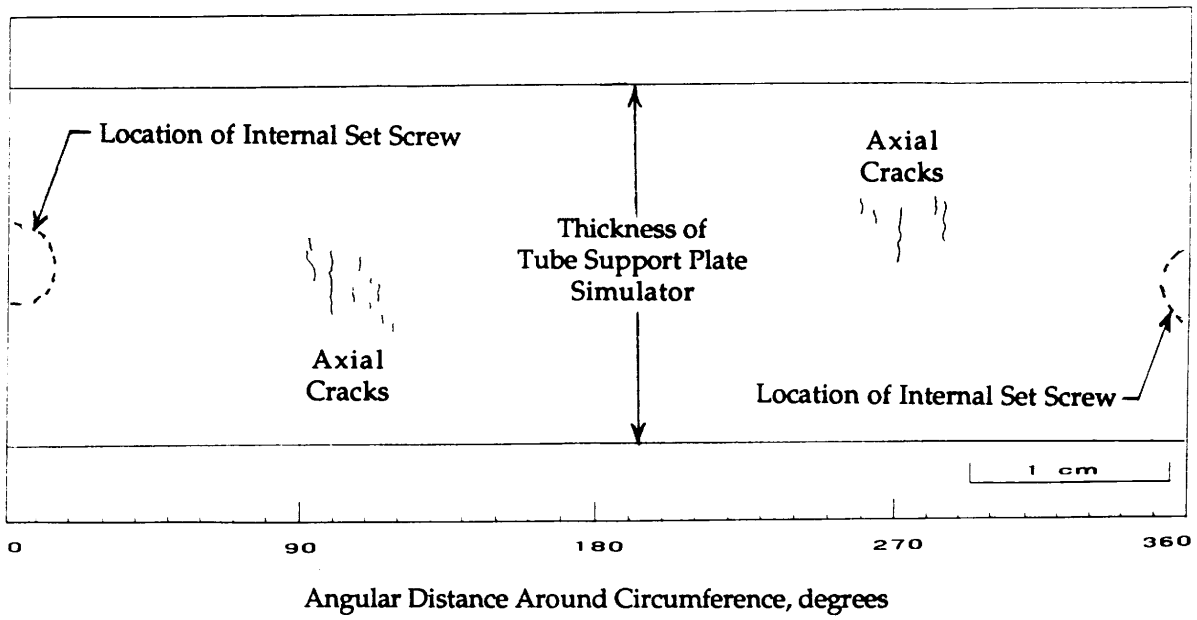

Figure 3-6
Surface Replica Map for Precracked Tube Intersection 13-16-3-1

Microanalysis

One tube intersection, 14-16-1-2, was analyzed by EDS to provide a baseline EDS analysis for comparison with other EDS analyses. Table 3-5 presents the results of analysis of crevice deposits and the tube free span.

Table 3-5
Results of EDS Analyses of Tube Intersection 14-16-1-2 from Precracking Test 14-16

	Weight Percent											
Area	Fe	Cr	Ni	Na	Cu	Ti	Al	Zn	Si	Mn	Ca	K
Crevice Deposit	7.2	0.9	3.1	2.6	0.6	0.1	7.6	0.3	58.6	0.4	6.1	11.9
Crevice Deposit	36.9	5.4	18.6	1.7	0.4	0.0	1.4	0.0	29.3	1.1	1.3	3.8
At the screw	70.7	6.3	19.0	0.0	0.3	0.5	0.5	0.2	1.4	1.0	0.1	0.0
Tube Free Span	39.4	11.6	44.8	0.0	0.8	0.4	1.2	0.0	0.5	1.0	0.1	0.1

The crevice deposits from Intersection 14-16-1-2 demonstrate the great variability that can be observed between deposits from the same TSP crevice. One deposit was composed primarily of Si, K, Al, Ca and Na. The other was primarily Fe, Si, Ni and Cr. At the screw contact point the composition was again different and was primarily Fe, Ni and Cr. The tube free span had a composition closer to the base metal composition and was primarily Ni, Fe and Cr.

After the completion of the precracking tests, deposits were removed from the inside the shells of Boiler 13, 14, 15, and 16 and analyzed by EDS to identify any possible materials that could assist in explaining the differences in the extent of corrosion among the four precracking tests. Prior to the precracking tests all four shells had been shot blasted with Al_2O_3 and cleaned with acetic acid to try to remove from the interior of the boiler shells any residual material from previous tests. Table 3-6 presents the results of the analyses of the four boiler shells.

Table 3-6
Results of EDS Analyses of Shell Deposits from Boilers 13, 14, 15 and 16

	Weight Percent											
Area	Fe	Cr	Ni	Na	Cu	Ti	Al	Zn	Si	S	Mn	Ce
Boiler 13	89.5	0.3	1.1	2.2	1.5	0.1	1.2	0.6	1.3	1.2	0.9	0.0
Boiler 14	71.5	0.5	0.8	0.0	22.7	0.0	1.2	0.3	0.7	1.7	0.5	0.0
Boiler 15	78.6	0.6	0.8	4.6	9.8	0.0	0.7	1.3	0.8	1.5	0.6	0.4
Boiler 16	77.9	0.3	0.6	0.0	15.6	0.1	1.1	1.2	0.7	1.7	0.5	0.0

All shell deposits showed the major constituent to be iron with varying amounts of copper present (i.e., from 1.5% to 22.7%). The deposit from Boiler 15 showed a 0.4% residual of cerium from the previous model boiler test series. It is possible that the residual cerium influenced the lack of precracking observed in precracking Test 15-15. This influence on IGSCC inhibition correlates with Test 12-9 from the first series of model boiler tests reported in Volume 2 of this report. However, it does not correlate with the poor results of the cerium acetate Test 15-15 reported herein.

Correlation With Time and Caustic Concentration

C.E.A. has performed a number of precracking tests in the past using mill annealed alloy 600 and sodium hydroxide as the feedwater pollutant. Table 3-7 shows the results of past tests for virgin tube materials together with the precracking results of Tests 13-16, 14-16, 15-15 and 16-14, and Reference Tests 13-17 and 13-18 for virgin tube materials. The tests are ranked by the total ppm-days (i.e., Na^+ feedwater tank concentration in ppm times the days to the first leak) to the detection of the first through wall leak. Two types of sludge were injected into the boilers: the French type and the Westinghouse type (W) as noted in the table.

For the Vallourec tubing, Heat No. NX3332, the ppm-days to cracking ranges from 8 to 62. The long time (i.e., 170 days and 61 ppm-days) necessary to obtain cracking in Test 9-10 is believed to be due to the release of sulfate ions from the preceding acid sulfate test period (i.e., sulfate in the blowdown was 0.25 mg-kg^{-1}). Tests 8-12, 12-9, 13-16, 13-

17, 13-18, 14-16, 15-15 and 16-14 used Babcock & Wilcox tubing, Heat No. 96834, and the range was from 8 ppm-days to 54 ppm-days for tests that obtained cracking. No through wall leaks occurred in Test 15-15 after 24 days (54 ppm-days). Note that the corrosion morphology in Test 8-12, which cracked in 13 ppm-days, was primarily IGSCC, whereas, the corrosion in Test 12-9 (47 ppm-days) was a mixture of IGA and IGSCC. One hypothesis for the difference is that Test 8-12 operated at a higher potential which promoted a more rapid IGSCC than the IGA plus IGSCC of Test 12-9.

In comparing the ppm-days to first cracking results of Reference Tests 13-17 and 13-18 with the four precracking Tests 13-16, 14-16, 15-15 and 16-14, there does not appear to be a good correlation with ppm-days. The time to first cracking in these six tests, in the range of 1 $mg\text{-}kg^{-1}$ to 4 $mg\text{-}kg^{-1}$ (1 ppm to 4 ppm) NaOH, does not appear to be proportional to the feedwater NaOH concentration; in fact, the tests with the lower NaOH concentrations, Tests 13-17 and 13-18, cracked in shorter times than the others.

Summary

There were significant differences in the extent of IGSCC among the four precracking tests. There is no obvious reason for the observed differences. Prior to the precracking tests, the four boiler shells were grit blasted with alumina and washed with dilute acetic acid to try to remove any residual materials resulting from the shell's previous test environment. It may be significant that the previous test environment for 15-15 was cerous acetate and that cerium was found in the deposits (0.4% Ce) on the inside of the boiler shell following the completion of precracking Test 15-15. Also, the previous test environment for Test 14-16 was phosphates. Although Test 14-16 had one leaking tube, the extent of corrosion was significantly less than in Tests 13-16 and 16-14, whose previous test environments did not include materials that could possibly buffer or inhibit IGSCC. However, EDS did not identify phosphorous in the surface deposit of Test 14-16.

Table 3-7
Summary of Results of Mill Annealed Alloy 600 Precracking Boiler Tests for Virgin Tube Materials

Boiler Test No.	Heat No.	Type Sludge	Make-Up Tank Na^+ Conc.	Time to First Leak	ppm-days to First Leak	Morphology
(CEA 4)*	Vallourec NX3332	French	0.58 ppm	13 days	8	Primarily IGSCC
13-17	B&W 96834	W	0.58 ppm	14 days	8	Primarily IGSCC
13-18	B&W 96834	W	0.58 ppm	19 days†	11	Primarily IGSCC
(CEA 5)*	Vallourec NX3332	French	0.58 ppm	21 days	12	Primarily IGSCC
8-12	B&W 96834	French	2.20 ppm	6 days	13	Primarily IGSCC
(CEA 1)*	Vallourec NX3332	French	2.30 ppm	6 days	14	Primarily IGSCC
(CEA 2)*	Vallourec NX3332	French	2.30 ppm	18 days	41	Primarily IGSCC
12-9	B&W 96834	French	2.35 ppm	20 days	47	IGA + IGSCC
16-14	B&W 96834	W	2.23 ppm	21 days	47	Primarily IGSCC
14-16	B&W 96834	W	2.39 ppm	21 days	50	Primarily IGSCC
13-16	B&W 96834	W	2.56 ppm	21 days	54	Primarily IGSCC
15-15	B&W 96834	W	2.26 ppm	No leak in 24 days	54+	Primarily IGSCC
9-10	Vallourec NX3332	French	0.34 ppm 0.42 ppm	(for 122 days) (for 48 days) 170	41 20 61	Primarily IGSCC; Boiler previously exposed to sulfate and had residual sulfates
(CEA 3)*	Vallourec NX3332	French	2.30 ppm	27 days	62	Primarily IGSCC

* Results from other CEA tests not related to the EPRI program.

† Test 13-18 was a mixture of virgin and precracked tubes. Not certain when the virgin tubes cracked through wall, but test period was 19 days long.

Reference Tests 13-17 and 13-18

Two reference tests, Tests 13-17 and 13-18, were conducted on the same AJAX loop simultaneously with the boric acid and candidate inhibitor tests. Test 13-17 experienced a through wall leak in 14 days and Test 13-18 experienced a through wall leak in just 9 days. These were shorter times to the first leak than all four of the precracking tests even though Tests 13-17 and 13-18 operated with 1 mg-kg^{-1} (ppm) NaOH instead of the 4 mg-kg^{-1} (ppm) used in the precracking tests.

Reference Test 13-17 was configured with all virgin tube intersections; see Table 2-20 for its test assembly configuration. Reference Test 13-18 was configured with a mixture of virgin (5) and precracked (7) tube intersections. Four of the precracked intersections were from ENSA. See Table 2-24 for its test assembly configuration.

Destructive Examinations

Destructive examinations were performed on all 12 intersections from Test 13-17. Four intersections experienced 100% through wall leaks, and one intersection had no IGSCC. Six intersections had varying degrees of IGSCC. One intersection, 13-17-1-3, suffered IGSCC that was characteristic of cracking influenced by an over-tightened TSP set screw even through the set screws were exterior to the TSP. Table 3-8 summarizes the destructive examination results for Test 13-17. There is no significant difference between the degradation of tubes with concentric, prepacked TSPs and those with eccentric TSPs.

Destructive examinations were performed on all 12 intersections from Test 13-18. Five intersections, three virgin and two precracked, experienced 100% through wall leaks. All other intersections had varying degrees of IGSCC. Four intersections, 13-16-1-3, 13-18-3-1, 13-18-3-2 and ENSA E2-A suffered IGSCC that was characteristic of cracking influenced by an over-tightened TSP set screw, even through three of the tubes had set screws that were exterior to their TSP. Table 3-9 summarizes the destructive examination results for Test 13-18. There is no significant difference between the degradation of tubes with concentric, prepacked TSPs and those with eccentric TSPs, or with virgin and precracked material.

Table 3-8
Destructive Examination Results for Reference Test 13-17

Intersection No.	TSP Type	Type of Material	TSP Set Screw	Destructive Examination, % Through Wall	Comments
13-17-1-1	Concentric	Virgin	Exterior	100%	Tube leaked
13-17-1-2	Concentric	Virgin	Exterior	IGSCC	
13-17-1-3	Concentric	Virgin	Exterior	IGSCC	Screw effect
13-17-2-1	Concentric	Virgin	Exterior	IGSCC	
13-17-2-2	Concentric	Virgin	Exterior	IGSCC	
13-17-2-3	Concentric	Virgin	Exterior	IGSCC	
13-17-3-1	Eccentric	Virgin	Exterior	100%	Tube leaked
13-17-3-2	Eccentric	Virgin	Exterior	100%	Tube leaked
13-17-3-3	Eccentric	Virgin	Exterior	Zero	
13-17-4-1	Eccentric	Virgin	Exterior	100%	Tube leaked
13-17-4-2	Eccentric	Virgin	Exterior	IGSCC	
13-17-4-3	Eccentric	Virgin	Exterior	IGSCC	

All concentric TSPs are also prepacked with sludge.

Table 3-9
Destructive Examination Results for Reference Test 13-18

Intersection No.	TSP Type	Type of Material	TSP Set Screw	Destructive Examination, % Through Wall	Comments
13-16-1-1	Eccentric	Precracked	Interior	100%	Tube leaked
13-16-1-2	Eccentric	Precracked	Interior	50%	
13-16-1-3	Eccentric	Precracked	Interior	50%	Screw effect
ENSA E7-A	Concentric	Precracked	Exterior	80%	
ENSA E7-C	Concentric	Precracked	Exterior	IGSCC	
ENSA E7-F	Free Span	Precracked	-	IGSCC	
13-18-3-1	Concentric	Virgin	Exterior	IGSCC	Screw effect
13-18-3-2	Concentric	Virgin	Exterior	100%	Screw effect & Tube leaked
13-18-3-3	Concentric	Virgin	Exterior	100%	Tube leaked
ENSA E2-A	Concentric	Precracked	Exterior	100%	Screw effect & Tube leaked
13-18-4-2	Eccentric	Virgin	Exterior	100%	Tube leaked
13-18-4-3	Concentric	Virgin	Exterior	IGSCC	

All concentric TSPs are also prepacked with sludge.

Microanalysis

The only microanalyses performed on any intersection from Reference Tests 13-17 or 13-18 were Auger and XPS on a section of free span tubing 13-16-1 exposed to precracking test 13-16 and Reference Test 13-18. Table 3-10 shows the Auger results and Table 3-11 shows the results of the XPS. The absence of chromium in the surface oxide layer correlates with the existence of a highly caustic environment. Auger and XPS were also performed on sections of free span tubing from Tests 14-17 (boric acid), 15-15 (cerous acetate) and 16-15 (titanium dioxide), these analysis results will be reported later in this section.

Table 3-10
Auger Analysis of Tube Free Span 13-16-1 from Reference Test 13-18

Depth	Weight Percent											
	All Elements									A-600 Metals		
Å	O	Cr	Fe	Ni	Si	S	Cl	C	Ti	Cr	Fe	Ni
0	46.9	0.0	30.1	4.3	3.8	0.0	0.2	14.2	0.5	0.0	87.6	12.4
100	52.0	0.0	34.5	4.6	3.5	0.0	0.1	4.9	0.3	0.0	88.1	11.9
500	53.7	0.0	37.8	4.7	2.0	0.0	0.0	1.5	0.2	0.0	88.9	11.1
2000	49.6	0.0	41.1	8.9	0.4	0.0	0.0	0.0	0.1	0.0	82.2	17.8
5000	47.9	0.0	43.2	8.8	0.0	0.0	0.0	0.0	0.1	0.0	83.0	17.0

Table 3-11
XPS Analysis of Tube Free Span 13-16-1 from Reference Test 13-18

Element	Form
Fe	Fe_3O_4
Ni	Ni_XO_y
Cu	Cu or Cu_2O

Boric Acid Test 14-17

One boiler, SG14, on the AJAX loop was operated with boric acid added to the auxiliary makeup tank so that the combined makeup would have a molar ratio of about 18 [B]: 1 [Na] for each of the three series following the precracking series. Those three runs are designated 14-17 Run 1, 14-17 Run 2 and 14-17 Run 3. The configuration for Run 1 consisted of 9 virgin tube intersections and three precracked intersections. See Table 2-21 for the Run 1 test assembly configuration. The configuration for Run 2 was modified by removing two of the virgin intersections and replacing them with two

ENSA precracked intersections. The configuration for Run 3 was the same as for Run 2. See Table 2-25 for the Run 2 and 3 test assembly configuration.

Destructive Examinations

Destructive examinations were performed on all 14 intersections from Test 14-17. Two virgin material intersections experienced about 4% through wall cracks, and two ENSA precracked intersections had crack depths of 70% and 80%. The pretest crack depths of those two intersections were 45 to 77% and 42 to 48%. There is no definitive means to determine whether those cracks grew with the two run exposure to NaOH plus boric acid. Ten intersections had no detected IGSCC by their destructive examination. Table 3-12 summarizes the destructive examination results for Test 14-17. There is no significant difference between the lack of degradation of tubes with concentric, prepacked TSPs and those with eccentric TSPs, or with virgin and precracked material.

Table 3-12
Destructive Examination Results for Boric Acid Test 14-17

Intersection No.	Run	TSP Type	Type of Material	TSP Set Screw	Destructive Exam, % Through Wall	Comments
14-16-1-1	1, 2, 3	Eccentric	Precracked	Interior	Zero	
16-14-1-1	1, 2, 3	Eccentric	Precracked	Interior	15%	
14-16-1-3	1, 2, 3	Eccentric	Precracked	Interior	Zero	
14-17-2-1	1, 2, 3	Eccentric	Virgin	Exterior	4%	
14-17-2-2	1, 2, 3	Eccentric	Virgin	Exterior	Zero	
14-17-2-3	1, 2, 3	Eccentric	Virgin	Exterior	4%	
14-17-3-1	1, 2, 3	Concentric	Virgin	Exterior	Zero	
14-17-3-2	1	Concentric	Virgin	Exterior	Zero	E9-B replaced
ENSA E9-B	2, 3	Free Span	Precracked	-	70%	14-17-3-2
14-17-3-3	1	Concentric	Virgin	Exterior	Zero	E9-C replaced
ENSA E9-C	2, 3	Concentric	Precracked	Exterior	80%	14-17-3-3
14-17-4-1	1, 2, 3	Concentric	Virgin	Exterior	Zero	
14-17-4-2	1, 2, 3	Concentric	Virgin	Exterior	Zero	
14-17-4-3	1, 2, 3	Concentric	Virgin	Exterior	Zero	

All concentric TSPs are also prepacked with sludge.

Microanalysis

EDS. EDS was performed on precracked intersection 14-16-1-3. Four areas were analyzed: two TSP crevice deposits, one area near a deposit, and the tube free span outside of the TSP crevice. Boron cannot be detected by the EDS method used. The highest concentration materials detected are identified in Table 3-13. The deposits are primarily iron and silicon deposits. The area near the deposit is primarily an iron

oxide, and the tube free span area is primarily the base tube material with iron oxide. These results are what would be expected for the test environment. Note that there was 0.3% Ti at the tube free span surface because Ti is commonly contained in Alloy 600.

Table 3-13
Results of EDS Analyses of Tube Intersection 14-16-1-3 from Test 14-17

	Weight Percent											
Area	Fe	Cr	Ni	Na	Cu	Ti	Al	Si	Mn	S	Ca	K
Crevice Deposit	43.3	1.5	6.2	0.9	1.1	0.0	1.2	41.4	1.2	0.1	1.2	1.7
Crevice Deposit	28.5	0.5	1.6	4.8	1.3	0.0	4.2	44.9	0.7	0.2	6.9	6.2
Near Deposit	70.7	3.4	16.4	0.0	0.2	0.0	0.4	5.8	1.6	0.0	0.8	0.5
Tube Free Span	41.1	11.2	43.0	0.0	1.6	0.3	1.2	0.5	0.9	0.0	0.0	0.0

Auger and XPS. Auger and XPS analyses were performed on a section of free span of tube 14-17-1 from Test 14-17, Run 1. Table 3-14 shows the Auger results and Table 3-15 shows the results of the XPS. The absence of chromium in the surface oxide layer correlates with the existence of a highly caustic environment.

Table 3-14
Auger Analysis of Tube Free Span 14-17-1 from Boric Acid Test 14-17 Run 1

	Weight Percent											
Depth	All Elements									A-600 Metals		
Å	O	Cr	Fe	Ni	Cu	S	Cl	C	Ti	Cr	Fe	Ni
0	42.1	0.0	26.8	5.9	1.7	3.2	1.8	18.2	0.3	0.0	81.9	18.1
100	47.0	0.0	31.7	4.1	2.3	2.7	1.3	10.7	0.2	0.0	88.6	11.4
500	49.4	0.0	35.2	4.8	1.7	2.7	0.7	5.5	0.1	0.0	88.0	12.0
2000	49.4	0.0	39.9	5.6	0.8	1.9	0.4	1.9	0.0	0.0	87.6	12.4
5000	48.8	0.0	43.0	6.6	0.3	0.8	0.1	0.3	0.0	0.0	86.6	13.4

Table 3-15
XPS Analysis of Tube Free Span 14-17-1 from Boric Acid Test 14-17 Run 1

Element	Form
Fe	Fe_3O_4
Ni	Ni_xO_y
Cu	Cu or Cu_2O

Summary

The lack of cracking with NaOH and boric acid is consistent with previous model boiler tests performed by C.E.A. with boric acid in the AJAX loops. These results have been reported in References (1) and (2). There was sufficient boric acid added to the feedwater tank to neutralize the sodium hydroxide present. The boric acid may also form a surface film that assists in the inhibition of crack initiation and growth. However, there is insufficient data generated in these studies to confirm this hypothesis.

Cerium Acetate Inhibitor Test 15-15

One boiler, SG15, on the AJAX loop was operated with cerous acetate added to the feedwater with a molar ratio of about 6 [Na]: 1 [Ce] for the two series following the precracking series. Those two runs are designated 15-15 Run 1 and 15-15 Run 2. The configuration for Run 1 consisted of 5 virgin tube intersections and 7 precracked intersections from the 15-15 precracking test. See Table 2-22 for the Run 1 test assembly configuration. The configuration for Run 2 was modified by removing two of the virgin intersections that had cracked 100% through wall and replacing them with two ENSA precracked intersections. See Table 2-26 for the Run 2 test assembly configuration.

Destructive Examinations

Destructive examinations were performed on 13 of the 14 intersections from Test 15-15. One tube free span precracked tube from ENSA was not examined. By the end of Run 1 two virgin material intersections with concentric prepacked TSPs had experienced 100% through wall cracks, and were replaced by two ENSA precracked intersections having crack depths of 59% and 59 to 72% (free span location). Following the completion of Run 2, 11 intersections were destructively examined with the following results:

- For all intersections the distribution of maximum crack depths were:
  - Six intersections had 100% through wall cracks
  - Two intersections had 90% through wall cracks
  - One intersection had 40% through wall cracks
  - Two intersections had zero cracks
- Two precracked eccentric TSP intersections with interior set screws had a crack morphology characteristic of an overtightened set screw. Those two intersections had maximum crack depths of 90% and 100%.

- The four concentric prepacked intersections had maximum crack depths of 90%, 100%, 100% and 100%. Two cracked through wall after Run 1.
- The two virgin eccentric TSP intersection both cracked 100%, although one was affected by an overtightened set screw.
- The seven precracked eccentric TSP intersections had a distribution of maximum crack depths of:
  - Three intersections had 100% through wall cracks
  - One intersection had 90% through wall cracks, but had a screw effect
  - One intersection had 40% through wall cracks
  - Two intersections had zero cracks

Table 3-16 summarizes the destructive examination results for Test 15-15. There appears to be no significant difference between the severity of degradation of tubes with concentric, prepacked TSPs and those with eccentric TSPs, or between virgin and precracked material. Overall, the cerous acetate did not appear to provide inhibition against IGSCC. The severity of degradation was comparable to that observed in the Reference Tests 13-17 and 13-18. However, the times to failure were different. Through wall leakage was detected after 9 days in Test 13-18 and after 14 days in Test 13-17, but Test 15-15 was in operation for 39 days before the first leak was detected.

Table 3-16
Destructive Examination Results for Cerous Acetate Test 15-15

Intersection No.	Run	TSP Type	Type of Material	TSP Set Screw	Destructive Exam, % Through Wall	Comments
15-15-1-1b	1, 2	Concentric	Virgin	Exterior	90%	
15-15-1-2b	1	Concentric	Virgin	Exterior	100%	E9-D replaced
ENSA E9-D	2	Free Span	Precracked	-	87%	See Fig. 3-5
15-15-1-3b	1	Concentric	Virgin	Exterior	100%	E9-E replaced
ENSA E9-E	2	Concentric	Precracked	Exterior	100%	
15-15-2-1	1, 2	Eccentric	Precracked	Interior	100%	Tube leaked
15-15-2-2	1, 2	Eccentric	Precracked	Interior	100%	Tube leaked
15-15-2-3b	1, 2	Eccentric	Virgin	Exterior	100%	
15-15-3-1	1, 2	Eccentric	Precracked	Interior	Zero	
15-15-3-2	1, 2	Eccentric	Precracked	Interior	90%	Screw effect
15-15-3-3	1, 2	Eccentric	Precracked	Interior	40%	
15-15-4-1	1, 2	Eccentric	Precracked	Interior	Zero	
15-15-4-2	1, 2	Eccentric	Precracked	Interior	100%	Tube leaked
15-15-4-3b	1, 2	Eccentric	Virgin	Exterior	100%	Screw effect & Tube leaked

All concentric TSPs are also prepacked with sludge.

Microanalysis

EDS. EDS was performed on four intersection from Test 15-15. Those intersections analyzed were:

- 15-15-1-1b: Virgin material concentric TSP intersection having 90% maximum crack depth after Run 1 and Run 2 exposures. Cerium content at the tube free span, crack mouth and along the depth of a crack face was analyzed.

- 15-15-2-2: Precracked eccentric TSP intersection having 100% maximum crack depth after Run 1 and Run 2 exposures. Crevice deposits and the tube free span were analyzed.

- 15-15-2-3b: Virgin material concentric TSP intersection having 100% maximum crack depth after Run 1 and Run 2 exposures. Crevice deposits and the tube free span were analyzed.

- 15-15-4-3b: Virgin material concentric TSP intersection having 100% maximum crack depth after Run 1 and Run 2 exposures. Crevice deposits and the tube free span were analyzed.

The results are presented in Tables 3-17 through 3-20. The cerium results shown in Tables 3-18 through 3-20 indicate that cerium is able to penetrate and concentrate in both the eccentric open crevices (Intersection 15-15-2-2 from 2.8 to 3.2 % Ce) and the prepacked concentric crevices (Intersections 15-15-2-3b and 15-15-4-3b from 0.4 to 3.2% Ce). However, the results from Table 3-17 show that while cerium may be able to concentrate on the tube surface within the crevice, it was not able to significantly penetrate the crack. Cerium concentration is 1.6% at the crack mouth, 0.2% 50µm into the crack, and undetectable 100µm into the crack. On the tube free span surface the cerium concentration varied between 0.1 and 1.1%, less than that observed within the crevice. Results of EDS analysis of a crack face from intersection 12-9-3-2b from the first phase of Task 2a are shown in Table 3-21, along with EDS results of the tube free span and a crevice deposit. Intersection 12-9-3-2b was exposed to 84 days of cerous acetate environment plus 4 $mg\text{-}kg^{-1}$ (ppm) NaOH. These results also show the inability of cerium to penetrate into the crack as compared to its concentration within the crevice.

These results are somewhat different from the EDS results of tube intersections from Test 12-9 in the first phase of Task 2a. In Test 12-9 the cerium content in crevice deposits varied from 13 to 50% for the 12 tube intersections analyzed. Even at the point of contact of the eccentrically loaded tubes with their TSP there were cerium concentrations up to 1.8%. Also, cerium content at the tube free span varied from 16 to 23% for the 12 tubes analyzed from Test 12-9.

Table 3-17
Results of EDS Analyses of Crack Face and Tube Free Span of Tube Intersection 15-15-1-1b from Test 15-15

	Weight Percent											
Area	Fe	Cr	Ni	Mg	Cu	Al	Si	Mn	Ce	Zn	Ca	K
Tube Free Span	50.6	8.5	30.8	0.0	0.8	3.3	1.4	0.8	0.9	3.0	0.0	0.0
Crack Mouth	12.6	20.5	55.0	0.5	0.5	1.8	4.1	1.3	1.6	0.3	1.4	0.5
50 µm Depth	7.6	14.2	65.4	1.0	0.0	4.0	7.0	0.3	0.2	0.0	0.2	0.0
100 µm Depth	7.8	15.3	69.2	2.1	0.0	2.3	3.2	0.0	0.0	0.0	0.1	0.0

Table 3-18
Results of EDS Analyses of Tube Intersection 15-15-2-2 from Test 15-15

	Weight Percent										
Area	Fe	Cr	Ni	Mg	Cu	Al	Si	Mn	Ce	Ca	Zn
Crevice Deposit	48.4	9.7	25.2	0.8	0.9	1.2	2.8	1.2	4.5	2.8	2.6
Crevice Deposit	47.8	4.2	16.2	0.0	0.0	9.0	10.5	0.9	6.8	3.2	1.4
Tube Free Span	58.9	1.5	3.0	0.5	10.2	0.4	0.3	0.7	23.2	0.1	1.2

Table 3-19
Results of EDS Analyses of Tube Intersection 15-15-2-3b from Test 15-15

	Weight Percent											
Area	Fe	Cr	Ni	Na	Cu	Ti	Al	Zn	Si	Mn	Ce	Ca
Crevice Deposit	50.1	4.0	19.7	4.6	0.5	0.1	1.4	1.5	12.4	0.7	2.4	2.5
Crevice Deposit	28.5	6.9	36.1	1.4	0.3	0.1	3.8	1.7	18.0	0.6	0.4	2.0
Tube Free Span	64.7	6.0	21.0	0.0	0.2	0.1	2.8	2.5	0.7	0.9	0.8	0.1s

Table 3-20
Results of EDS Analyses of Tube Intersection 15-15-4-3b from Test 15-15

	Weight Percent											
Area	Fe	Cr	Ni	Na	Cu	Ti	Al	Zn	Si	Mn	Ce	Ca
Crevice Deposit	45.5	2.2	13.4	5.8	0.7	0.0	2.1	1.7	18.3	0.7	3.2	6.1
Crevice Deposit	44.9	4.5	16.5	8.1	0.8	0.2	6.0	1.5	10.9	1.0	2.5	2.1
Tube Free Span	62.9	6.2	21.4	0.0	0.2	0.1	3.3	2.5	0.9	0.8	1.1	0.1

Table 3-21
Results of EDS Analyses of Tube Free Span, Crevice Deposit and Crack Face of Tube Intersection 12-9-3-2b from Test 12-9

	Weight Percent										
Area	Fe	Cr	Ni	Mg	Cu	Al	Si	Mn	Ce	Zn	Ca
Tube Free Span	21.7	2.8	9.0	-	14.2	0.5	0.3	0.2	16.9	34.4	-
Crevice Deposit	45.0	1.1	4.6	-	1.3	0.7	1.9	0.3	35.6	9.5	-
Crack Face, Depth											
First 200 µm	12.1	15.3	61.1	1.4	0.7	4.2	3.4	0.3	0.3	1.0	0.2
200 to 400 µm	9.1	14.7	65.3	1.5	0.5	4.8	2.9	0.4	0.3	0.3	0.2
400 to 600 µm	7.7	14.6	64.9	1.5	1.9	5.7	2.2	0.3	0.2	0.8	0.2
600 to 800 µm	7.5	14.5	63.6	1.4	2.7	6.0	1.2	0.7	0.4	2.1	0.1

Auger and XPS. Auger and XPS analyses were performed on a section of tube free span from Test 15-15, Runs 1 and 2. Table 3-22 shows the Auger results and Table 3-23 shows the results of the XPS. Auger results show that the cerium was incorporated into the tube surface oxide film. Also note that chromium is found in the surface oxide film, which is different from that observed in the reference tests and test with boric acid and titanium dioxide.

Table 3-22
Auger Analysis of Tube Free Span from Cerous Acetate Test 15-15 Runs 1 and 2

	Weight Percent											
Depth	All Elements									A-600 Metals		
Å	O	Cr	Fe	Ni	Cu	Ce	Cl	C	Ti	Cr	Fe	Ni
0	43.1	8.3	14.0	3.8	7.4	4.4	2.5	16.1	0.4	31.8	53.5	14.7
100	48.4	9.8	17.4	3.7	5.5	7.1	1.5	6.5	0.0	31.7	56.5	11.8
500	49.7	9.8	19.7	4.3	4.1	9.1	0.7	2.5	0.1	20.1	58.2	12.7
2000	46.9	9.8	21.0	5.5	3.3	12.3	0.4	0.8	0.0	27.1	57.8	15.1
5000	46.0	9.8	21.5	6.1	3.2	13.1	0.2	0.0	0.0	26.3	57.4	16.3

Table 3-23
XPS Analysis of Tube Free Span from Cerous Acetate Test 15-15 Runs 1 and 2

Element	Form
Cr	Cr_xO_y
Fe	Fe_3O_4
Ni	Ni_xO_y
Ce	CeO_4

Auger analysis was also performed on areas of tube intersection 15-15-1-3b. This tube was not exposed to a precracking environment. The results showed that no cerium was found on the tube OD nor on the fracture face of the largest crack. Chromium depletion was found near the crack mouth but at the crack tip. The film on the tube OD near the crack mouth was an Fe, Cr, Ni mixed oxide.

Summary

The continuous injection of cerous acetate did not have an inhibiting effect as was expected based on the results from Test 12-9 in the first phase of Task 2a. The reasons for this lack of inhibition of IGSCC are not apparent. EDS analysis demonstrated that while cerium was able to penetrate and concentrate in both open eccentric and prepacked concentric TSP crevices in Test 15-15, cerium did not concentrate to the extent that it did in Test 12-9 when the cerium acetate was injected on a daily basis. In addition, EDS analysis showed that cerium was not able to penetrate down into the crack from the tube surface. A difference between Test 12-9 and Test 15-15 is the difference in the type of sludge injected, which could have changed the oxidation potential.

Titanium Dioxide Inhibitor Tests 16-15 and 16-16

One boiler, SG16, on the AJAX loop was operated with titanium dioxide added to the feedwater with a molar ratio of about 6 [Na]: 1 [Ti] for two test series, 16-15 and 16-16, following the precracking series. Test 16-15 had only one test period and is designated as 16-15. There were two runs for Test 16-16 and these are designated 16-16 Run 1 and 16-16 Run 2. The configuration for Test 16-15 consisted of 6 virgin tube intersections and 6 precracked intersections from precracking Tests 13-16 and 16-14. See Table 2-23 for the Test 16-15 assembly configuration.

The configuration for Test 16-16 Run 1 consisted of 2 virgin tube intersections and 10 precracked intersections from precracking Test 14-16 (6 intersections) and ENSA (4 intersections). See Table 2-27 for the Run 1 test assembly configuration. The configuration for Run 2 was modified by removing one intersection that had cracked 100% through wall and replacing it with a section of tube with no TSP simulator. See Table 2-28 for the Run 2 test assembly configuration.

Destructive Examinations

Destructive examinations were performed on all 12 intersections from Test 16-15. The destructive examinations results are:

- For all intersections the distribution of maximum crack depths were:

  - Three intersections had 100% through wall cracks
  - One intersection had 90% through wall cracks
  - Three intersection had 30 to 40% through wall cracks
  - Five intersections had zero cracks
- No cracked intersections with interior or exterior set screws reported a crack morphology characteristic of an overtightened set screw.
- The three virgin concentric TSP intersections had zero, 90% and 100% cracks.
- The three virgin eccentric TSP intersections had zero cracking reported.
- The six precracked eccentric TSP intersections had maximum crack depths of:
  - Two intersections had 100% through wall cracks
  - Three intersections had 30 to 40% through wall cracks
  - One intersection had zero cracks

Table 3-24 summarizes the destructive examination results for Test 16-15. There appears to be a significant difference between the severity of degradation of tubes with concentric, prepacked TSPs and those with eccentric TSPs. Also, there is a difference between the ability to inhibit cracking from initiating with virgin material and stopping crack growth in precracked material. Two of the six precracked intersection grew to 100% through wall. The crack growth of three intersections is not clear since their final crack depths were 30 to 40%, which is near the limit of detection for the nondestructive methods used to assess crack depth after the precracking tests, thus they experienced from no crack growth to 30 to 40% crack growth during Test 16-15. Overall, titanium dioxide did appear to provide inhibition against IGSCC, provided the crevice was open and not prepacked. The overall severity of degradation was significantly less than that observed in the Reference Tests 13-17 and 13-18.

Table 3-24
Destructive Examination Results for Titanium Dioxide Test 16-15

Intersection No.	TSP Type	Type of Material	TSP Set Screw	Destructive Exam, % Through Wall	Comments
16-15-1-1	Eccentric	Virgin	Exterior	Zero	
16-15-1-2	Eccentric	Virgin	Exterior	Zero	
16-15-1-3	Eccentric	Virgin	Exterior	Zero	
16-15-2-1	Concentric	Virgin	Exterior	Zero	
16-15-2-2	Concentric	Virgin	Exterior	90%	
16-15-2-3	Concentric	Virgin	Exterior	100%	
16-14-2-1	Eccentric	Precracked	Interior	Zero	
16-14-2-3	Eccentric	Precracked	Interior	100%	Tube leaked
13-16-3-3	Eccentric	Precracked	Interior	30%	
13-16-4-1	Eccentric	Precracked	Interior	40%	
13-16-4-2	Eccentric	Precracked	Interior	100%	Tube leaked
13-16-4-3	Eccentric	Precracked	Interior	40%	

All concentric TSPs are also prepacked with sludge.

Destructive examinations were performed on 9 of the 11 intersections and one tube free span from Test 16-16. The destructive examinations results are:

- For all intersections and the tube free span the distribution of maximum crack depths were:
  - Four intersections had 100% through wall cracks
  - Two intersection had 35 to 50% through wall cracks
  - Four intersections had zero cracks
- Two 100% cracked intersections with interior, and then exterior, set screws reported a crack morphology characteristic of an overtightened set screw.
- The two virgin eccentric TSP intersections had zero cracking reported.
- The six C.E.A. precracked eccentric TSP intersections had a distribution of maximum crack depths of:
  - Three intersections had 100% through wall cracks (two had set screw effect)
  - One intersection had a 35% through wall crack

— Two intersections had zero cracks

Table 3-25 summarizes the destructive examination results for Test 16-16. There is too little data to determine a significant difference between the severity of degradation of tubes with concentric, prepacked TSPs and those with eccentric TSPs. There does appear to be a difference between the ability to inhibit cracking from initiating with virgin material and stopping crack growth in precracked material. Three of the six C.E.A precracked intersection grew to 100% through wall; the crack growth of one intersection is not clear since the final crack depth was 35%, which is near the limit of detection for the nondestructive methods used to assess crack depth after the precracking tests. Overall, titanium dioxide did appear to provide inhibition against IGSCC, provided the crevice was open and not prepacked. The overall severity of degradation was significantly less than that observed in the Reference Tests 13-17 and 13-18.

Microanalysis

EDS. EDS was performed on two intersections from Test 16-15 and one intersection from Test 16-16. Those intersections analyzed were:

- 13-16-4-3: Precracked eccentric TSP intersection from Test 16-15 having 40% maximum crack depth. A crevice deposit and the tube free span were analyzed.

- 16-15-2-3: Virgin material concentric TSP intersection from Test 16-15 having 100% maximum crack depth. Analyzed prepacked deposits in the TSP split region included an area where some prepacked material was lost, and a tube free span area. See Figure 3-7 for diagram of the areas analyzed.

- 14-16-4-3: Precracked eccentric TSP intersection from Test 16-16 having 100% maximum crack depth after Run 1 exposure. This intersection had a configuration of cracks that is characterized by an overtightened TSP set screw. Areas along the crack depth were analyzed.

Table 3-25
Destructive Examination Results for Titanium Dioxide Test 16-16

Intersection No.	Run	TSP Type	Type of Material	TSP Set Screw	Destructive Exam, % Through Wall	Comments
ENSA E12-A	1, 2	Concentric	Precracked	Exterior	100%	
ENSA E12-B	1, 2	Concentric	Precracked	Exterior	Not Performed	
ENSA E1-F	1, 2	Concentric	Precracked	Exterior	Not Performed	
16-16-2-1	1, 2	Eccentric	Virgin	Exterior	Zero	
16-16-2-2	1, 2	Eccentric	Virgin	Exterior	Zero	
ENSA E5-D	1, 2	Free Span	Precracked	-	50%	
14-16-3-1	1, 2	Eccentric	Precracked	Interior*	100%	Tube leaked
14-16-3-2	1, 2	Eccentric	Precracked	Interior*	35%	
14-16-3-3	1, 2	Eccentric	Precracked	Interior*	100%	Screw effect
14-16-4-1	1, 2	Eccentric	Precracked	Interior*	Zero	
14-16-4-2	1, 2	Eccentric	Precracked	Interior*	Zero	
14-16-4-3	1	Eccentric	Precracked	Interior*	100%	Screw effect

All concentric TSPs are also prepacked with sludge.

* Set screw were on the interior for the precracking test and then moved to the exterior for Test 16-16.

The results are presented in Tables 3-26 through 3-28. Significant quantities of titanium were found in the crevice deposit and on the tube free span of Intersection 13-16-4-3. This is an indication that the titanium was able to get to the tube OD surface within the TSP crevice. By contrast, no titanium was found in Zone 1 of Intersection 16-15-2-3, which in the center of prepacked simulated plant sludge, indicating the titanium could not penetrate the sludge deposit. Significant quantities of titanium were found in Zone 2, Zone 3 and the tube free span of Intersection 16-15-2-3. Intersection 13-16-4-3 did not crack through wall, whereas, Intersection 16-15-2-3 did crack through wall.

EDS of Intersection 14-16-4-3 showed significant titanium through the crack examined. This would appear to indicate that the titanium had no inhibiting effect. However, this intersection's cracking is complicated by the adverse effect of an overtightened TSP set screw during the precracking phase of the test. It cannot be determined how much of an effect the overtightened screw had of the cracking, but from previous tests reported in Volume 2 of this report it is known that the effect can be significant.

Table 3-26
Results of EDS Analyses of Tube Intersection 13-16-4-3 from Test 16-15

	Weight Percent						
Area	Fe	Cr	Ni	Si	Mn	Ti	Na
Deposit within the TSP crevice	60.9	0.7	1.1	0.3	0.9	28.8	7.1
Deposit + 20 min. cleaning*	44.9	0.0	1.6	0.3	0.9	43.4	9.0
Deposit + 20 min. cleaning* + sanding	58.2	4.3	17.2	2.7	7.0	7.6	3.0
Tube Free Span	43.5	8.5	24.6	0.1	0.7	22.6	0.0
Tube Free Span + 20 min. cleaning*	79.3	3.6	14.4	0.3	0.6	1.9	0.0
Tube Free Span + 20 min. cleaning*	64.8	3.2	11.6	0.2	0.5	19.9	0.0
Contact Zone between Tube and TSP	65.9	4.3	21.6	6.0	0.9	0.2	1.1

* Cleaning involved 20 minutes immersed in an ultrasonic bath

Table 3-27
Results of EDS Analyses of Tube Intersection 16-15-2-3 from Test 16-15

	Weight Percent							
Area	Fe	Cr	Ni	Si	Mn	Ti	Na	Ca
Zone 1	94.3	0.8	1.8	0.5	1.2	0.0	1.4	ND
Zone + 20 min. cleaning*	94.3	1.6	1.6	0.4	0.8	0.0	1.1	0.2
Zone 2	51.7	1.1	4.1	6.6	1.6	21.6	13.4	ND
Zone 2 + 20 min. cleaning*	24.2	12.3	39.0	1.5	0.3	16.0	1.5	5.4
Zone 3	35.1	11.0	31.0	0.2	0.4	22.3	0.0	ND
Zone 3 + 20 min. cleaning*	25.0	18.0	51.7	0.4	0.0	4.5	0.0	0.3
Tube Free Span	53.6	7.6	21.3	0.3	0.6	16.6	0.0	ND
Tube Free Span + 20 min. clean.*	16.3	19.1	63.6	0.4	0.0	0.7	0.0	ND
Tube Free Span + 20 min. clean.*	19.8	18.3	60.3	0.2	0.6	0.8	0.0	ND

Zone 1 - Center of prepacked simulated plant sludge
Zone 2 - On the bottom of the prepacked sludge
Zone 3 - At the split of the TSP where prepacked sludge had loosened
* Cleaning involved 20 minutes immersed in an ultrasonic bath

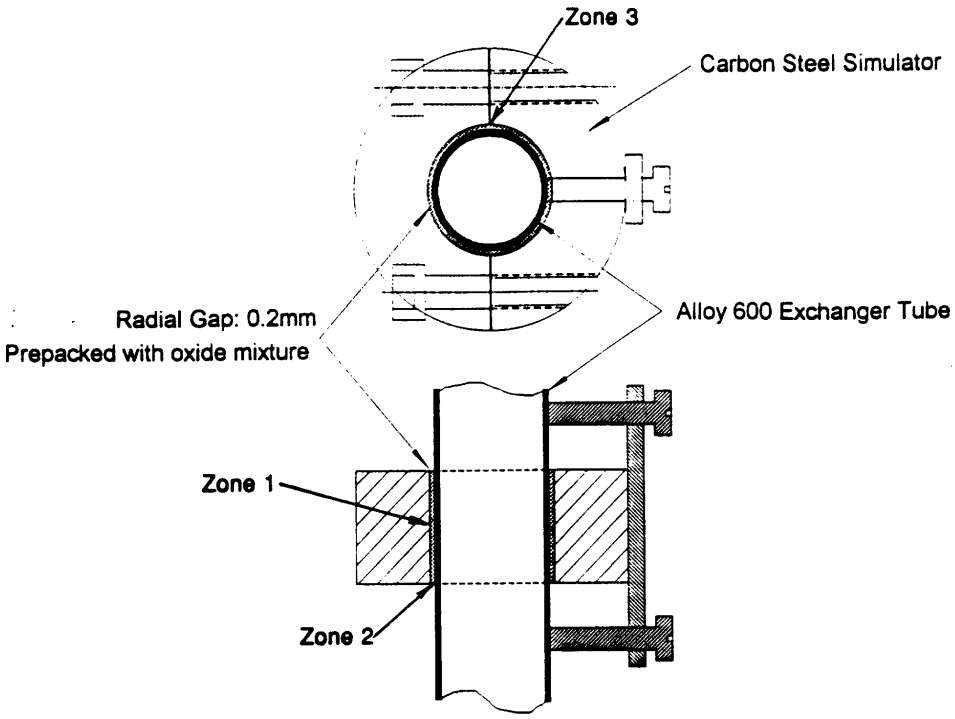

Figure 3-7
Areas of EDS Analyses of Tube Intersection 16-15-2-3 from Test 16-15

Table 3-28
Results of EDS Analyses of a Through Wall Crack Face, At or Near Crack Mouth of Tube Intersection 14-16-4-3 and Tube Free Span from Test 16-16

	Weight Percent								
Area	Fe	Cr	Ni	Cu	Ti	Al	Zn	Si	Mn
50 µm Depth from OD	14.0	7.5	28.8	0.8	46.2	0.8	0.9	0.9	0.5
100 µm Depth from OD	31.6	7.0	56.8	0.0	23.5	0.2	0.3	0.3	0.3
200 µm Depth from OD	21.7	11.1	44.5	0.0	21.0	0.2	0.0	1.2	0.3
1/2 Tube Wall from OD	20.0	13.5	58.3	0.0	6.3	0.2	0.5	0.3	0.3
3/4 Tube Wall from OD	22.4	13.4	57.9	0.4	2.6	0.7	0.7	1.5	0.5
50 µm from ID	13.3	13.6	56.0	0.5	15.0	0.6	0.0	1.1	0.0
OD Face at Crack Mouth	34.8	5.4	14.0	1.4	41.8	0.8	0.0	1.2	0.5
OD Face Near Crack Mouth	33.8	3.4	11.9	0.5	41.1	3.8	0.0	5.2	0.3
OD Face Near Crack Mouth	17.1	16.6	58.6	0.4	4.3	0.3	0.0	1.7	0.6
OD Face Near Crack Mouth	17.1	4.4	16.4	0.0	60.8	0.2	0.0	1.2	0.0
1/2 Tube Wall from OD	69.2	4.0	19.1	0.0	5.6	0.5	0.0	0.9	0.8
1/2 Tube Wall from OD	65.9	4.1	13.5	0.0	10.7	2.3	0.0	2.6	0.9
Tube Free Span	65.6	5.8	17.6	1.2	7.0	0.3	1.0	0.6	0.8
Tube Free Span	40.4	12.2	40.6	0.0	3.8	1.2	0.4	0.6	0.7

XRD. X-ray diffraction (XRD) analysis was performed by NWT (CAMET) on a number of deposit samples. These included:

- Samples of filtered sludges from the drains of Tests 13-17 (Reference) and 16-15 (TiO_2), plus a sample of the Westinghouse simulated plant sludge filtered from pure water. In the case of the filtered sludges, samples were prepared by both C.E.A. and NWT. These analyses were performed to determine the crystalline form of the iron and titanium in these tests. The results are shown in Table 3-29. Samples 1 and 4 should be similar, as should samples 2 and 5. Sample 3 (pure Westinghouse simulated plant sludge) is included as a reference.

- Tube intersection 14-16-3-1 from Test 16-16 was sent to NWT to analyze various locations in and around the TSP crevice. These results are presented in Table 3-30.

- Samples filtered from the drains of Test 16-15 (TiO_2) and Test 16-16 (TiO_2 with $NaAlO_2$). These results are presented in Table 3-31.

The XRD results show that much of the titanium injected into the model boiler reacts with the magnetite present to form ilmenite. The percentages of ilmenite found in Test 16-15 (TiO_2 only) and Test 16-16 (TiO_2 and $NaAlO_2$) drains were similar. Deposits from within the TSP crevice also showed significant quantities of ilmenite present.

Table 3-29
XRD Analysis of Samples Filtered (0.3 µm Filter) from Drains of Tests 13-17 (Reference) and 16-15 (TiO_2)

			Weight Percent				
Sample	Lab No.	NWT No.	TiO_2 Anatase	TiO_2 Rutile	$FeTiO_3$ Ilmenite	Fe_3O_4 Magnetite	Fe_2O_3 Hematite
Test 13-17 Drain - NWT	1898-1	1	-	-	-	97	3
Test 16-15 Drain - NWT	1898-2	2	8	5	62	25	-
W Simulated Sludge	1898-3	3	-	-	-	97	-
Test 13-17 Drain - CEA	1898-4	4	-	-	-	97	3
Test 16-15 Drain - CEA	1898-5	5	10	-	60	30	-

Table 3-30
XRD Analysis of Samples Taken from Tube Intersection 14-16-3-1 from Test 16-16 (TiO_2 with $NaAlO_2$)

	Weight Percent			
Sample	TiO_2	$FeTiO_3$ Ilmenite	Fe_3O_4 Magnetite	Fe_2O_3 Hematite
Tube OD, crevice, ~90° from TSP contact	-	-	87	-
Tube OD, tube free span, below TSP	-	18	52	-
TSP ID, crevice, ~45° from TSP contact	6	33	48	3
TSP ID, crevice, ~135° from TSP contact	-	22	51	15
TSP, top of ring	12	65	17	-

Table 3-31
XRD Analysis of Samples Filtered (0.3 µm Filter) from Drains of Tests 16-15 (TiO_2) and 16-16 (TiO_2 with $NaAlO_2$)

		Weight Percent				
Sample	Drain Date	TiO_2 Anatase	TiO_2 Rutile	$FeTiO_3$ Ilmenite	Fe_3O_4 Magnetite	Fe_2O_3 Hematite
Test 16-15 Drain - NWT	4/11/94	9%	-	59%	31%	-
Test 16-16 Drain - NWT	9/9/94	26%	-	59%	15%	-

Auger and XPS. Auger and XPS analyses were performed on a section of tube free span 13-16-3 from Test 16-15. Table 3-32 shows the Auger results and Table 3-33 shows the results of the XPS. Auger results show that the titanium was incorporated into the tube oxide film. The absence of chromium in the surface oxide layer correlates with the existence of a highly caustic environment.

Table 3-32
Auger Analysis of Tube 13-16-3 Free Span from Titanium Dioxide Test 16-15

Depth	Weight Percent											
	All Elements									A-600 Metals		
Å	O	Cr	Fe	Ni	Cu	S	Cl	C	Ti	Cr	Fe	Ni
0	42.9	0.0	10.2	5.0	2.1	2.6	1.5	32.2	3.7	0.0	67.2	32.8
100	44.5	0.0	21.7	5.5	1.5	3.1	1.0	19.0	3.7	0.0	79.7	20.3
500	47.9	0.0	26.9	5.6	1.1	2.7	0.8	11.5	3.5	0.0	82.7	17.3
2000	49.1	0.0	34.8	6.6	0.7	1.7	0.4	3.7	3.0	0.0	84.0	16.0
5000	49.1	0.0	39.3	6.5	0.3	0.8	0.2	1.2	2.6	0.0	85.7	14.3

Table 3-33
XPS Analysis of Tube 13-16-3 Free Span from Titanium Dioxide Test 16-15

Element	Form
Fe	Fe_3O_4
Ni	Ni_xO_y
Ti	TiO_2
Cu	Cu or Cu_2O

Summary

The continuous injection of titanium dioxide with or without sodium aluminate did appear to have an inhibiting effect on initiation and growth of IGA/IGSCC in caustic environments. This is different from the conclusions drawn from Test 8-12 in the first phase of Task 2a when the titanium dioxide - silicon dioxide sol-gel was injected on a daily basis. EDS analysis demonstrated that in Tests 16-15 and 16-16 titanium was able to penetrate and concentrate in open, eccentric TSP crevices, but not in prepacked, concentric TSP crevices. In addition, EDS analysis showed that titanium, in the form of TYZOR LA, was able to penetrate deep down into a crack from the tube surface during a 150°C, 12 hour long soak.

If titanium is able to penetrate and concentrate in the crevice, then it appears to be able to inhibit IGSCC. Since the solubility of titanium dioxide in water is very low, it probably exists as a colloid. As a colloid, it is difficult to penetrate packed solids.

References

1. J. Daret and G. Pinard Legry, Intergranular Attack (IGA) of PWR's Steam Generator Tubing: Evaluation of Remedial Properties of Boric Acid, Environmental Degradation of Materials in Nuclear Power Systems - Water Reactors, The Metallurgical Society, 1988.

2. J. Daret and D. Feron, Intergranular Attack of Alloy 600: Simulation and Remedial Action Tests, NP-6115-SD, Electric Power Research Institute, Palo Alto, CA, February 1989.

4

CONCLUSIONS

Cracking in Caustic

Precracking of mill annealed alloy 600 tubes was performed in boiler Tests 13-16, 14-16, 15-15 and 16-14. With a concentration of 4 ppm sodium hydroxide in the make-up tank (2.3 ppm Na^+) and simulated plant sludge injections of 1 gram daily for 16 days, through wall leaks were detected in Tests 13-16, 14-16, and 16-14 after 21 days exposure to caustic. No through wall cracking was detected in Tests 15-15 after 24 days of exposure. All four boilers operated until 24 days of caustic exposure when they were taken out of service. The time to the first through wall leak for each boiler was within the band of failure times for previous C.E.A. model boiler tests with only sodium hydroxide as a contaminant (i.e., 6 to 27 days).

Nondestructive examination of the intersections from Test 13-16 showed three with 100% indications, three with 30% to 75% indications and six with less than 15% indications. Test 16-14 showed four with 100% indications, six with 30% to 90% indications and two with less than 15% indications. Test 14-16 only had one with a 100% indication and eleven intersections with less than 15% indications. Test 15-15 only had one with a 30% indication and eleven intersections with less than 15% indications.

All four boilers were operated identically and the tube intersections were the same materials and configuration. Prior to the precracking tests all four shells had been shot blasted with Al_2O_3 and cleaned with acetic acid to try to remove from the interior of the boiler shells any residual material from previous tests. Thus, there is no apparent reason for the differences seen in the degree of IGSCC in the four boilers. The one major difference was the environment of the previous test in each boiler. Boiler 14 had a previous phosphate test environment, however, no residual phosphate was found on the boiler shell after the acetic acid cleaning. Boiler 15 had a previous cerium acetate environment and residual cerium (0.4 weight %) was found in the boiler shell surface oxide.

Tests 13-17 and 13-18 were reference tests involving injection of sodium hydroxide with no other additives, i.e., no inhibitor or buffer. These tests were conducted with a concentration of 1 ppm sodium hydroxide in the make-up tank (0.6 ppm Na^+). The

amounts of injected simulated plant sludge differed: Test 13-17 injected 1 gram daily for 21 days and Test 13-18 injected 0.35 grams weekly for three weeks. Test 13-17 consisted of all virgin tube material, while Test 13-18 was configured with five intersections having virgin tube material and seven precracked intersections from Test 13-16 (three) and ENSA (four). Test 13-17 developed a through wall crack after only 14 days. A precracked tube intersection in Test 13-18 cracked through wall after nine days of exposure, while after 19 days of exposure three of the virgin tube intersections were found leaking by hydro testing but the exact time of failure could not be identified. Thus, the virgin tube materials in Tests 13-17 and 13-18 exposed to 1 ppm sodium hydroxide from their make-up tanks cracked in less time than the four precracking tests exposed to 4 ppm sodium hydroxide from their make-up tanks. Four tube intersections from Test 13-17 and five tube intersections from Test 13-18 had through wall cracks.

Based on the results from these six tests and on the results of other C.E.A. tests as reported in Table 3-7, the time to first cracking in the range of 1 $mg\text{-}kg^{-1}$ to 4 $mg\text{-}kg^{-1}$ (1 ppm to 4 ppm) NaOH does not appear to be proportional to the feedwater NaOH concentration or to the integrated exposure (i.e., ppm days).

A summary of the results for caustic cracking in the absence of an inhibitor or buffer is given in Table 4-1.

Table 4-1
Summary of Caustic Cracking Results in the Absence of Inhibitors or Buffers

Tube Material Condition	NaOH Conc. mg/kg	TSP Config.	Type of Sludge Injected	Total Sludge Injected	Time to First Failure	Total Test Duration	No. Leaked Per No. Tested
Virgin	4	Open	Fess.[1]	14 g	6 to 20 d	28 d	3/24
Virgin	4	Open	West.[2]	16 g	21 d	24 d	7/48
Virgin	1	Open	West.[2]	15 g	14 d	28 d	3/5
Virgin	1	Open	West.[2]	1 g	9 d	19 d	1/1
Virgin	1	Prepacked	West.[2]	N/A	9 to 14 d	19 to 28 d	3/11
Precracked	1	Open	West.[2]	1 g	9 d	19 d	1/3

1 Simulated Fessenheim plant sludge

2 Westinghouse simulated plant sludge

The first significant observation is the quasi-independence, for this alloy 600 tubing material in open and eccentrically mounted TSPs, of the time to get a throughwall crack (a detectable primary-to-secondary leak) on sodium hydroxide concentration, and on composition/oxidizing properties and quantity of injected sludge. For the material heat tested, the maximum crack propagation rate under the cracking reference chemistry was about 7 µm per hour, which represents extremely severe conditions for testing inhibitors.

The overall conclusions from these tests are:

- Alloy 600 tubing can rapidly crack at TSP intersections in model boilers with sodium hydroxide contamination. The maximum crack propagation rate is about 7 µm per hour.
- The significant differences in the degree of IGSCC observed in the four precracking test boilers are not well understood. The differences could have been related to the boiler's previous test environment.
- The degree of IGSCC attack did not appear to be significantly related to the makeup tank hydroxide concentration, the amount or type of simulated plant sludge added, or to the configuration of the TSP simulator.
- Nondestructive test results correlated with the results of the destructive examinations.

Cracking in Caustic With Addition of Boric Acid Buffer

One boiler, SG14, was operated with boric acid and sodium hydroxide added to the feedwater makeup tank so that the makeup flow would have a molar ratio of about 18 [B]: 1 [Na] for each of the three series following the precracking series. Those three runs are designated 14-17 Run 1, 14-17 Run 2 and 14-17 Run 3. The total test period for all three runs was 74 days. The configuration for Run 1 consisted of 9 virgin tube intersections and three precracked intersections. See Table 2-21 for the Run 1 test assembly configuration. The configuration for Run 2 was modified by removing two of the virgin intersections and replacing them with two ENSA precracked intersections. The configuration for Run 3 was the same as for Run 2. See Table 2-25 for the Run 2 and 3 test assembly configuration.

Destructive examinations were performed on all 14 intersections. Two virgin material intersections experienced about 4% through wall cracks, and two ENSA precracked intersections had crack depths of 70% and 80%. The pretest crack depths of those two intersections were 45 to 77% and 42 to 48%. There is no definitive means to determine whether those cracks grew with the two run exposure to NaOH plus boric acid. Ten intersections had no detected IGSCC by their destructive examination. There is no significant difference between the lack of degradation of tubes with concentric, prepacked TSPs and those with eccentric TSPs, or with virgin and precracked material.

The lack of cracking with NaOH and boric acid is consistent with previous model boiler tests performed by C.E.A. with boric acid in the AJAX loops. There was sufficient boric acid added to the feedwater tank to neutralize the sodium hydroxide present. The boric acid may also form a surface film that assists in the inhibition of

crack initiation and growth. However, there is insufficient data generated in these studies to confirm this hypothesis.

The overall conclusions from these tests are:

- Boric acid can neutralize sodium hydroxide if present in sufficient quantity. By adding both the boric acid and sodium hydroxide to the feedwater makeup tank, sodium borate was actually being injected into the model boiler.
- Virgin tube material experienced shallow intergranular penetrations of about 4% of tube wall in both open crevice and packed crevice TSP configurations.
- Precracked tube intersections did not crack through wall. Since the initial crack depths were not accurately known, the rate of crack growth could not be calculated.
- These results are consistent with previous model boiler tests performed by C.E.A.

Titanium Dioxide Inhibitor Test

Boiler SG16 was operated with sodium hydroxide in the feedwater makeup tank and titanium dioxide in the auxiliary makeup tank so that the combined makeup flow would have a molar ratio of about 6 [Na]: 1 [Ti] for the two test series following the precracking series. Those two tests are designated 16-15 and, 16-16 Run 1, 16-16 Run 2. The configuration for Test 16-15 consisted of six virgin tube intersections and six precracked intersections. See Table 2-23 for the Test 16-15 assembly configuration. The configuration for Test 16-16 Run 1 consisted of two virgin tube intersections and ten precracked intersections. The configuration for Test 16-16 Run 2 was identical to that for Test 16-16 Run 2 except that the intersection at the 3rd elevation on leg #4 was removed for Run 2. In addition, Intersection E5-D at the 3rd elevation of tube #2 had a free span crack approximately 55% through wall. See Tables 2-26 and 2-27 for the Test 16-16 Run 1 and Run 2 assembly configurations, respectively. Test 16-15 consisted of the addition of only titanium dioxide, whereas, Test 16-16 also added sodium aluminate as a zeta potential modifier. In addition, both tests had about a two day period of time soaking with 1.2% TYZOR LA.

The addition of titanium dioxide to Test 16-15 did, in some intersections, inhibit the growth of existing cracks and inhibit the initiation of new cracks. In other intersections there was no inhibition. The first through wall crack was found in a precracked intersection after 18 days of exposure to caustic plus titanium dioxide. The results of the destructive examination are given in Table 4-2. Inhibition was complete for virgin tube material with open eccentric TSP crevices. However, two of the three concentric, prepacked TSP intersections severely cracked while the third had cracking inhibited. In the precracked intersections with eccentric TSPs the degree of inhibition was also mixed: two of the intersections cracked through wall, one had no cracking and three

had 30% to 40% through wall cracking. All six precracked intersections came from aggressive precracking tests, i.e., Tests 13-16 and 16-14. Therefore, the crack growth rate for the three intersections with 30% to 40% through wall cracking cannot be determined since the crack depth found may have existed after the precracking tests. The overall conclusion from this test is that inhibition can occur with titanium dioxide if the material can be transported inside the crevice. The test results also suggest that the titanium is not dissolved in the bulk water, but consists of colloidal size particles that have difficulty penetrating packed crevices that can be penetrated by sodium ions.

The results of EDS analysis of TSP crevice deposits show titanium was able to accumulate in the eccentric open crevice of Intersection 13-16-4-3 in Test 16-15, whereas titanium was not found in the concentric prepacked crevice of Intersection 16-15-2-3 in Test 16-15. Intersection 13-16-4-3 was found to be 40% through wall cracked and Intersection 16-15-2-3 cracked 100% through wall.

Table 4-2
Summary of Caustic Cracking Results With Titanium Dioxide Inhibitor - Test 16-15

Intersection No.	TSP Type	Type of Material	TSP Set Screw	Destructive Exam, % Through Wall	Comments
16-15-1-1	Eccentric	Virgin	Exterior	Zero	
16-15-1-2	Eccentric	Virgin	Exterior	Zero	
16-15-1-3	Eccentric	Virgin	Exterior	Zero	
16-15-2-1	Concentric	Virgin	Exterior	Zero	
16-15-2-2	Concentric	Virgin	Exterior	90%	
16-15-2-3	Concentric	Virgin	Exterior	100%	
16-14-2-1	Eccentric	Precracked	Interior	Zero	
16-14-2-3	Eccentric	Precracked	Interior	100%	Tube leaked
13-16-3-3	Eccentric	Precracked	Interior	30%	
13-16-4-1	Eccentric	Precracked	Interior	40%	
13-16-4-2	Eccentric	Precracked	Interior	100%	Tube leaked
13-16-4-3	Eccentric	Precracked	Interior	40%	

All concentric TSPs are also prepacked with sludge.

The addition of titanium dioxide plus sodium aluminate to Test 16-16 did, in some intersections, inhibit the growth of existing cracks and inhibit the initiation of new cracks. In other intersections there was no inhibition. The results of the destructive examination are given in Table 4-3. Inhibition was complete for virgin tube material with open eccentric TSP crevices. However, cracking was not inhibited in concentric, prepacked TSP intersections. In the precracked intersections with eccentric TSPs the degree of inhibition was also mixed: three of the six intersections cracked through wall, two had no cracking and one had 35% through wall cracking. All six precracked intersections came from the relatively non-aggressive precracking Test 14-16. The crack

growth rate for the one intersection with 35% through wall cracking cannot be determined since the crack depth found may have existed after the precracking tests. Two of the 100% cracked intersections were affected by the interior set screw as evidenced by the unique cracking pattern. The overall conclusion from this test is that inhibition can occur with titanium dioxide if the material can be transported inside the crevice. The test results also suggest that the titanium is not dissolved in the bulk water, but consists of colloidal size particles that have difficulty penetrating packed crevices that can be penetrated by sodium ions.

Table 4-3
Destructive Examination Results for Titanium Dioxide Test 16-16

Intersection No.	Run	TSP Type	Type of Material	TSP Set Screw	Destructive Exam, % Through Wall	Comments
ENSA E12-A	1, 2	Concentric	Precracked	Exterior	100%	
ENSA E12-B	1, 2	Concentric	Precracked	Exterior	Not Performed	
ENSA E1-F	1, 2	Concentric	Precracked	Exterior	Not Performed	
16-16-2-1	1, 2	Eccentric	Virgin	Exterior	Zero	
16-16-2-2	1, 2	Eccentric	Virgin	Exterior	Zero	
ENSA E5-D	1, 2	Free Span	Precracked	-	50%	
14-16-3-1	1, 2	Eccentric	Precracked	Interior*	100%	Tube leaked
14-16-3-2	1, 2	Eccentric	Precracked	Interior*	35%	
14-16-3-3	1, 2	Eccentric	Precracked	Interior*	100%	Screw effect
14-16-4-1	1, 2	Eccentric	Precracked	Interior*	Zero	
14-16-4-2	1, 2	Eccentric	Precracked	Interior*	Zero	
14-16-4-3	1	Eccentric	Precracked	Interior*	100%	Screw effect

All concentric TSPs are also prepacked with sludge.

* Set screw were on the interior for the precracking test and then moved to the exterior for Test 16-16.

The overall conclusions from these two titanium dioxide tests are:

- Under favorable conditions titanium dioxide can inhibit IGSCC of alloy 600.
- IGSCC of virgin alloy 600 tube material in open, eccentric TSP crevices was completely inhibited by titanium dioxide with and without the sodium aluminate zeta potential modifier. None of the five intersections had any IGSCC identified at the completion of the two tests.
- The inhibition of IGSCC for precracked alloy 600 tube material in open, eccentric TSP crevices was mixed. Five of twelve intersections experienced through wall leaks. The IGSCC of two of the five 100% through wall cracked tubes was associated with overtightened TSP set screws. IGSCC in the remaining seven

intersections either grew slowly or not at all. Since the initial crack depths were not accurately known, the rate of crack growth could not be calculated.

- Titanium dioxide did not inhibit the IGSCC of intersections that had been packed with simulated plant sludge.
- Titanium dioxide can incorporate itself in the oxide film of alloy 600, if the surface is exposed to water containing titanium dioxide.
- Titanium dioxide will react with magnetite to form ilmenite and precipitate on heat transfer surfaces.
- Since titanium dioxide does not penetrate sludge deposits it is probably in the form of a fine or colloidal size solid as opposed to being dissolved.

Cerium Acetate Inhibitor Test

Boiler SG15 was operated with cerous acetate added to the feedwater with a molar ratio of about 6 [Na]: 1 [Ce] for two series following the precracking series. Those two runs are designated 15-15 Run 1 and 15-15 Run 2. The configuration for Run 1 consisted of 5 virgin tube intersections and 7 precracked intersections from the 15-15 precracking test. See Table 2-22 for the Run 1 test assembly configuration. The configuration for Run 2 was modified by removing two of the virgin intersections that had cracked 100% through wall and replacing them with two ENSA precracked intersections. See Table 2-26 for the Run 2 test assembly configuration.

The addition of cerium acetate to Test 15-15 did not inhibit the growth of existing cracks and inhibit the initiation of new cracks. Ten tube intersections experienced 90% to 100% through wall cracking in one or two runs. All five virgin tube materials suffered extensive cracking. The results of the destructive examination are given in Table 4-4.

Table 4-4
Destructive Examination Results for Cerous Acetate Test 15-15

Intersection No.	Run	TSP Type	Type of Material	TSP Set Screw	Destructive Exam, % Through Wall	Comments
15-15-1-1b	1, 2	Concentric	Virgin	Exterior	90%	
15-15-1-2b	1	Concentric	Virgin	Exterior	100%	E9-D replaced
ENSA E9-D	2	Free Span	Precracked	-	Not Performed	
15-15-1-3b	1	Concentric	Virgin	Exterior	100%	E9-E replaced
ENSA E9-E	2	Concentric	Precracked	Exterior	100%	
15-15-2-1	1, 2	Eccentric	Precracked	Interior	100%	Tube leaked
15-15-2-2	1, 2	Eccentric	Precracked	Interior	100%	Tube leaked
15-15-2-3b	1, 2	Eccentric	Virgin	Exterior	100%	
15-15-3-1	1, 2	Eccentric	Precracked	Interior	Zero	
15-15-3-2	1, 2	Eccentric	Precracked	Interior	90%	Screw effect
15-15-3-3	1, 2	Eccentric	Precracked	Interior	40%	
15-15-4-1	1, 2	Eccentric	Precracked	Interior	Zero	
15-15-4-2	1, 2	Eccentric	Precracked	Interior	100%	Tube leaked
15-15-4-3b	1, 2	Eccentric	Virgin	Exterior	100%	Screw effect & Tube leaked

All concentric TSPs are also prepacked with sludge.

The results of EDS analyses show that cerium was able to penetrate packed TSP crevices and accumulate in significant quantities. For example, in Intersection 15-15-1-1b there was 1.6% cerium near the mouth of a crack in the intersection crevice that had been prepacked with simulated plant sludge. Cerium concentrations of several percent were found in deposits of open eccentric TSP crevices.

The overall conclusions from these cerium acetate tests are:

- Cerium acetate did not inhibit IGSCC of alloy 600.
- 100% through wall IGSCC of alloy 600 tube material was experienced by: (1) open, eccentric TSPs with virgin tube material, (2) open, eccentric TSPs with precracked tube material, (3) prepacked, concentric TSPs with virgin tube material, and (4) prepacked, concentric TSPs with precracked tube material.
- Significant quantities of cerium were able to penetrate prepacked TSP crevices, but did not provide IGSCC inhibition.
- While complete IGSCC inhibition was not accomplished with cerium acetate, the time to failure with cerium acetate injection was a factor of two or more greater than with just sodium hydroxide alone.

Results Summary by TSP Intersection Configuration

Tables 4-5, 4-6 and 4-7 summarize the results of the model boiler testing by the configuration of the TSP intersection. From these data, boric acid neutralization of a caustic environment would appear to be the most favorable additive. Titanium dioxide was able to completely inhibit initiation of IGSCC in open, eccentric crevice with virgin tube material. Injection of titanium dioxide was less successful in inhibiting IGSCC in sludge prepacked concentric crevices and in precracked tubes in open eccentric intersections. Cerium acetate was uniformly ineffective in inhibiting the initiation and growth of IGSCC in all type of intersection configurations.

Table 4-5
Summary of Results Obtained With Inhibitors On Virgin Tubes With Open Crevices and Eccentric TSPs

Inhibitor Tested	Time to First Failure	Total Test Duration	No. Leaked Per No. Tested	IGSCC Range
None	6 to 21 d	19 to 28 d	14/78	0 to 100%
Boric Acid	N/A	74 d	0/3	0 to 4%
TiO_2	N/A	21 d	0/3	0%
TiO_2 + $NaAlO_2$	N/A	46 d	0/2	0%
Cerium Acetate	39 d	47 d	1/2	100%

Table 4-6
Summary of Results Obtained With Inhibitors On Precracked Tubes With Open Crevices and Eccentric TSPs

Inhibitor Tested	Time to First Failure	Total Test Duration	No. Leaked Per No. Tested	IGSCC Range
None	9 d	19 d	1/3	50 to 100%
Boric Acid	N/A	74 d	0/3	0 to 15%
TiO_2	19 d	21 d	2/6	0 to 100%
TiO_2 + $NaAlO_2$	19 d	19 d	1/1	100%
TiO_2 + $NaAlO_2$	45 d	46 d	2/5	0 to 100%
Cerium Acetate	39 d	47 d	3/7	0 to 100%

Table 4-7
Summary of Results Obtained With Inhibitors On Virgin Tubes With Sludge Prepacked Crevices and Concentric TSPs

Inhibitor Tested	Time to First Failure	Total Test Duration	No. Leaked Per No. Tested	IGSCC Range
None	9 to 14 d	19 to 28 d	3/11	0 to 100%
Boric Acid	N/A	74 d	0/6	0 to 4%
TiO_2	N/A	21 d	0/3	0 to 100%
Cerium Acetate	N/A	47 d	0/3	90 to 100%

A

MATERIAL CHARACTERISTICS

The tubing material used for this task is typical of tubing used in operating steam generators and was low temperature mill annealed alloy 600, 3/4 inch in diameter manufactured by Babcock & Wilcox, Heat No. 96834.

Tubing Material Chemistry and Heat Treatment

The chemical composition of the material heat is listed in Table A-1. The heat treatment parameters for the mill anneal is listed in Table A-2.

Table A-1
Tubing Material Chemistry

	Composition, Weight Percent													
Supplier/Heat No.	**C**	**Ni**	**Cr**	**Si**	**Mn**	**P**	**S**	**Cu**	**Co**	**Ti**	**Al**	**Fe**	**N2**	**B**
B & W/96834	.040	74.91	15.83	.30	.26	NM	.001	.01	.023	NM	NM	8.09	NM	NM

NM = Not Measured

Table A-2
Tubing Heat Treatment

Supplier/Heat No.	Material Type	Heat Treatment
B & W/96834	600 MA	Mill Anneal at 927°C (1700°F) for 3 to 5 minutes

Carbide Decoration

A sample of the tubing material was etched with bromine-methanol and examined for total and intergranular carbides. Tables A-3 and A-4 identify the total, intergranular and percent intergranular carbides for the exterior surface grains and the bulk material grains, respectively. Table A-5 identifies the percent intergranular carbides in the exterior surface grains and the bulk material grains.

Table A-3
Material Carbide Decoration in Exterior Surface Grains

		Average Carbides in Exterior Surface Grains		
Supplier/Heat No.	Material Type	Total No./100 μm^2	Intergranular No./100 μm^2	Percent Intergranular
B & W/96834	600 MA	18 ± 1	2 ± 0.1	11%

Table A-4
Material Carbide Decoration in Bulk Material Grains

		Average Carbides in Bulk Material Grains		
Supplier/Heat No.	Material Type	Total No./100 μm^2	Intergranular No./100 μm^2	Percent Intergranular
B & W/96834	600 MA	26 ± 5	3.4 ± 0.7	13%

Table A-5
Comparison of Carbide Decoration in Exterior Surface and Bulk Material Grains

		Percent Intergranular Carbides in Grains		
Supplier/Heat No.	Material Type	Exterior Surface	Bulk Material	Ratio of Bulk/Exterior
B & W/96834	600 MA	11%	13%	1.2

Figures A-1a, A-1b, A-6 and A-11 of Volume 2 of this report show the carbide distribution and microstructure of the B&W Heat No. 96834. Figures A-1a and A-1b show micrographs of the bulk material using the dual etch technique. The first micrograph, Figure A-1a, reveals all carbides after using the orthophosphoric acid etch. The second micrograph, Figure A-1b, reveals the grain boundaries following a slight repolishing and an oxalic acid etch. Figure A-6 shows the micrograph, after bromine - methanol etch, that was used to generate the bulk material total and intergranular carbides values. Figure A-11 shows the equivalent micrographs for the exterior surface grains for this mill annealed material.

Mechanical Characteristics

The mechanical properties of the material used in this task of the program are listed in Table A-6.

Table A-6
Tubing Mechanical Properties

		Properties at 208C		
Supplier/Heat No.	**Material Type**	**0.2% YS MPa (ksi)**	**UTS MPa (ksi)**	**Elongation %**
B & W/96834	600 MA	356 (51.7)	736 (106.7)	39

B

CHEMISTRY OF SECONDARY CIRCUITS

Titanium Dioxide Inhibitor Tests

The composition of the titanium dioxide used in Boiler Tests 16-15 and 16-16 is given in Table B-1. This material was manufactured by DuPont on a bench scale process and designated as Lot #E79503-13A. The surface area of this material was 660 m^2-g^{-1}.

Table B-1
Composition of Titanium Dioxide Inhibitor

Constituent	Weight Percent
TiO_2	99.9+%

Trace Impurities in mg-kg^{-1} (ppm): Acetate = 5,700 ppm; Sodium = 6.9; Calcium = <5; Magnesium = <1; Other Anions = <50

DuPont TYZOR LA is a 50% solution of lactic acid titanium chelate, ammonium salt in water. This results in a titanium concentration of 8.14% (weight) titanium in the 50% solution. The structure of TYZOR LA is given in Figure B-1.

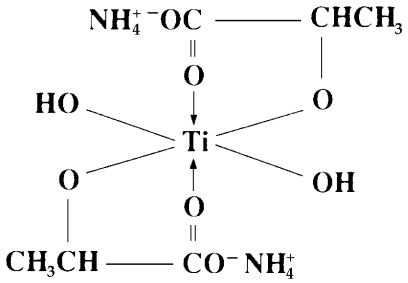

Figure B-1
Structure of DuPont TYZOR LA

Sodium aluminate, $NaAlO_2$, was added to the titanium dioxide solution for Test 16-16 to modify the zeta potential of the titanium dioxide. This material was obtained from ICB Biomedical, Inc., Lot #55339. No trace impurities were analyzed for the sodium aluminate.

Cerous Acetate Inhibitor Test

The composition of cerous acetate, $Ce(C_2H_3O_2)_2 \bullet X\ H_2O$, used in Boiler Test No. 15-15 is given in Table B-2. This material was from GFS Chemicals, Lot #BI. The material was reported to have 1.5 waters of hydration from GFS Chemicals, but was believed to have 6 waters of hydration based on tests by CEA. In preparing the test solutions a formula weight with 1.5 waters of hydration was used, 344.28 g-mole^{-1}. If the material had 6 waters of hydration (formula weight of 425.34 g-mole^{-1}), then the actual amount of cerium added to the feedwater tank would be 19% less than anticipated (i.e., a difference in formula weights of 425.34 g-mole^{-1} (6 waters) versus 344.28 g-mole^{-1} (1.5 waters)).

Table B-2
Composition of Cerous Acetate Inhibitor ($Ce(C_2H_3O_2)_3 \bullet X\ H_2O$)

Constituent	Weight Percent
Cerous Acetate	99.9+%

Trace Impurities in mg-kg^{-1} (ppm): Sodium = 250; Calcium = 150; Magnesium = 12; Potassium = <50; Copper = 1.2; Lead = 1.2

Composition of Test Drains

At the completion of a test period the AJAX boiler would be drained. The compositions of the drained liquid for each Reference, Boric Acid and Candidate Inhibitor test is presented in Table B-3. The amount of sulfate in the drains of each test is believed to be a result of the sulfate in the magnetite injected into each boiler as simulated plant sludge. The magnetite has been analyzed and found to contain 2800 mg-kg^{-1} (ppm) of sulfur. 15 to 21 grams of sludge was added to Tests 13-17, 14-17 Run 1, 15-15 Run 1, and 16-15 which had drain sulfate concentration of from 6.1 to 6.6 mg-kg^{-1} (ppm). The other tests only had 1.05 grams of sludge injected and had drain sulfate concentration of from 0.6 to 1.4 mg-kg^{-1} (ppm).

Table B-3
Composition of Liquid Drained from Tests

Test No.	13-17	13-18	14-17	14-17	14-17	15-15	15-15	16-15	16-16	1616
Run No.	-	-	1	2	3	1	2	-	1	2
pH @ 25°C	11.0	10.2	9.5	9.3	7.1	10.4	10.3	10.7	10.5	9.6
Total Cond, $\mu S\text{-}cm^{-1}$	195	80	125	79	17.4	94	81	129	98	73
Na^{+}, $mg\text{-}kg^{-1}$	31.1	7.2	31.8	22.6	11.7	10.9	6.4	15.8	10.8	17.8
SO_4^{2-}, $mg\text{-}kg^{-1}$	6.6	1.3	6.1	1.4	0.6	6.4	0.6	6.3	0.6	1.1
Si, $mg\text{-}kg^{-1}$	0.19	0.28	0.38	0.15	ND	0.27	0.47	0.44	0.40	ND
Al, $mg\text{-}kg^{-1}$	0.068	0.38	0.69	0.13	ND	0.63	0.30	0.06	0.49	ND
Zn, $mg\text{-}kg^{-1}$	0.002	0.007	0.006	<0.001	ND	0.003	<0.001	0.003	0.002	ND
B, $mg\text{-}kg^{-1}$	ND	ND	17.1	12.8	8.8	ND	ND	ND	ND	ND
B:Na Weight Ratio	-	-	0.54	0.57	0.75	-	-	-	-	-
Ce, $mg\text{-}kg^{-1}$	ND	ND	ND	ND	ND	<0.03	<0.05	ND	ND	ND
Acetate, $mg\text{-}kg^{-1}$	ND	ND	ND	ND	ND	2.24	1.65	ND	ND	ND
Soluble Ti, $mg\text{-}kg^{-1}$	ND	ND	ND	ND	ND	ND	ND	0.086	0.245	ND

ND = Not Determined

C

NONDESTRUCTIVE EXAMINATION RESULTS

Two methods of nondestructive examination were used, eddy current testing and ultrasonic testing.

Eddy Current Examination

All eddy current examination results are taken from Reference (1). All eddy current examinations were performed on the four precracking tests, 13-16, 14-16, 15-15 and 16-14, after exposure to the sodium hydroxide environment. No exams were performed on tubes from other tests. Table C-1 identifies the maximum depth crack found at each tube-to-tube support plate intersection for the four precracking tests. For details of each examination refer to Reference (1).

Two types of eddy current examinations were conducted, one using a conventional bobbin coil probe for 3/4 inch tubes and the other using a special laboratory rotating probe for both 3/4 and 7/8 inch tubes (1). The design of the bobbin coil is that which is commonly used for in-service inspection on French steam generators. For 3/4 inch tubes it works in the differential mode at three frequencies: 600, 280 and 120 kHz. Calibration is performed using a standard tube with 10, 30 and 40% of wall thickness slots and with four 100% depth holes, 1 mm in diameter, located at 90° apart around the circumference. Combining 280 and 120 kHz frequencies eliminates the TSP signal. Evaluation of the crack depth is based on the phase angle.

The design of the rotating probe is based on a ferrite coil, 1 mm in diameter, working in the absolute mode at four frequencies: 600, 280, 120 and 30 kHz for 3/4 inch tubes; and 500, 240, 100 and 30 kHz for 7/8 inch tubes. Calibration is performed using a standard tube with 10, 30 and 40% of wall thickness EDM notches (15 mm in length) and four 100% depth holes, 1 mm in diameter, located 90° apart around the circumference. Displacement of the probe through the tube is helical, with a step of 0.5 mm per 360° rotation at a linear speed of 2.5 mm per second (i.e., five complete rotations per second). Signals are normalized to the 100% hole signal and reported either on a three dimensional map (i.e., elevation, angular position and voltage) or on iso-voltage plots.

Table C-1
Eddy Current Results for Precracking in Boiler Tests 13-16, 14-16, 15-15 and 16-14

Intersection Number	Maximum Crack Depth, % Through Wall*			
	Test 13-16	Test 14-16	Test 15-15	Test 16-14
1-1	<40%	<40%	<40%	<40%
1-2	<40%	100%	<40%	100%
1-3	<40%	<40%	<40%	90%
2-1	100%	<40%	<40%	<40%
2-2	70%	50%	<40%	<40%
2-3	90%	<40%	<40%	<40%
3-1	50%	<40%	<40%	100%
3-2	90%	<40%	<40%	90%
3-3	<40%	<40%	<40%	100%
4-1	<40%	<40%	<40%	80%
4-2	<40%	<40%	<40%	70%
4-3	<40%	<40%	<40%	100%

* An eddy current result value of <40% indicates that no significant signal was found and the actual crack depth can be from zero to 40%.

Ultrasonic Examination

All ultrasonic examination results are taken from Reference (2). All ultrasonic examinations were performed on the four precracking tests, 13-16, 14-16, 15-15 and 16-14, after exposure to the sodium hydroxide environment. No exams were performed on tubes from other tests. Table C-2 identifies the maximum depth crack found at each tube-to-tube support plate intersection for the four precracking tests. For details of each examination refer to Reference (2).

Ultrasonic inspections were carried out from the inside of the tube, which was filled with water to allow the transmission of the ultrasonic waves between the transducers and the surface of the tube, using focused ultrasonic transducers. For complete inspection of the area of interest, the transducer was displaced along a helical path so that the combination of the rotational speed, the steps along the helix and the repetition frequency of the ultrasonic pulses produced a lattice of measurement points with satisfactory coverage (2).

Three types of ultrasonic measurements were taken: (1) profiling and thickness measurements, (2) detection and measurement of circumferential (transverse) cracks, and (3) detection and measurement of axial (longitudinal) cracks. Thickness measurements were carried out using a transducer with a central frequency of 15 MHz,

and an active diameter of 5.5 mm, which was focused at 30 mm in the water, generating longitudinal waves at 0° in the tube material. The recordings of the profile of the internal surface of the tubes were obtained by measuring the variations in the depth of the water path between the transducer and the internal surface. The uncertainty in the measurement is of the order of 15 µm. Data acquisition was carried out along four vertical paths spaced at 90° intervals around the circumference.

Detection of circumferential cracks were made using a 15 MHz transducer with an active diameter of 5.5 mm, which was focused at 30 mm in the water, generating refraction shear waves at 45° in the tube material. The axis of emission of the waves coincides with the tube axis, with a propagation along the tube support plates towards the tube sheet. The defects looked for were those on the outside tube wall and these were detected by the presence of a corner echo. The overall sensitivity of the measurement chain was adjusted by a prior calibration on a tube mock-up containing EDM notches with depths varying from 20 to 80% of the nominal tube thickness. This was set so that the saturation of the amplifying stages occurred for the 80% notch reflection.

Detection of axial cracks were made using a 12 MHz transducer with an active diameter of 5.5 mm, which was focused at 30 mm in the water, generating refraction shear waves at 45° in the tube material. The axis of emission of the waves was perpendicular to the tube axis, with a propagation direction clockwise for an observer looking at the tubes from above the tube sheet. The reference for zero angle is the TSP set screw. The defects looked for were those on the outside tube wall and these were detected by the presence of a corner echo. The overall sensitivity of the measurement chain was adjusted by a prior calibration on a tube mock-up containing EDM notches with depths varying from 20 to 80% of the nominal tube thickness. This was set do that the saturation of the amplifying stages occurred for the 80% notch reflection.

The position of defects is given by two coordinates: (1) the distance, Z, from the top of the tube sheet, and (2) the angle, ∅, with ∅ = 0° being the TSP set screw location. The positive direction of ∅ is counter-clockwise for an observer looking at the tubes from above the tube sheet. The location of each tube support plate (TSP) is given with respect to the tube sheet; the closest is designated TSP1, then TSP2 and TSP3.

Table C-2
Ultrasonic Examination Results for Precracking in Boiler Tests 13-16, 14-16, 15-15 and 16-14

Intersection Number	Maximum Crack Depth, % Through Wall*			
	Test 13-16	Test 14-16	Test 15-15	Test 16-14
1-1	<15%	<15%	30%	<15%
1-2	<15%	100%	<15%	100%
1-3	<15%	<15%	<15%	100%
2-1	100%	<15%	<15%	<15%
2-2	75%	<15%	<15%	75%
2-3	100%	<15%	<15%	30%
3-1	75%	<15%	<15%	100%
3-2	100%	<15%	<15%	90%
3-3	30%	<15%	<15%	100%
4-1	<15%	<15%	<15%	90%
4-2	<15%	<15%	<15%	75%
4-3	<15%	<15%	<15%	90%

* An ultrasonic result value of <15% indicates that no significant signal was found and the actual crack depth can be from zero to 15%.

References

1. Besnard, R., "Controle Par Courants de Foucault de Maquettes de Generateur de Vapeur Soumises a la Corrosion Maquettes 13-16, 14-16, 15-15, 16-14," Laboratoire de Controle par Methodes Electromagnetiques, STA/LCME-94/DT 1625, September 1994.

2. Gondard, C., "Controle Par Ultrasons de Maquettes de Tubes de GV Soumis a de la Corrosion du Milieu Secondaire Maquettes AJAX 13/16, 14/16, 15/15, 16/14 Decembre 93," Laboratoire de Controle par Ultrasons, STA/LCUS DT 1585, May 1994.

D

SURFACE REPLICATION MAPS

After completion of all nondestructive examinations, the section of the tube including the TSP was cut from the tube bundle and the TSP simulators were removed from the tubes. A plastic replica was made of the exterior surface of many of the tubes at the intersection with their TSP. The replica was viewed under a microscope and a complete, detailed mapping of cracks on the exterior surface of each tube-to-TSP intersection was made. In order to make the cracks of some tubes more visible they were bulged (expanded) by inserting a flexible plug inside the tube and compressing the plug hydraulically. Tubes so expanded are noted on their map's figure title. These surface replication maps are useful in identifying axial cracks with transverse components and circumferential cracks. Through the use of these maps, selected exterior surface areas were chosen for micrographs. Table D-1 lists the tubes with surface maps, and Figures D-1 through D-49 show the maps which were produced.

Table D-1
List of Tube Intersections with Surface Replication Maps

Tube Intersection Number	Figure Number	Exposures
13-16-1-1	D-1	13-16 (NaOH Precracking) & 13-18 (NaOH Reference)
13-16-1-2	D-2	13-16 (NaOH Precracking) & 13-18 (NaOH Reference)
13-16-1-3	D-3	13-16 (NaOH Precracking) & 13-18 (NaOH Reference)
13-16-2-2	D-4	13-16 (NaOH Precracking)
13-16-2-3	D-5	13-16 (NaOH Precracking)
13-16-3-1	D-6	13-16 (NaOH Precracking)
13-16-3-2	D-7	13-16 (NaOH Precracking)
13-16-3-3	D-8	13-16 (NaOH Precracking)
13-16-4-1	D-9	13-16 (NaOH Precracking)
13-16-4-2	D-10	13-16 (NaOH Precracking)
13-16-4-3	D-11	13-16 (NaOH Precracking)
13-17-1-2	D-12	13-17 (NaOH Reference)
13-17-1-3	D-13	13-17 (NaOH Reference)
13-17-2-1	D-14	13-17 (NaOH Reference)
13-17-2-2	D-15	13-17 (NaOH Reference)
13-17-2-3	D-16	13-17 (NaOH Reference)
13-17-3-1	D-17	13-17 (NaOH Reference)
13-17-3-2	D-18	13-17 (NaOH Reference)
13-17-4-1	D-19	13-17 (NaOH Reference)
13-17-4-3	D-20	13-17 (NaOH Reference)
13-18-2-2	D-21	ENSA E7-C, D, E (Precracking) & 13-18 (NaOH Reference)
13-18-3-1	D-22	13-18 (NaOH Reference)
13-18-3-2	D-23	13-18 (NaOH Reference)
13-18-3-3	D-24	13-18 (NaOH Reference)
13-18-4-1	D-25	ENSA E2-A (Precracking) & 13-18 (NaOH Reference)
13-18-4-2	D-26	13-18 (NaOH Reference)
13-18-4-3	D-27	13-18 (NaOH Reference)

Table D-1 (Continued)
List of Tube Intersections with Surface Replication Maps

Tube Intersection Number	Figure Number	Exposures
14-16-1-1	D-28	14-16 (NaOH Precracking) & 14-17-1, 14-17-2, 14-17-3 (Boric Acid)
14-16-3-2	D-29	14-16 (NaOH Precracking) & 16-16-1, 16-16-2 (TiO_2 + $NaAlO_2$)
14-16-3-3	D-30	14-16 (NaOH Precracking) & 16-16-1, 16-16-2 (TiO_2 + $NaAlO_2$)
14-17-3-2	D-31	ENSA E9-B (Precracking) & 14-17-2, 14-17-3 (Boric Acid)
14-17-3-3	D-32	ENSA E9-C (Precracking) & 14-17-2, 14-17-3 (Boric Acid)
15-15-1-1b	D-33	15-15-1, 15-15-2 (Cerium Acetate)
15-15-1-2b	D-34	15-15-1 (Cerium Acetate)
15-15-2-2	D-35	15-15 (NaOH Precracking) & 15-15-1, 15-15-2 (Cerium Acetate)
15-15-2-3b	D-36	15-15-1, 15-15-2 (Cerium Acetate)
15-15-3-2	D-37	15-15 (NaOH Precracking) & 15-15-1, 15-15-2 (Cerium Acetate)
15-15-3-3	D-38	15-15 (NaOH Precracking) & 15-15-1, 15-15-2 (Cerium Acetate)
15-15-4-2	D-39	15-15 (NaOH Precracking) & 15-15-1, 15-15-2 (Cerium Acetate)
15-15-4-3b	D-40	15-15-1, 15-15-2 (Cerium Acetate)
16-14-1-1	D-41	16-14 (NaOH Precracking) & 14-17-1, 14-17-2, 14-17-3 (Boric Acid)
16-14-2-2	D-42	16-14 (NaOH Precracking)
16-14-4-1	D-43	16-14 (NaOH Precracking)
16-14-4-2	D-44	16-14 (NaOH Precracking)
16-14-4-3	D-45	16-14 (NaOH Precracking)
16-15-2-2	D-46	16-15 (TiO_2)
16-15-2-3	D-47	16-15 (TiO_2)
16-16-1-1	D-48	ENSA E12-A (Precracking) & 16-16-1, 16-16-2 (TiO_2 + $NaAlO_2$)
16-16-2-3	D-49	ENSA E5-D (Precracking) & 16-16-1, 16-16-2 (TiO_2 + $NaAlO_2$)

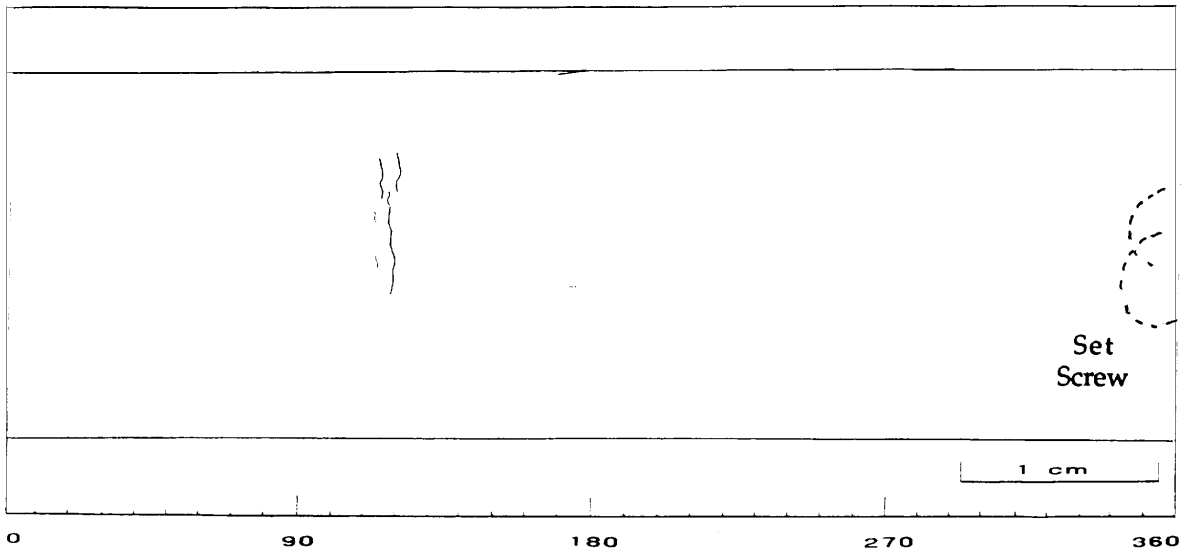

Figure D-1
Exterior Surface Replication Map of Intersection 13-16-1-1 (After bulging)

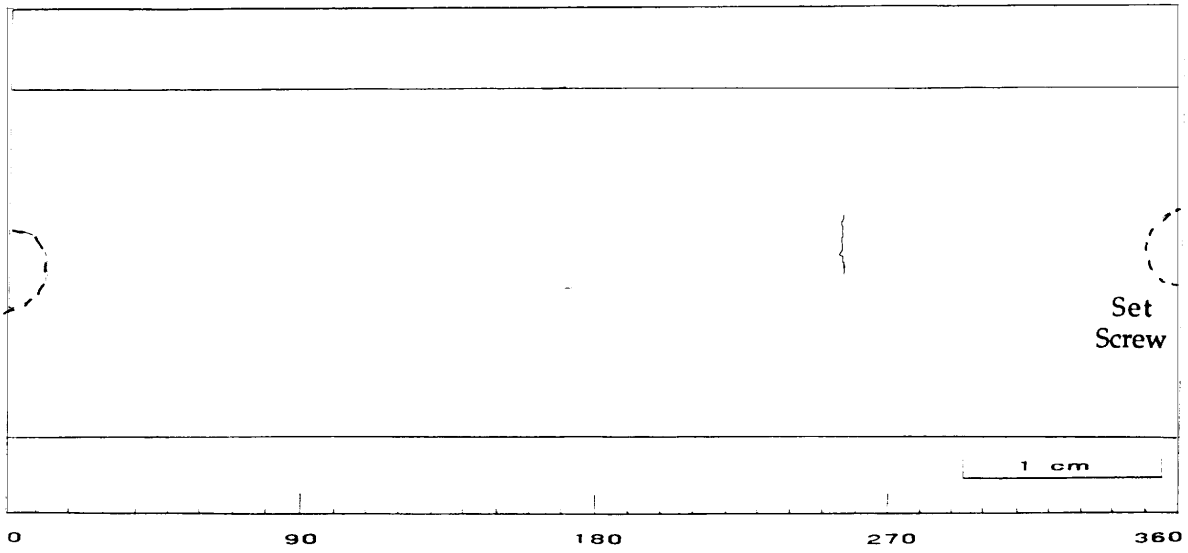

Figure D-2
Exterior Surface Replication Map of Intersection 13-16-1-2 (After bulging)

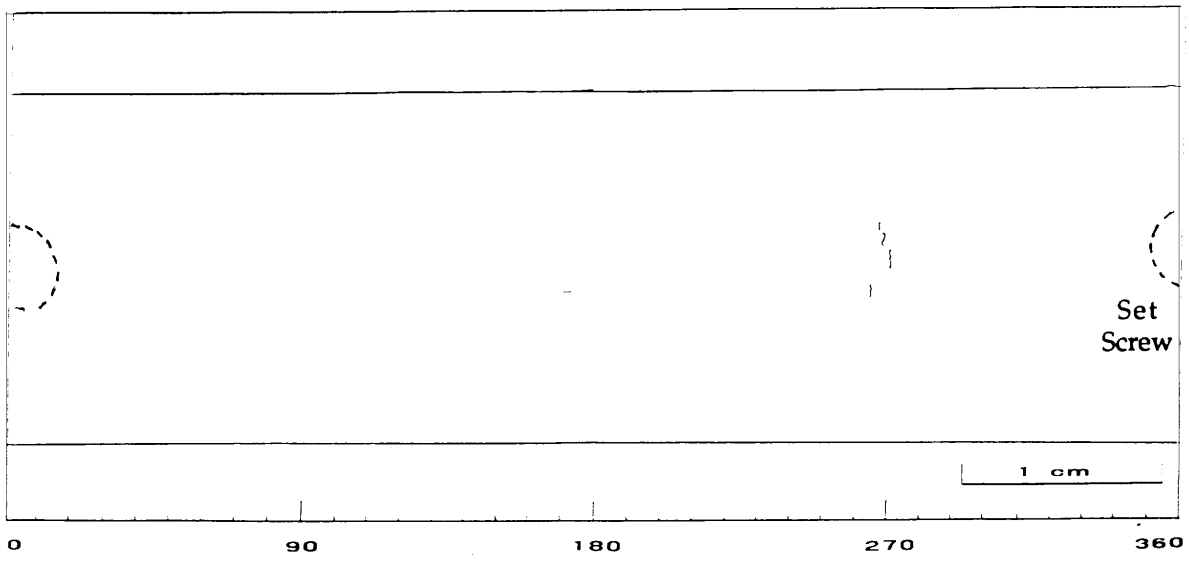

Figure D-3
Exterior Surface Replication Map of Intersection 13-16-1-3 (After bulging)

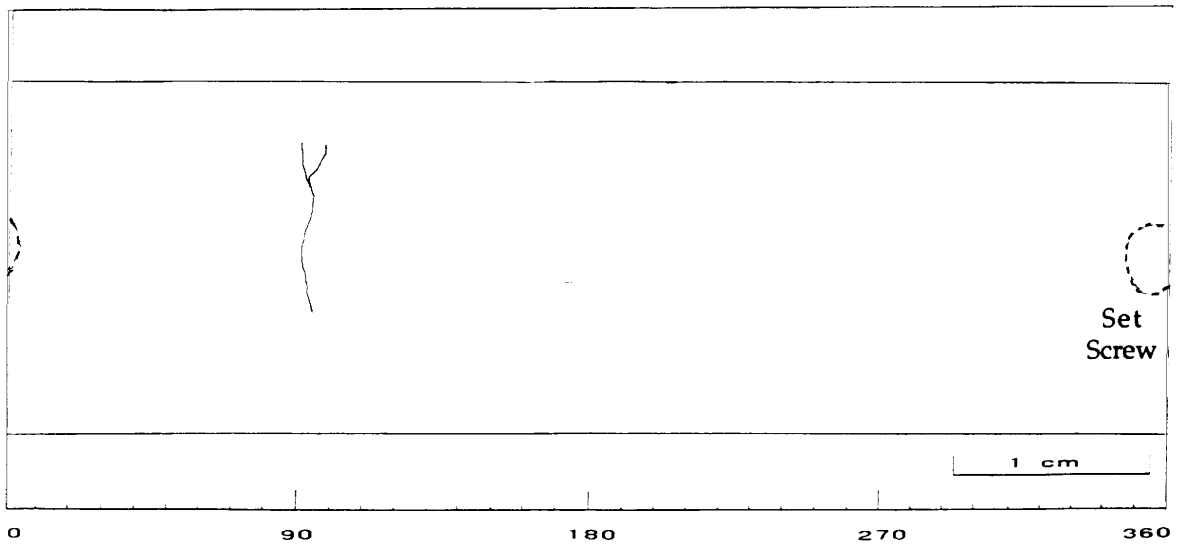

Figure D-4
Exterior Surface Replication Map of Intersection 13-16-2-2 (After bulging)

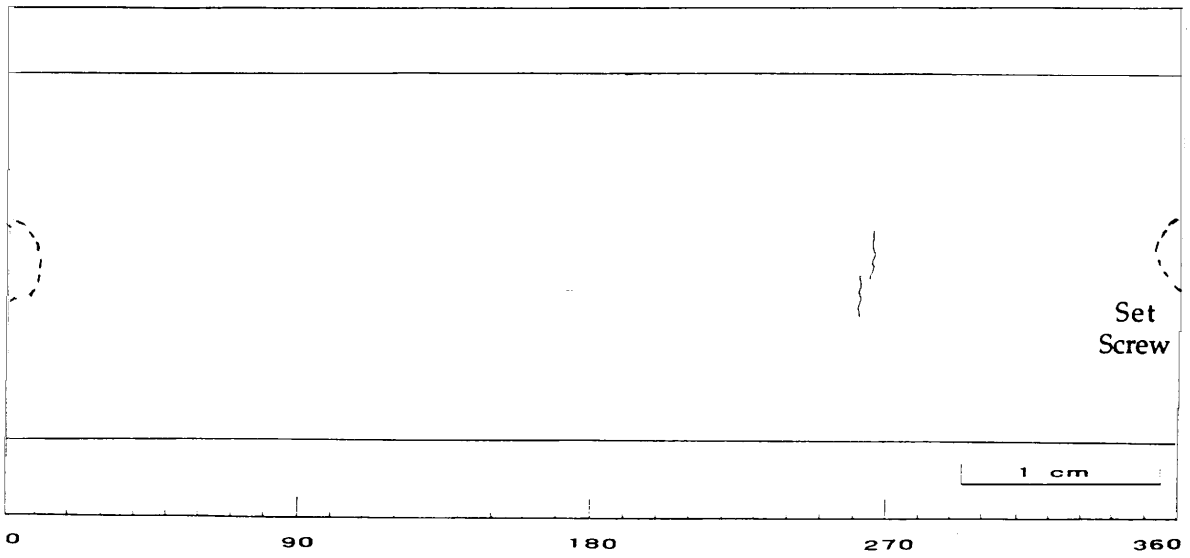

Figure D-5
Interior Surface Replication Map of Intersection 13-16-2-3 (After bulging)

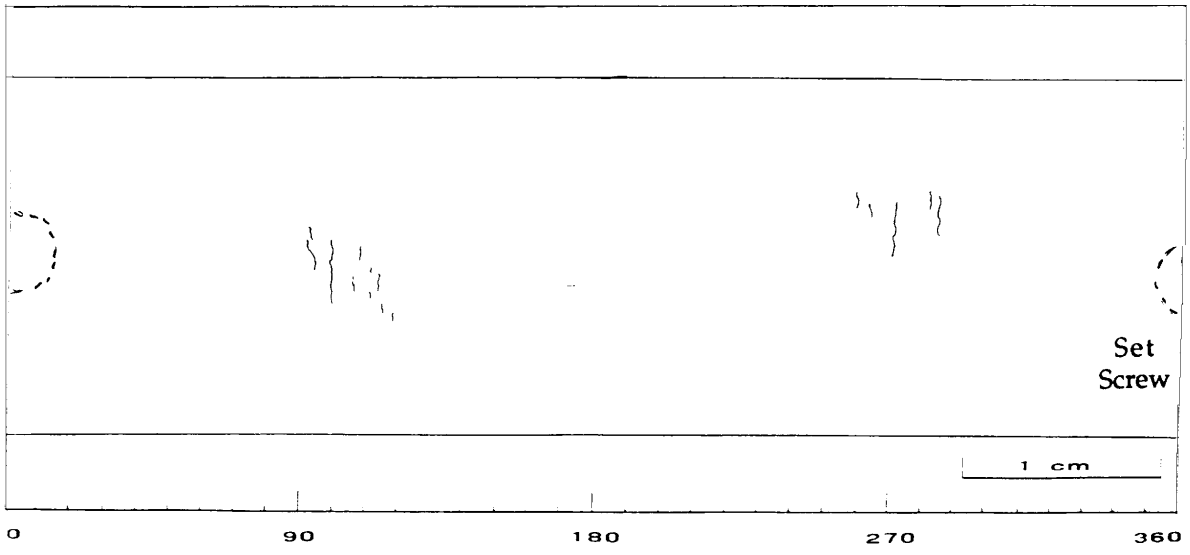

Figure D-6
Exterior Surface Replication Map of Intersection 13-16-3-1 (After bulging)

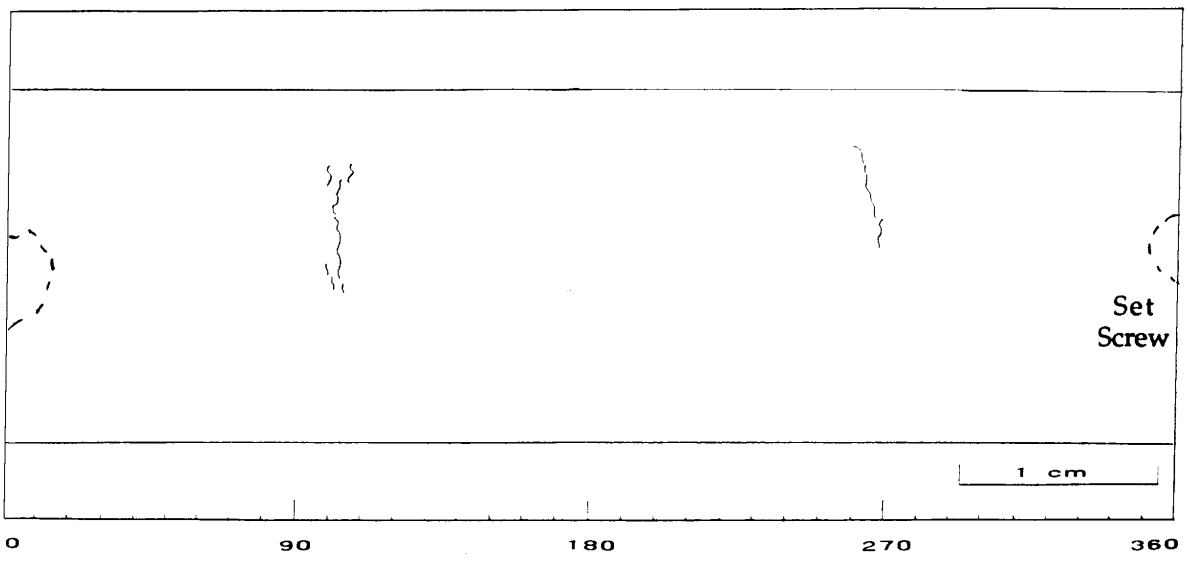

Figure D-7
Exterior Surface Replication Map of Intersection 13-16-3-2 (After bulging)

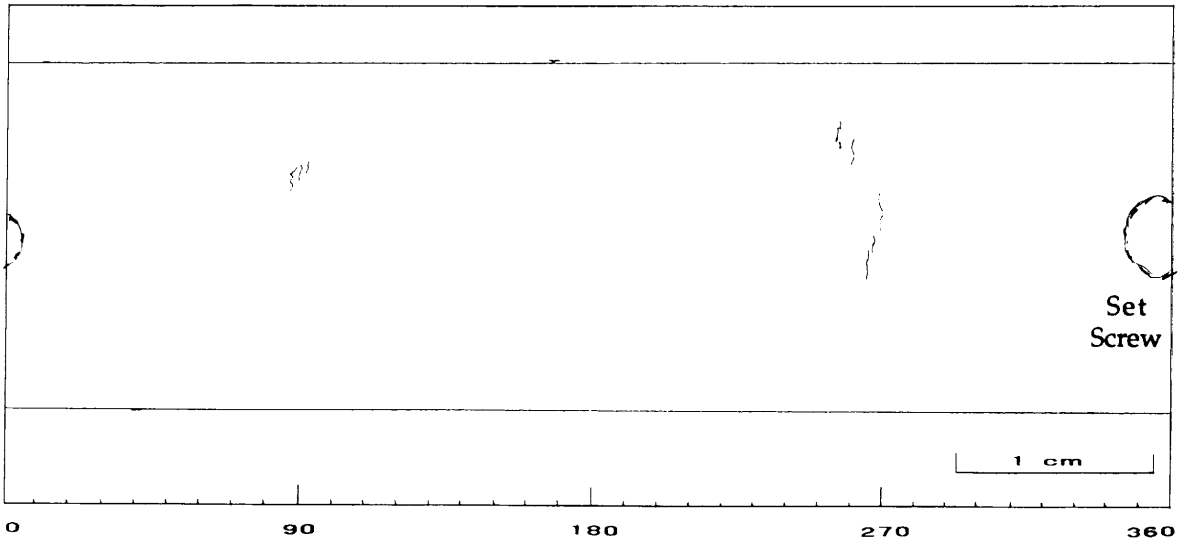

Figure D-8
Interior Surface Replication Map of Intersection 13-16-3-3 (After bulging)

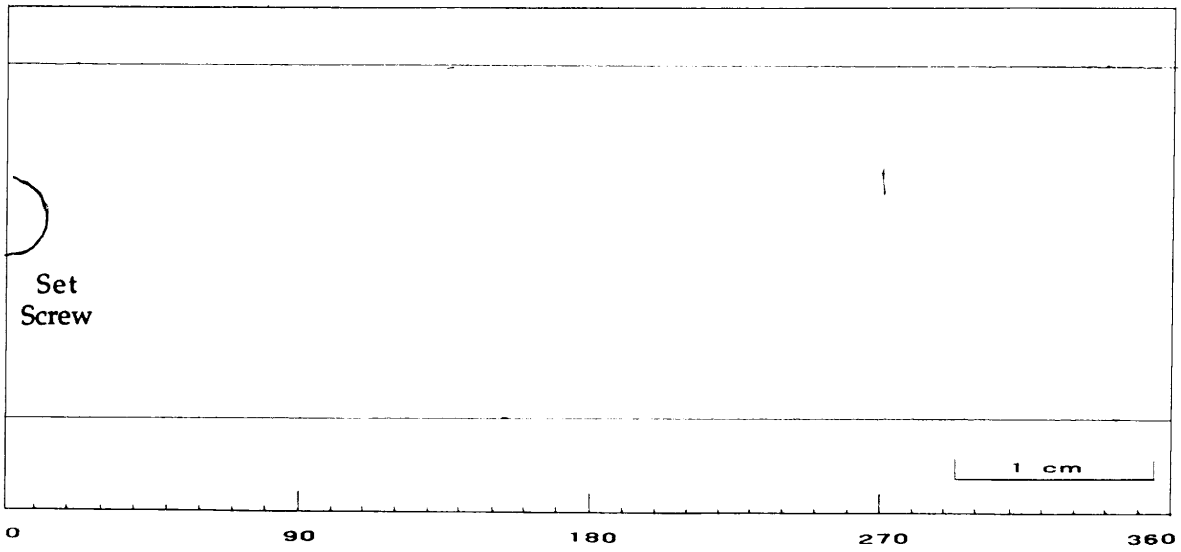

Figure D-9
Exterior Surface Replication Map of Intersection 13-16-4-1 (After bulging)

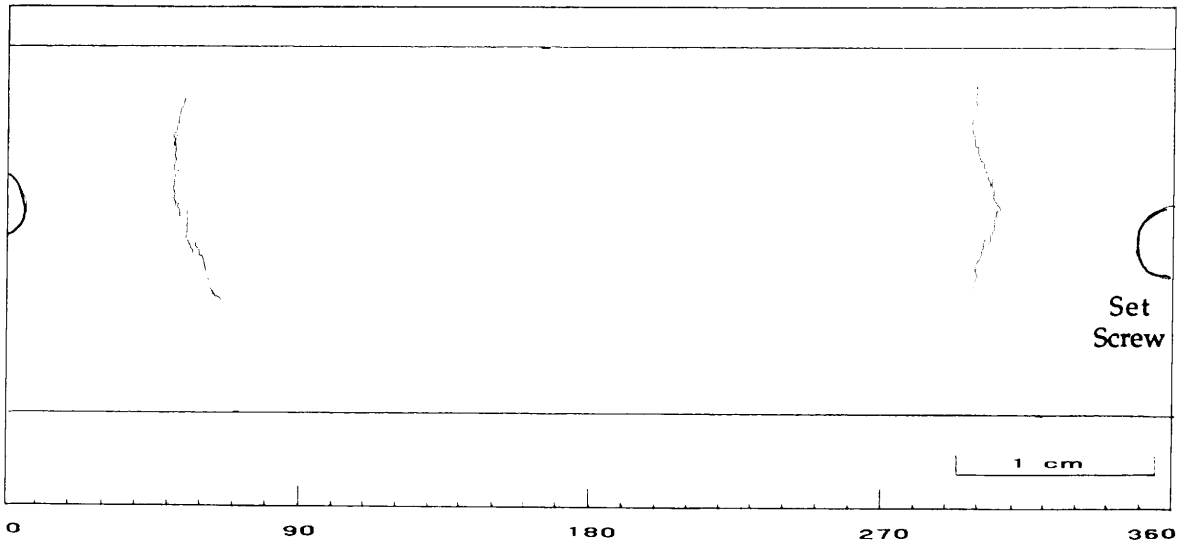

Figure D-10
Exterior Surface Replication Map of Intersection 13-16-4-2

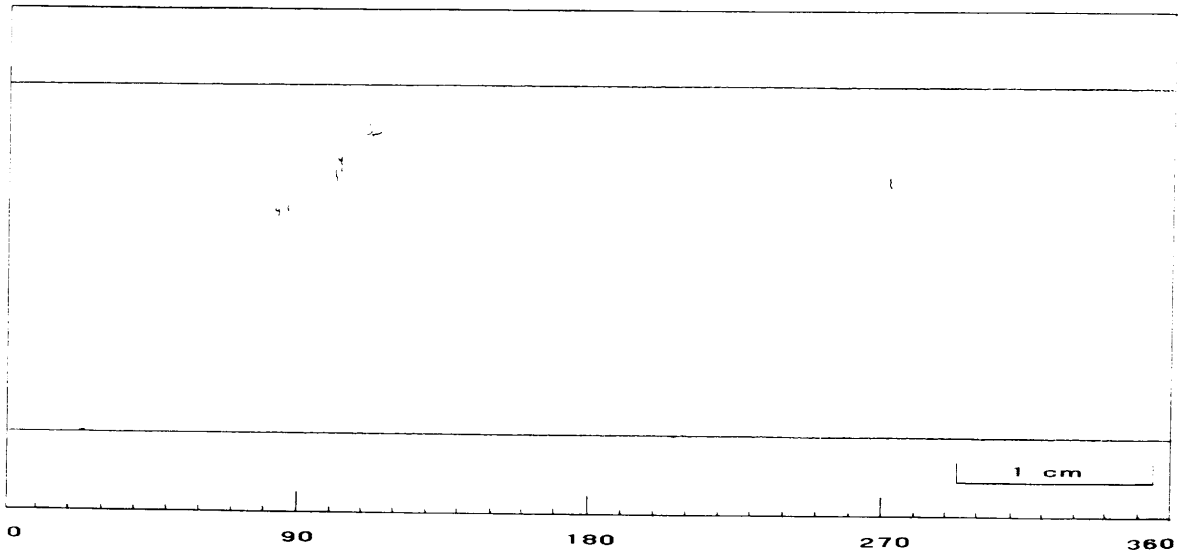

Figure D-11
Exterior Surface Replication Map of Intersection 13-16-4-3 (After bulging)

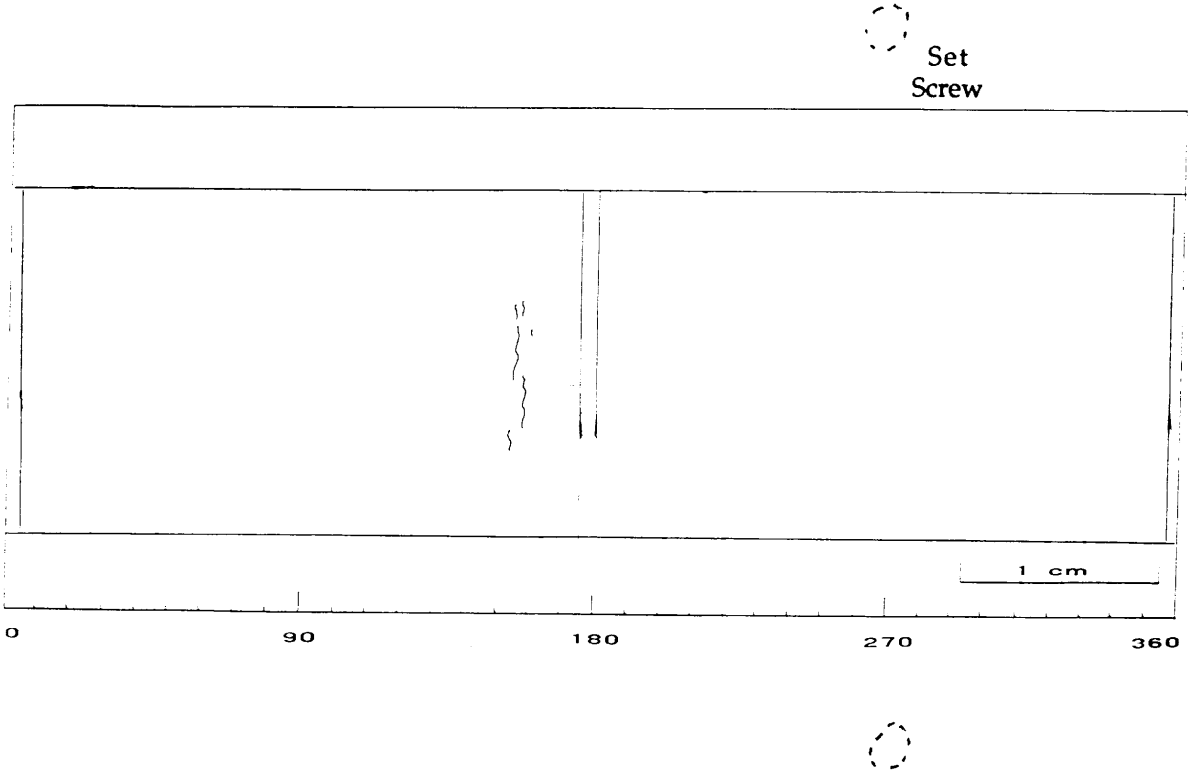

Figure D-12
Exterior Surface Replication Map of Intersection 13-17-1-2 (After bulging)

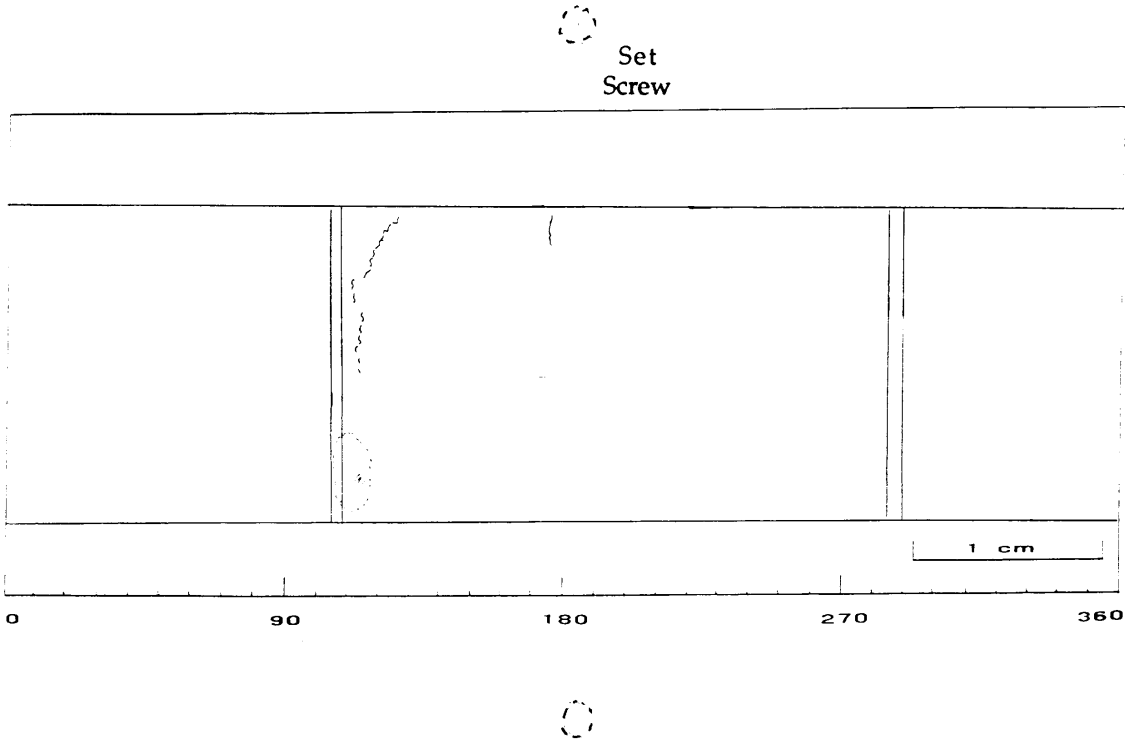

Figure D-13
Exterior Surface Replication Map of Intersection 13-17-1-3 (After bulging)

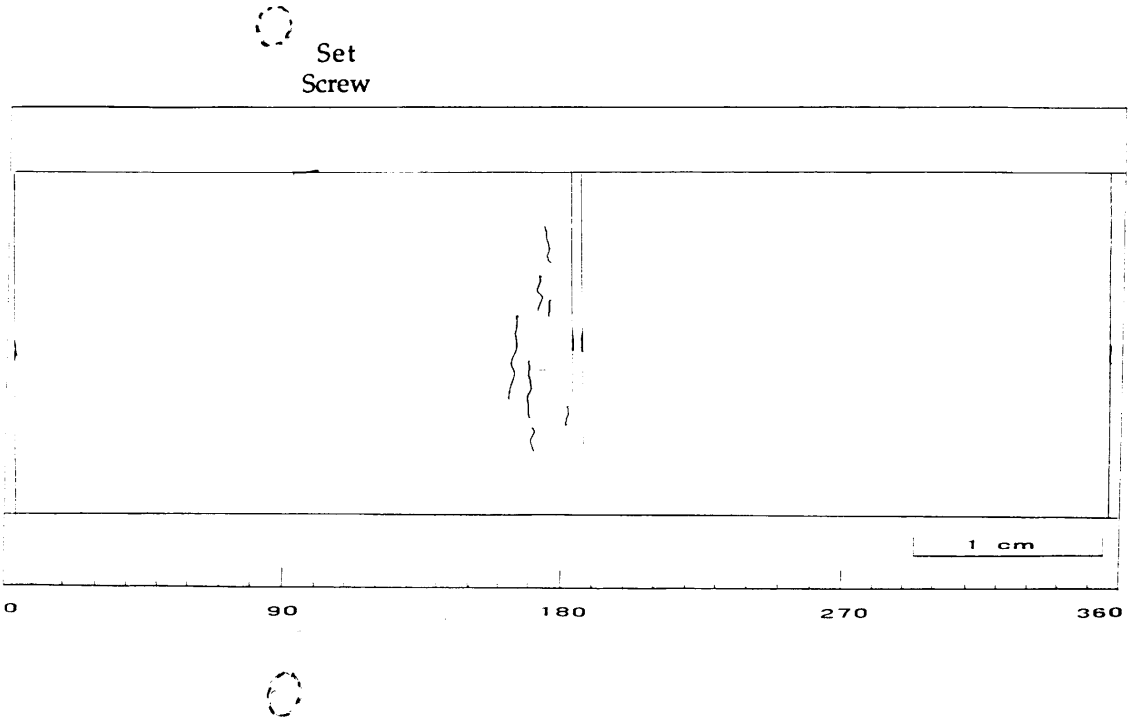

Figure D-14
Exterior Surface Replication Map of Intersection 13-17-2-1 (After bulging)

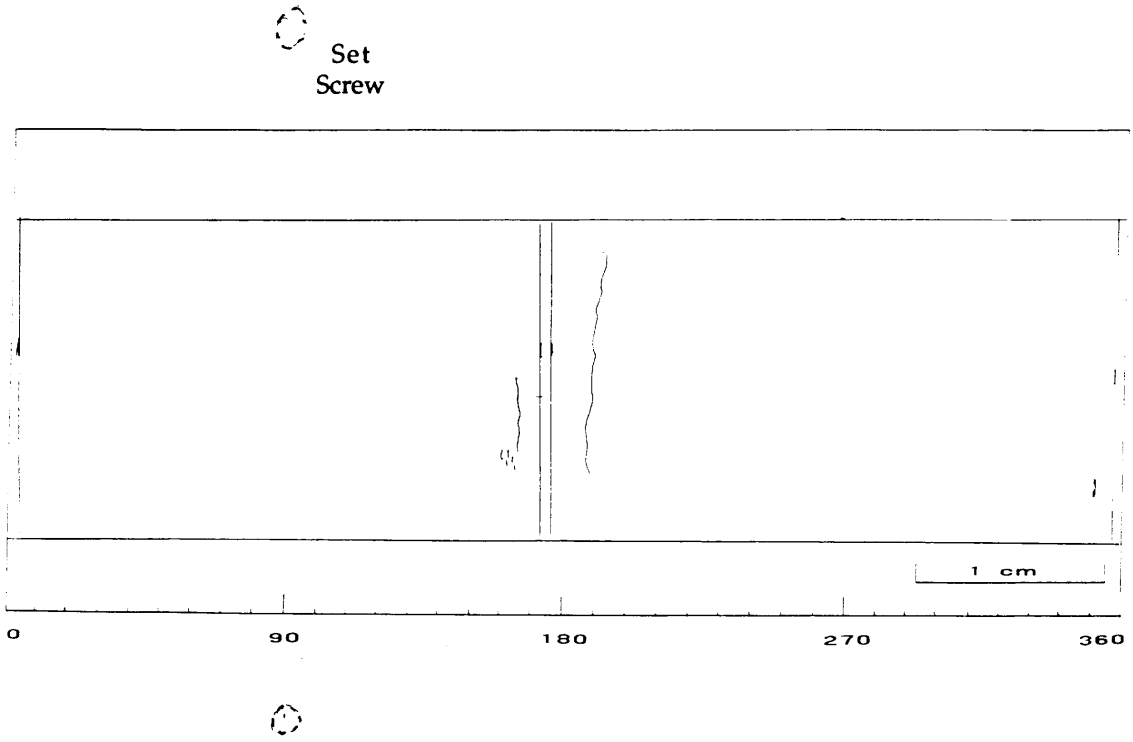

Figure D-15
Exterior Surface Replication Map of Intersection 13-17-2-2 (After bulging)

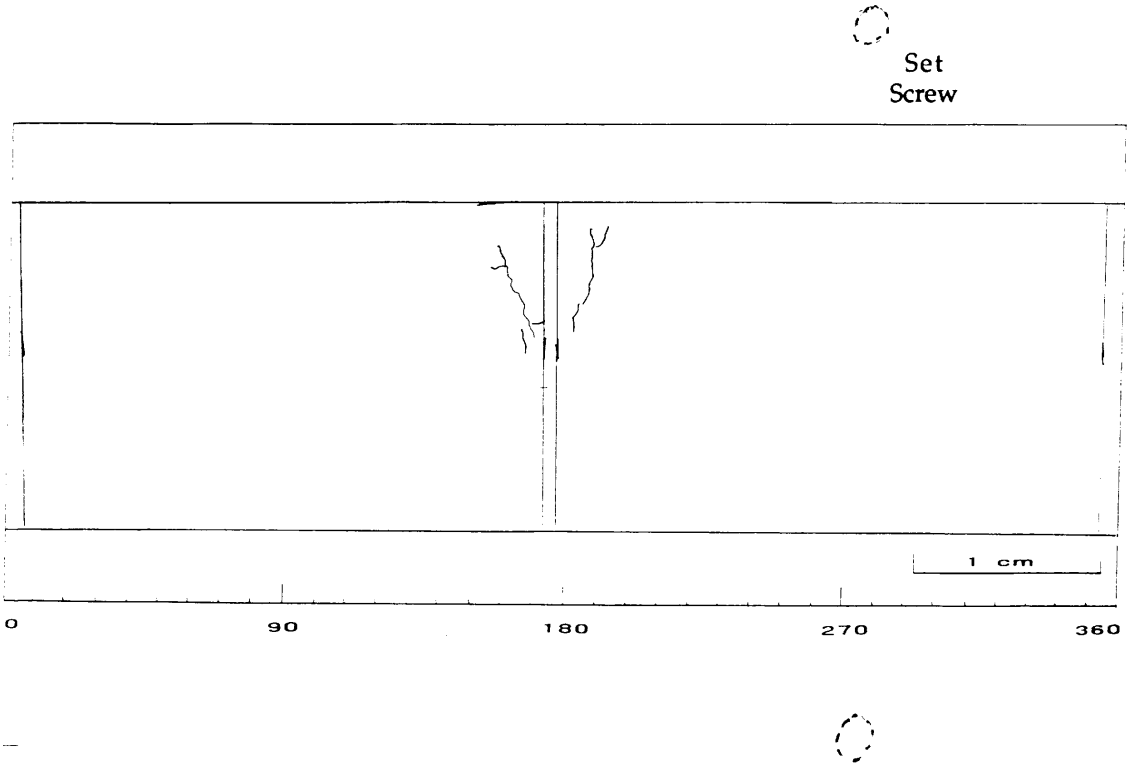

Figure D-16
Exterior Surface Replication Map of Intersection 13-17-2-3 (After bulging)

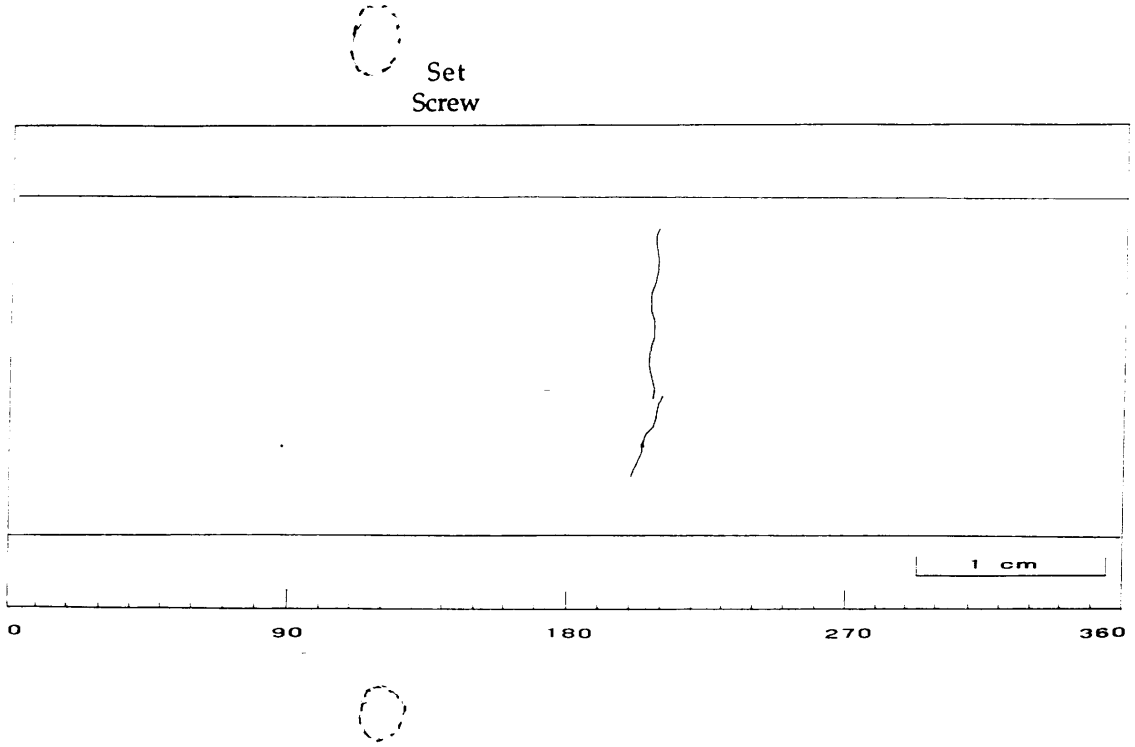

Figure D-17
Exterior Surface Replication Map of Intersection 13-17-3-1 (After bulging)

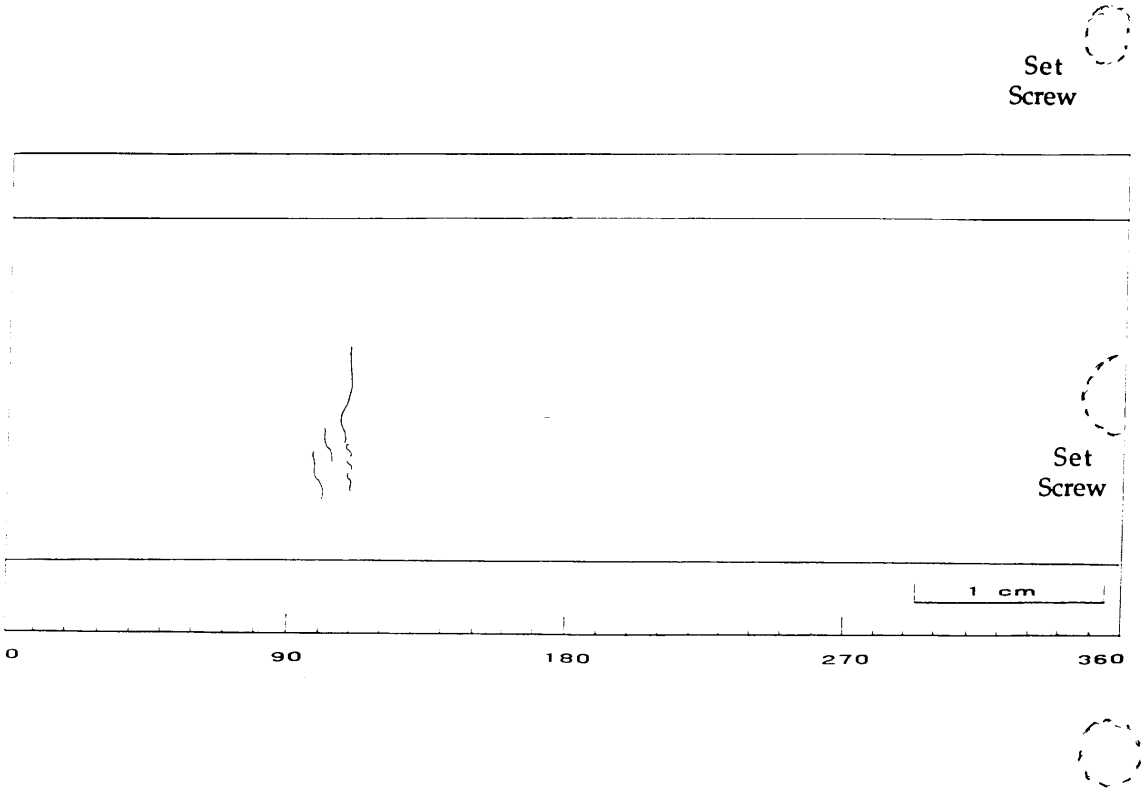

Figure D-18
Exterior Surface Replication Map of Intersection 13-17-3-2 (After bulging)

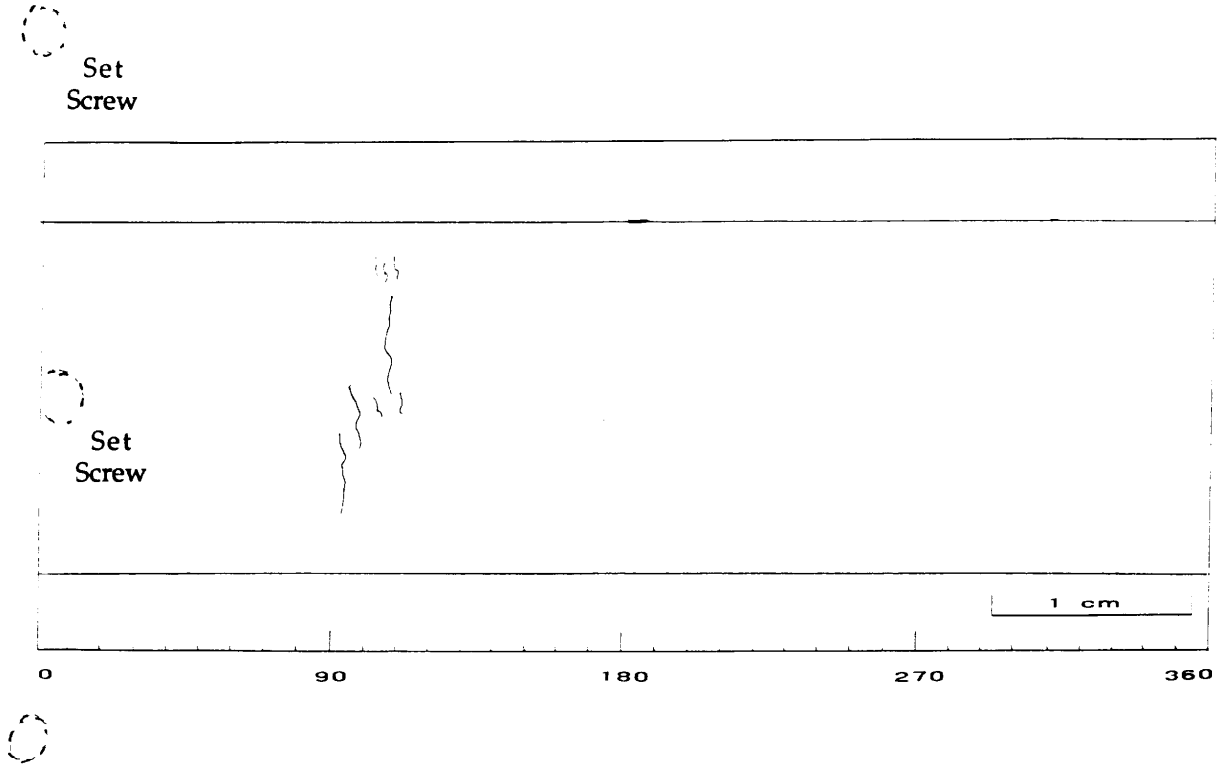

Figure D-19
Exterior Surface Replication Map of Intersection 13-17-4-1 (After bulging)

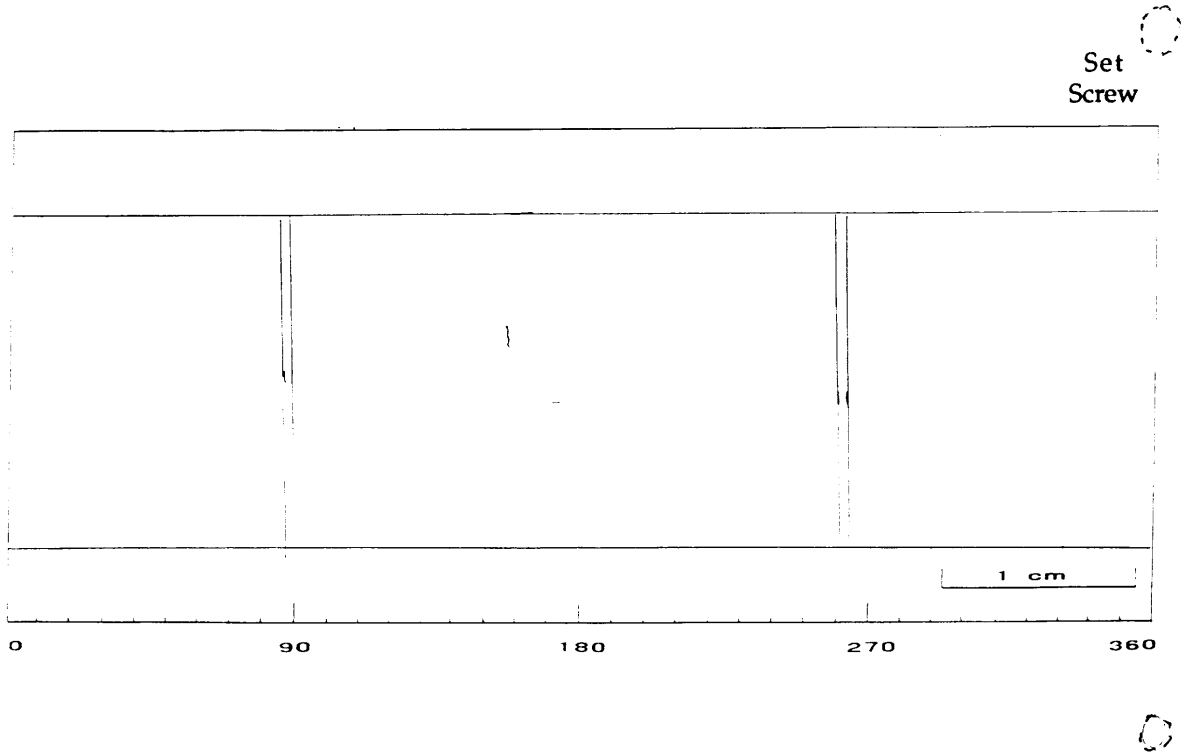

Figure D-20
Exterior Surface Replication Map of Intersection 13-17-4-3 (After bulging)

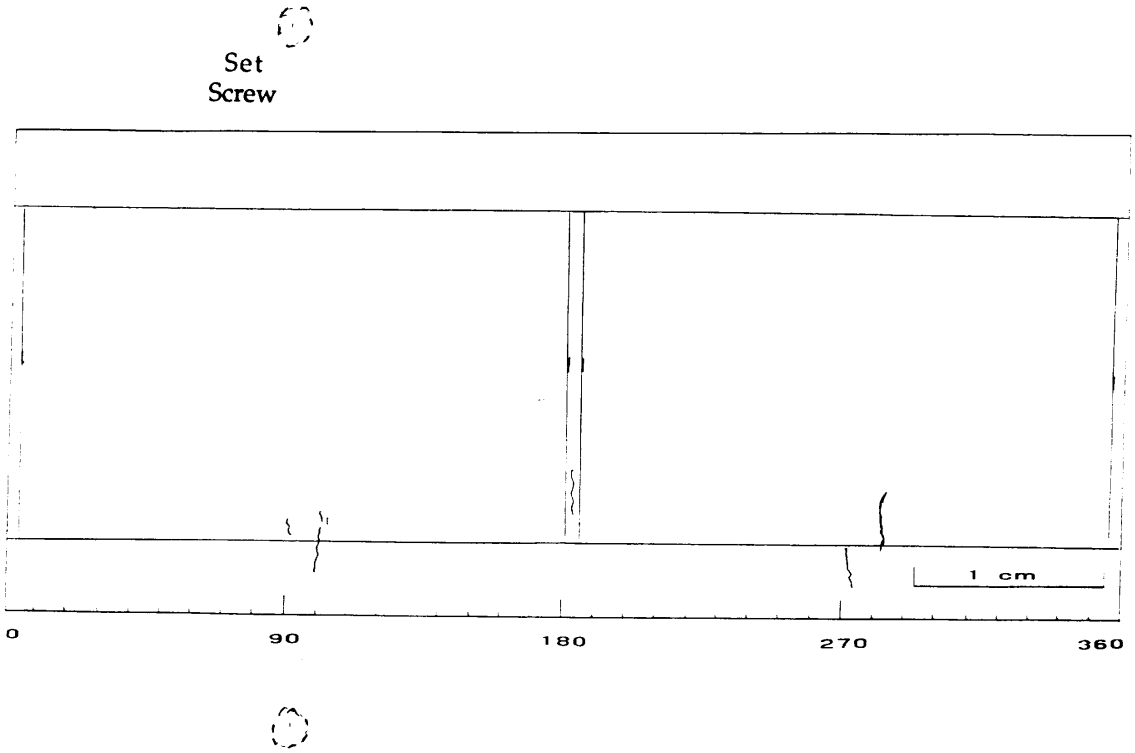

Figure D-21
Exterior Surface Replication Map of Intersection 13-18-2-2 (After bulging)

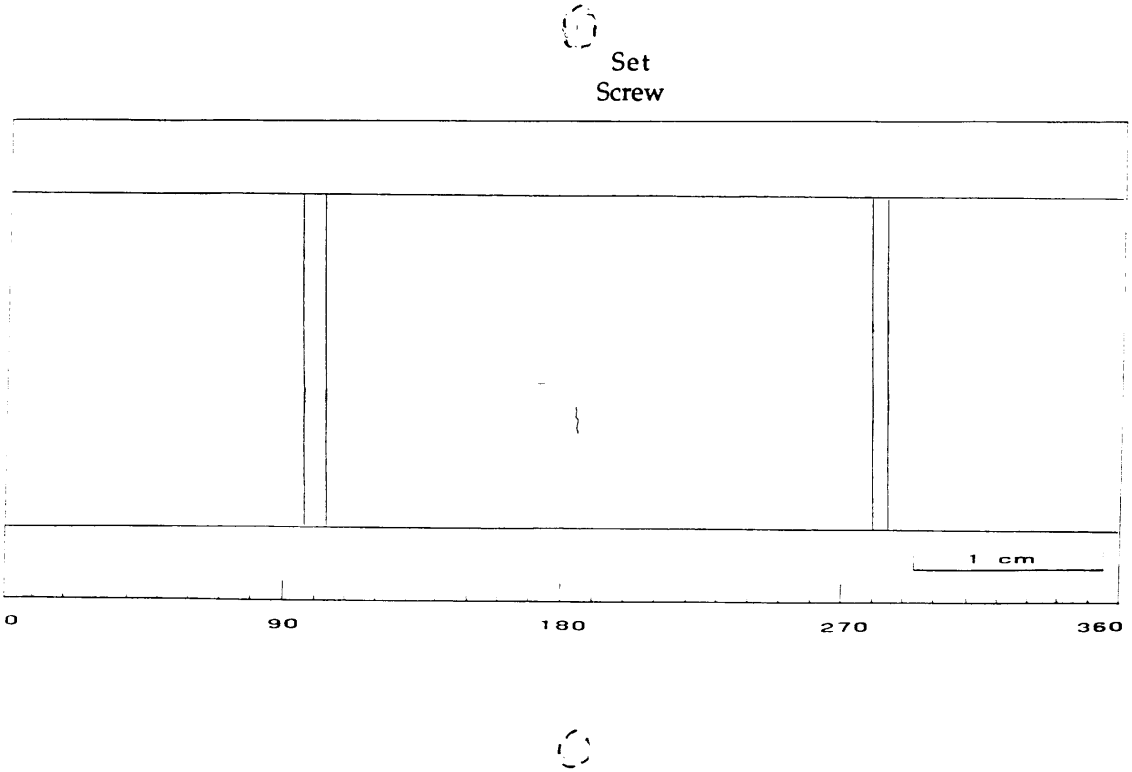

Figure D-22
Exterior Surface Replication Map of Intersection 13-18-3-1 (After bulging)

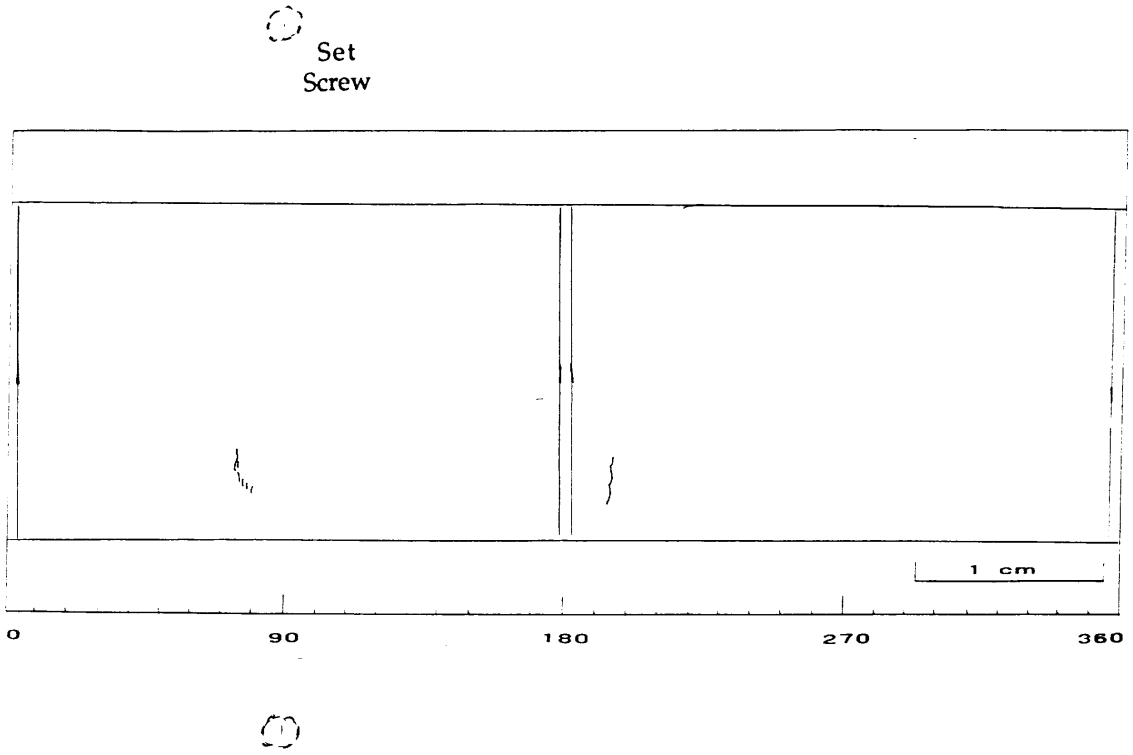

Figure D-23
Exterior Surface Replication Map of Intersection 13-18-3-2 (After bulging)

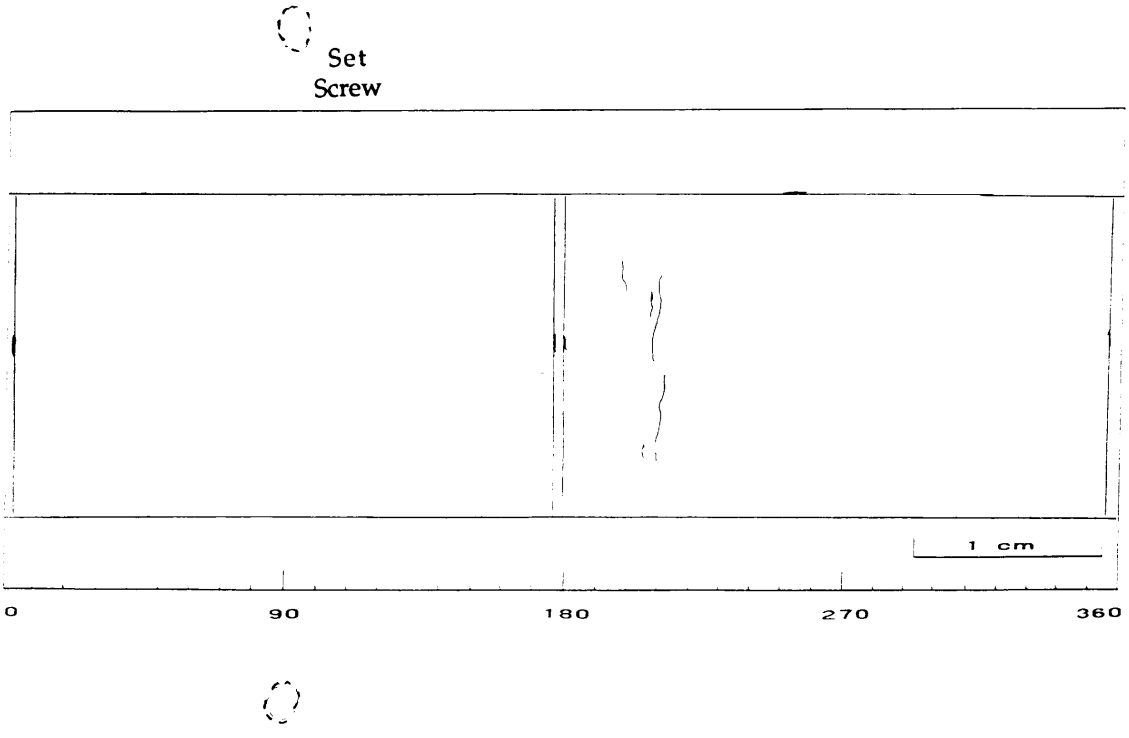

Figure D-24
Exterior Surface Replication Map of Intersection 13-18-3-3 (After bulging)

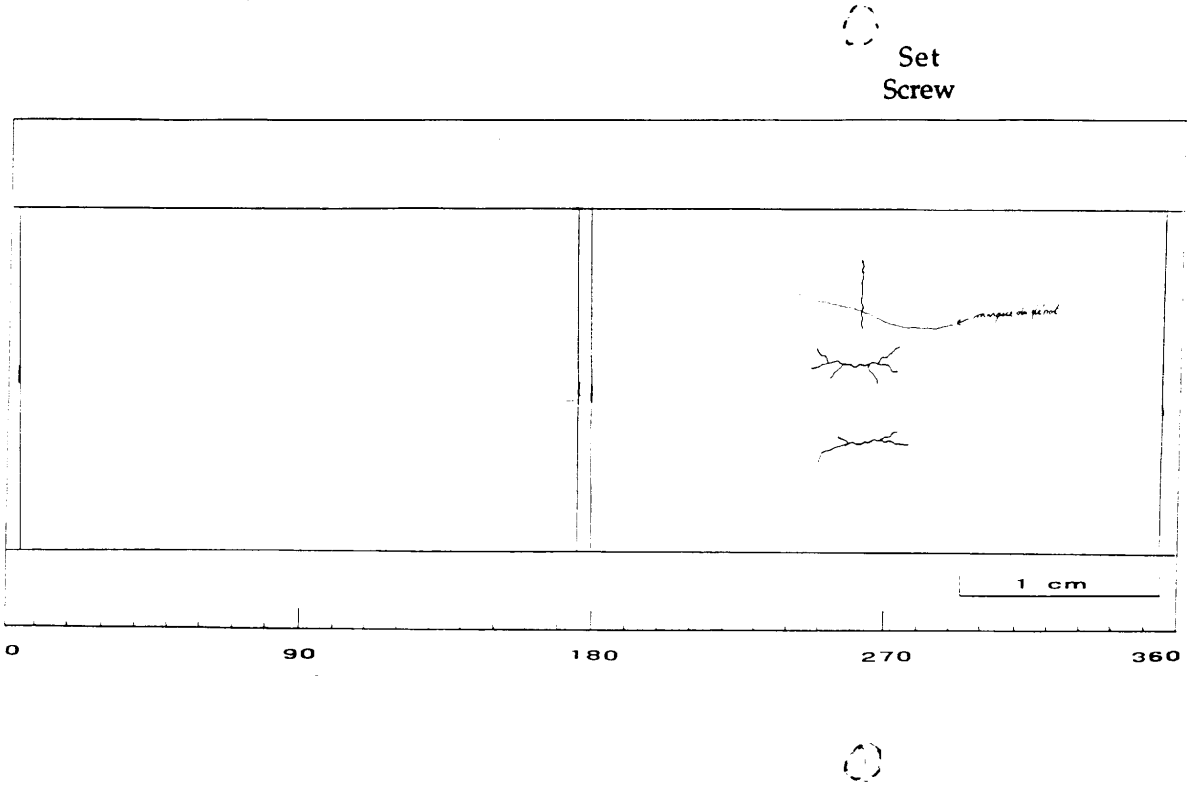

Figure D-25
Exterior Surface Replication Map of Intersection 13-18-4-1 (After bulging)

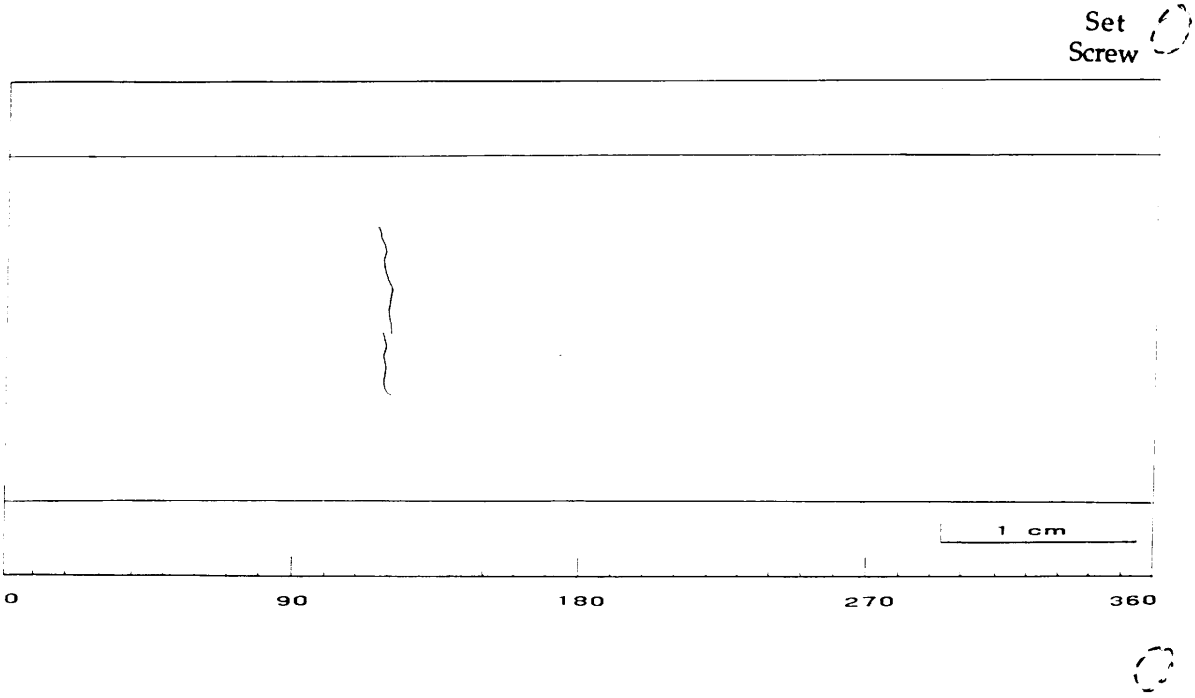

Figure D-26
Exterior Surface Replication Map of Intersection 13-18-4-2 (After bulging)

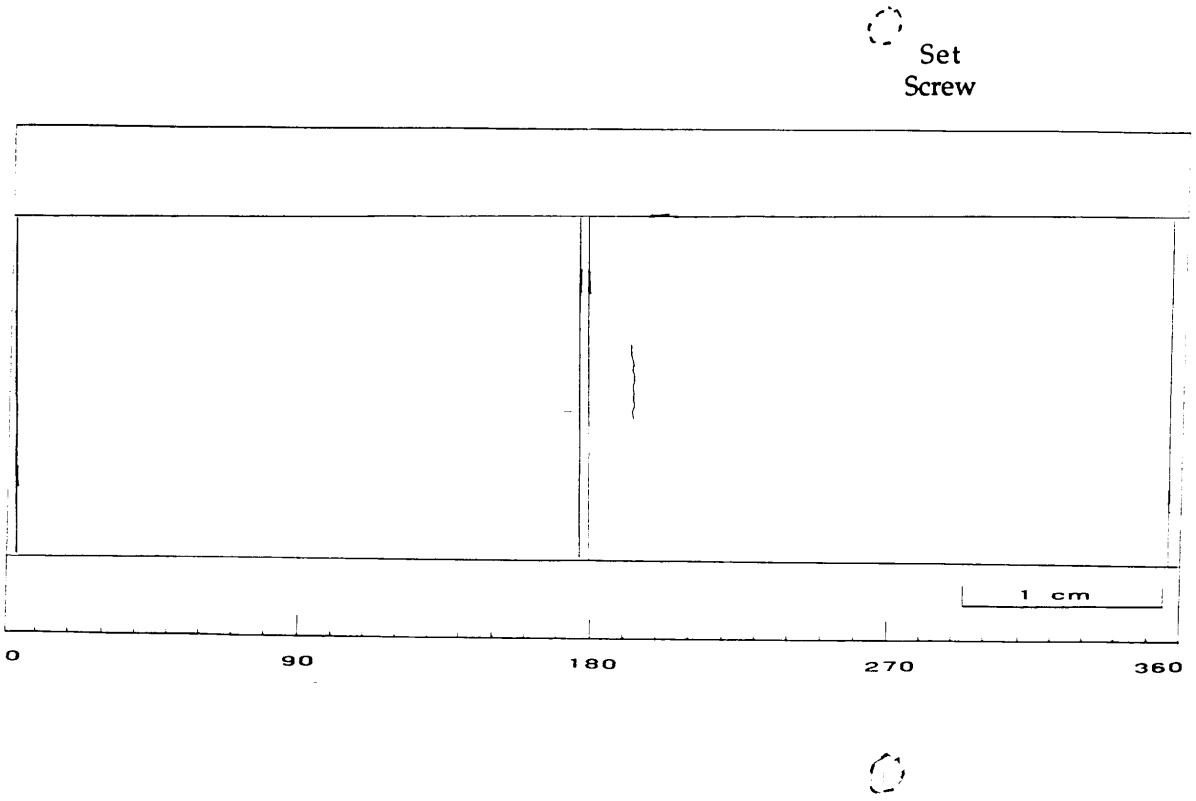

Figure D-27
Exterior Surface Replication Map of Intersection 13-18-4-3 (After bulging)

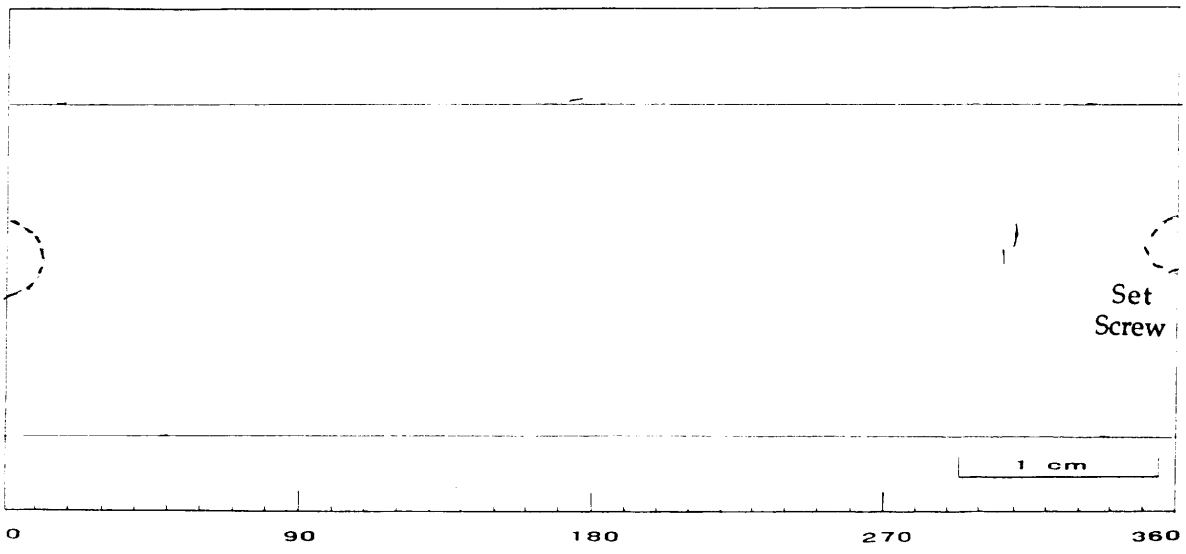

Figure D-28
Exterior Surface Replication Map of Intersection 14-16-1-1 (After bulging)

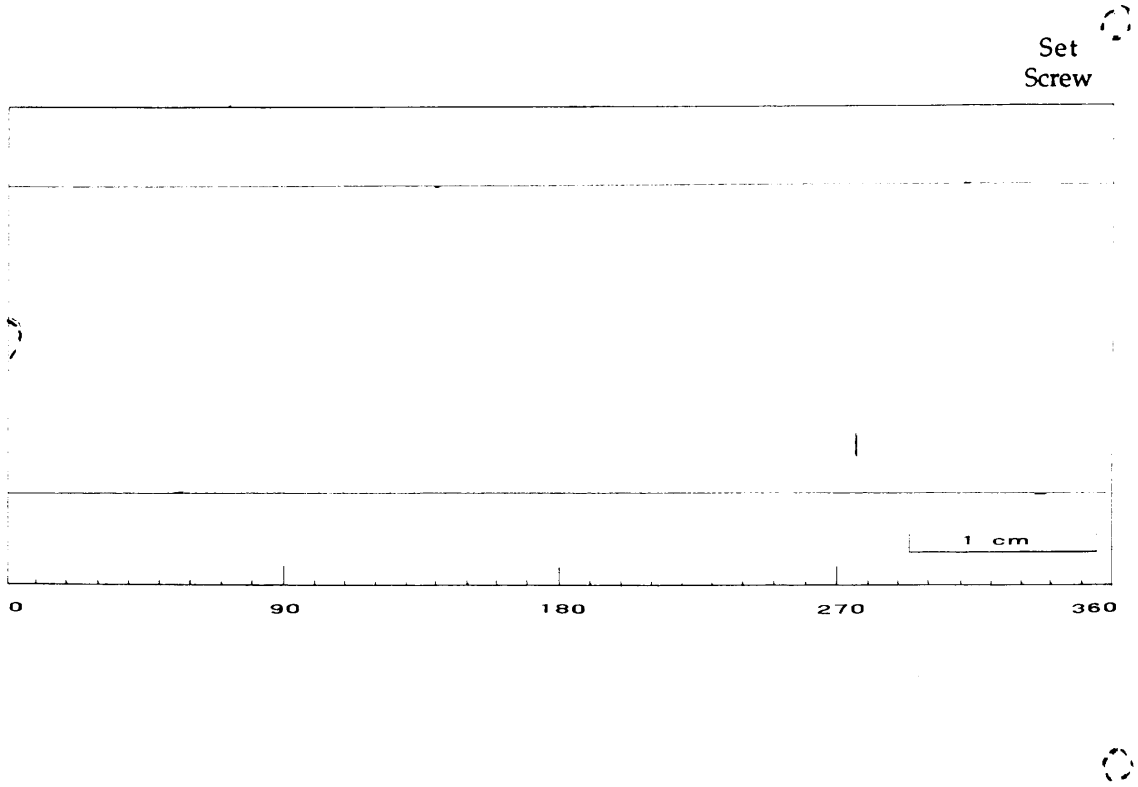

Figure D-29
Exterior Surface Replication Map of Intersection 14-16-3-2 (After bulging)

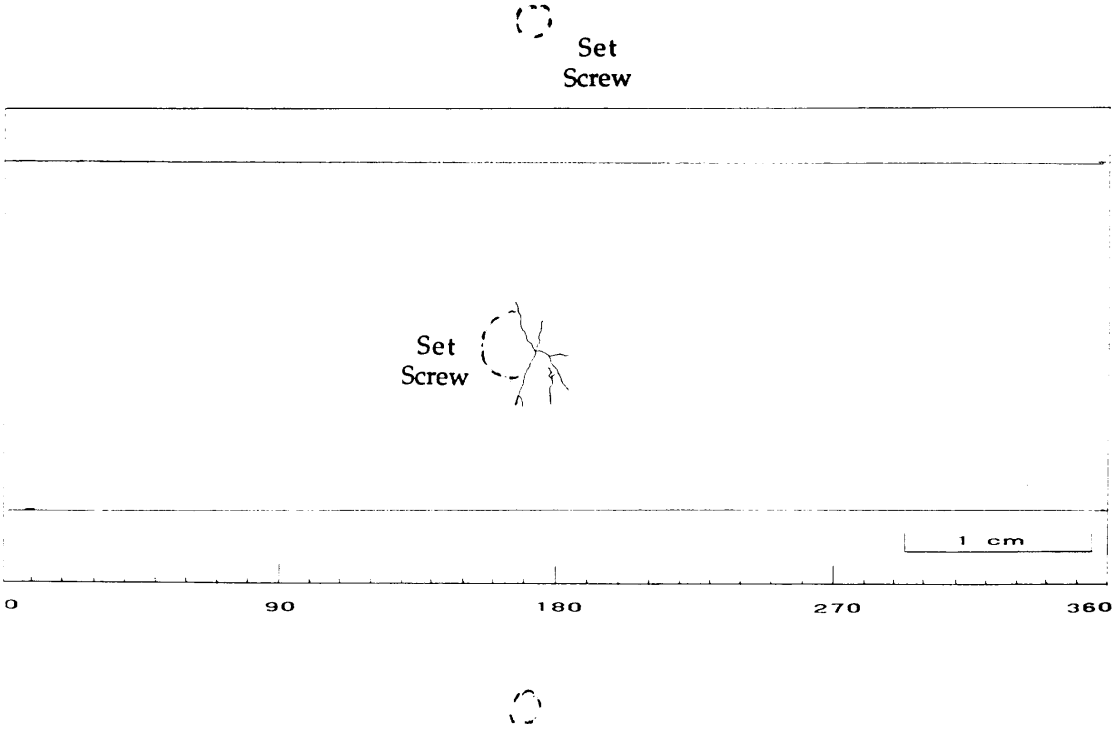

Figure D-30
Exterior Surface Replication Map of Intersection 14-16-3-3 (After bulging)

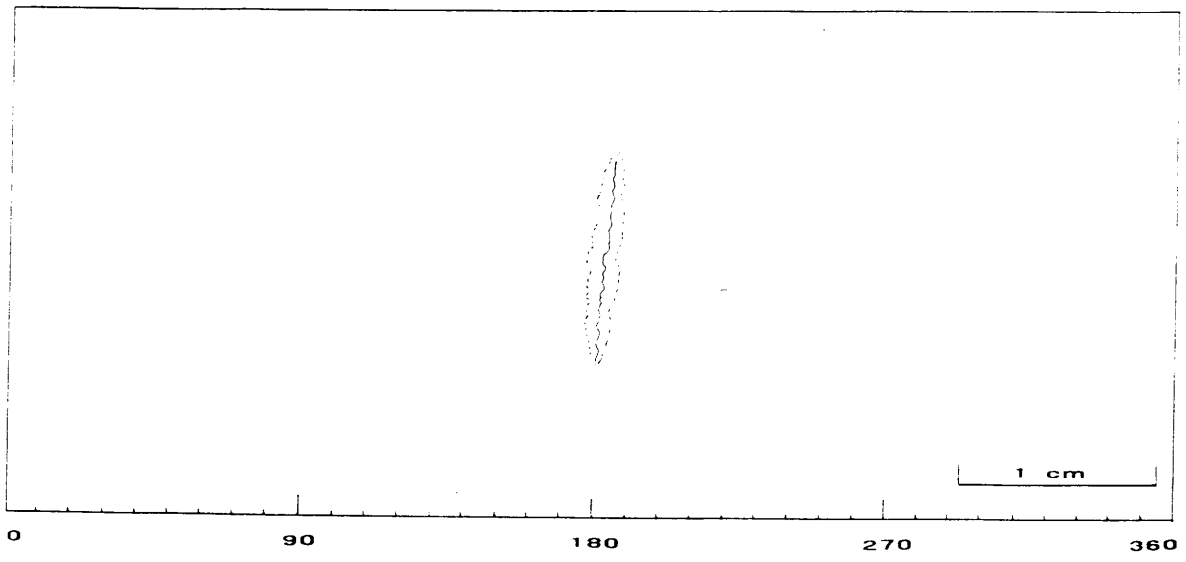

Figure D-31
Exterior Surface Replication Map of Intersection 14-17-3-2 (After bulging)

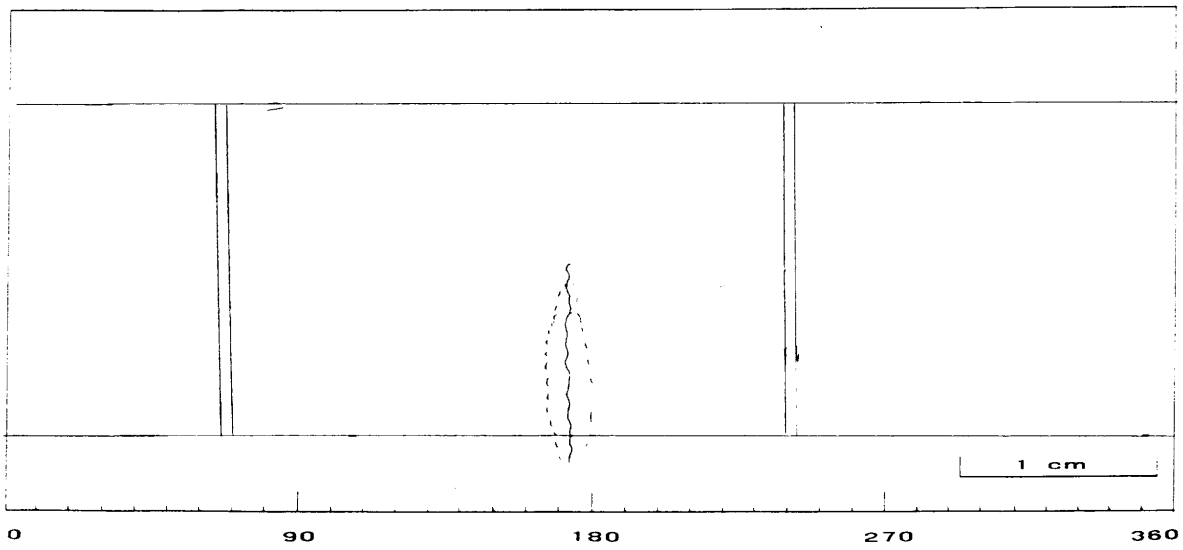

Figure D-32
Exterior Surface Replication Map of Intersection 14-17-3-3 (After bulging)

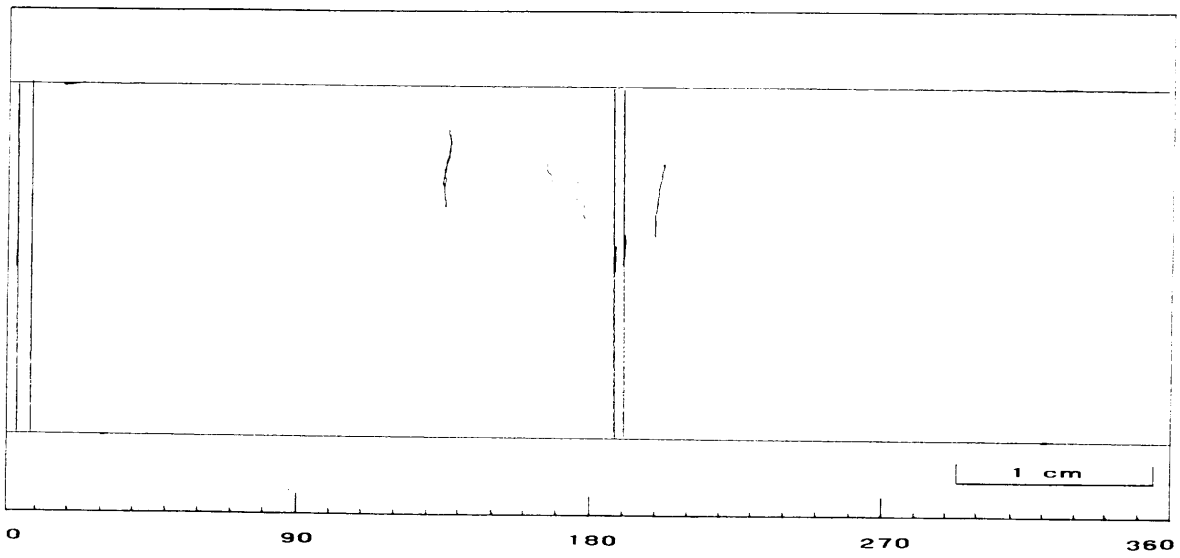

Figure D-33
Exterior Surface Replication Map of Intersection 15-15-1-1b (After bulging)

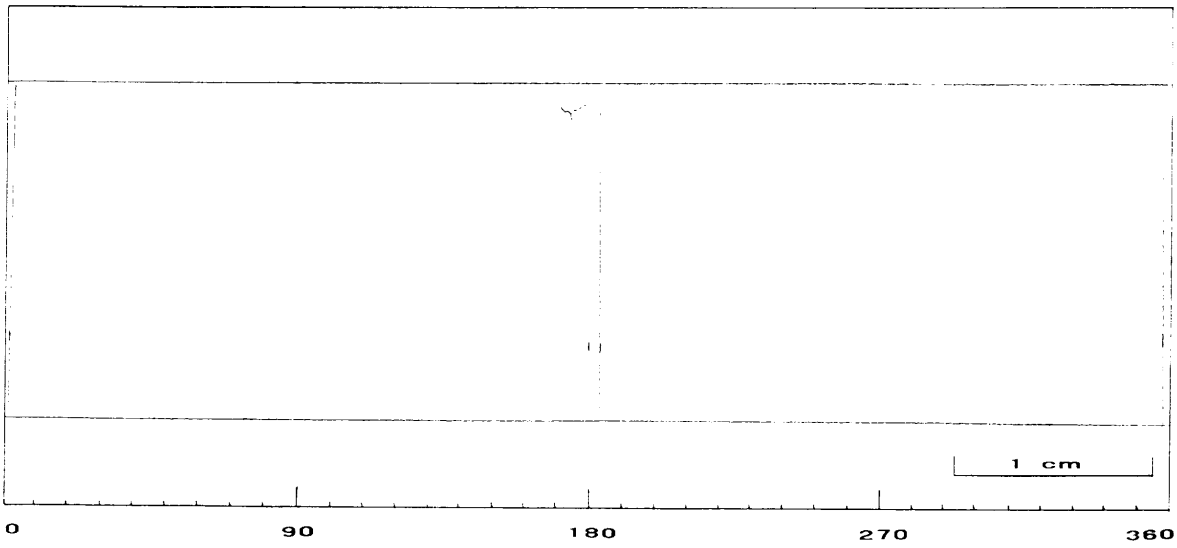

Figure D-34
Exterior Surface Replication Map of Intersection 15-15-1-2b (After bulging)

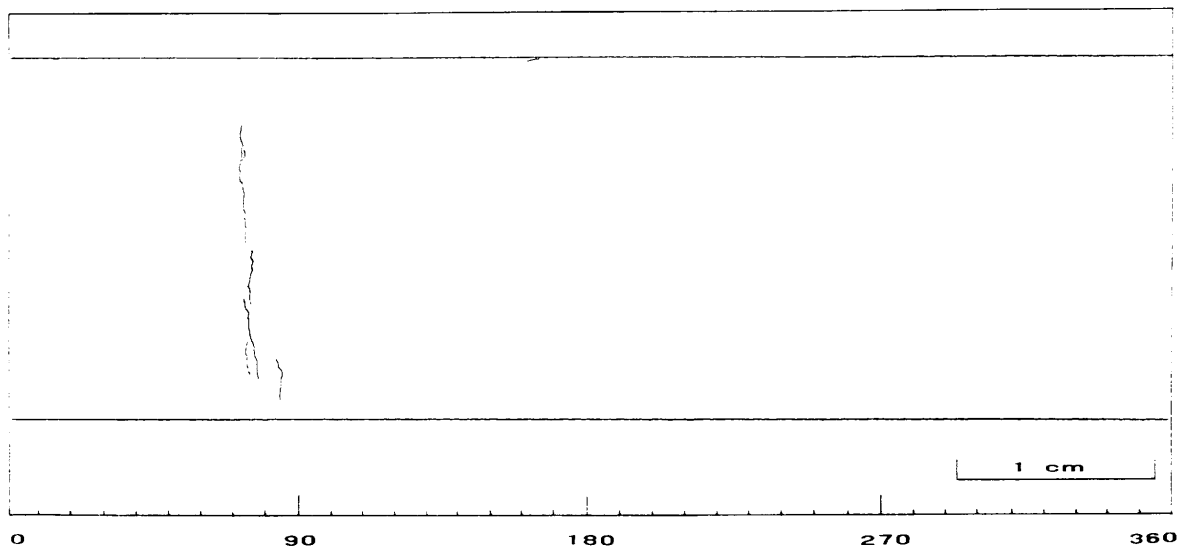

Figure D-35
Exterior Surface Replication Map of Intersection 15-15-2-2

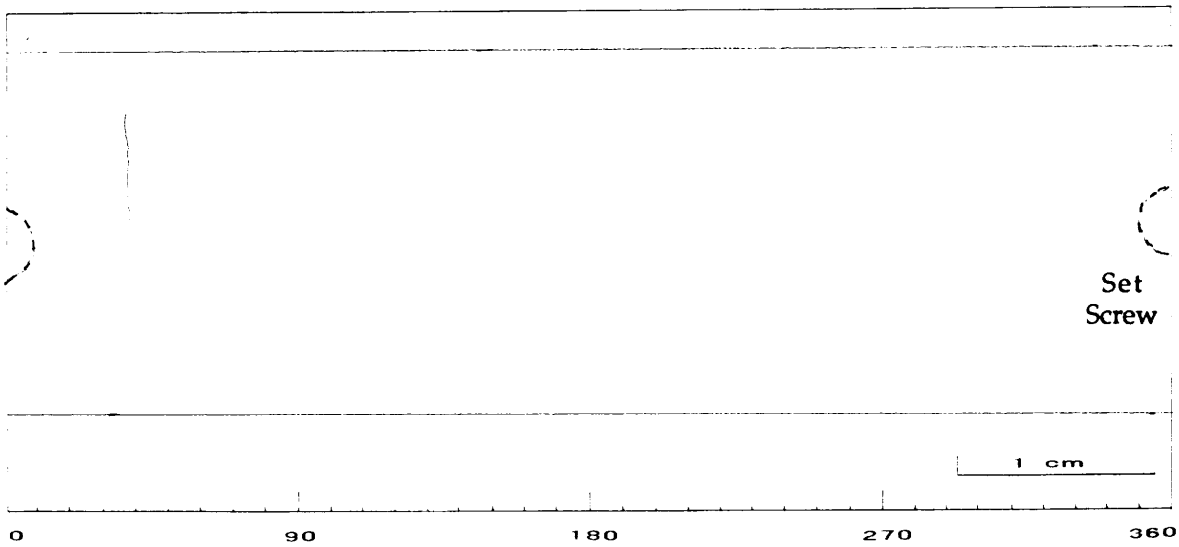

Figure D-36
Exterior Surface Replication Map of Intersection 15-15-2-3b (After bulging)

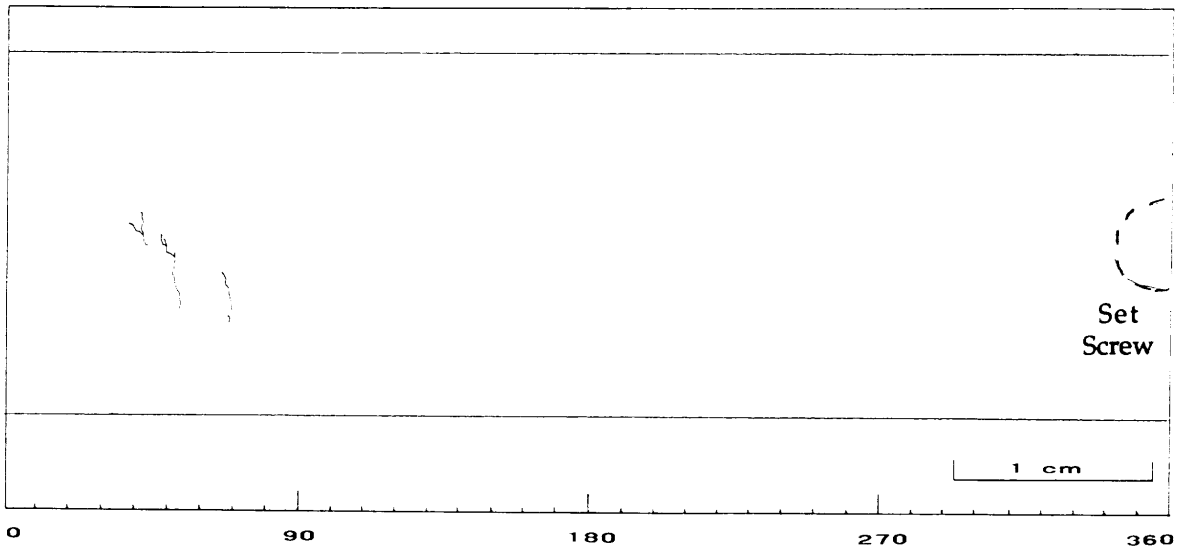

Figure D-37
Exterior Surface Replication Map of Intersection 15-15-3-2

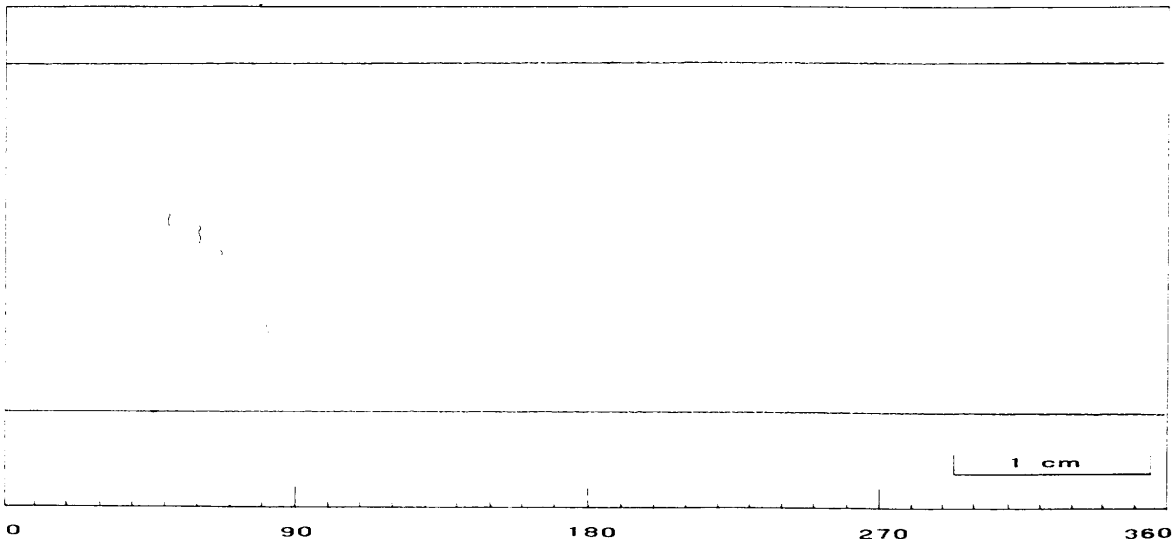

Figure D-38
Exterior Surface Replication Map of Intersection 15-15-3-3 (After bulging)

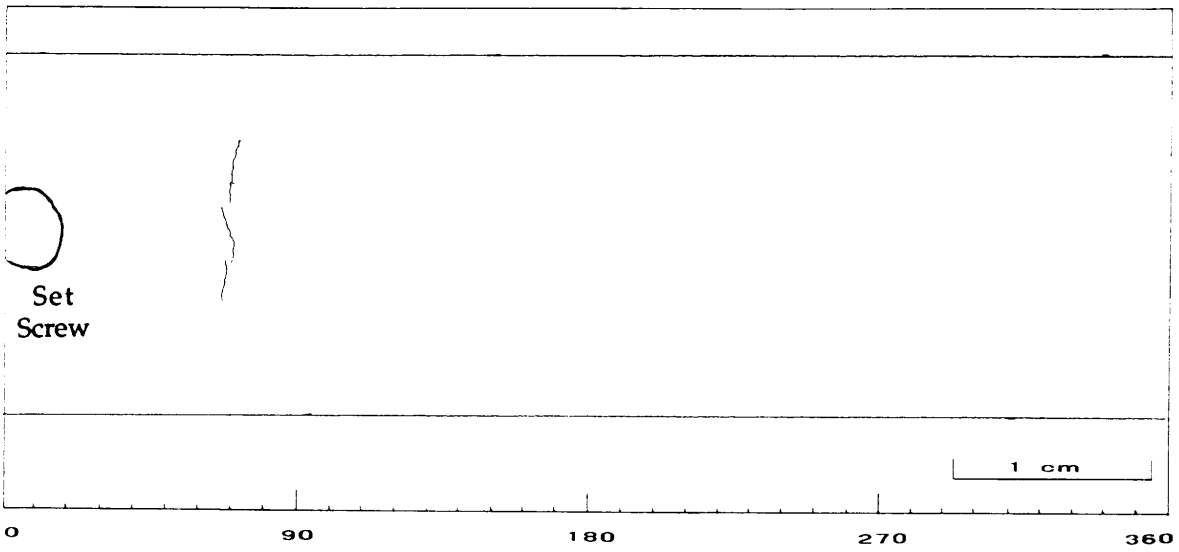

Figure D-39
Exterior Surface Replication Map of Intersection 15-15-4-2

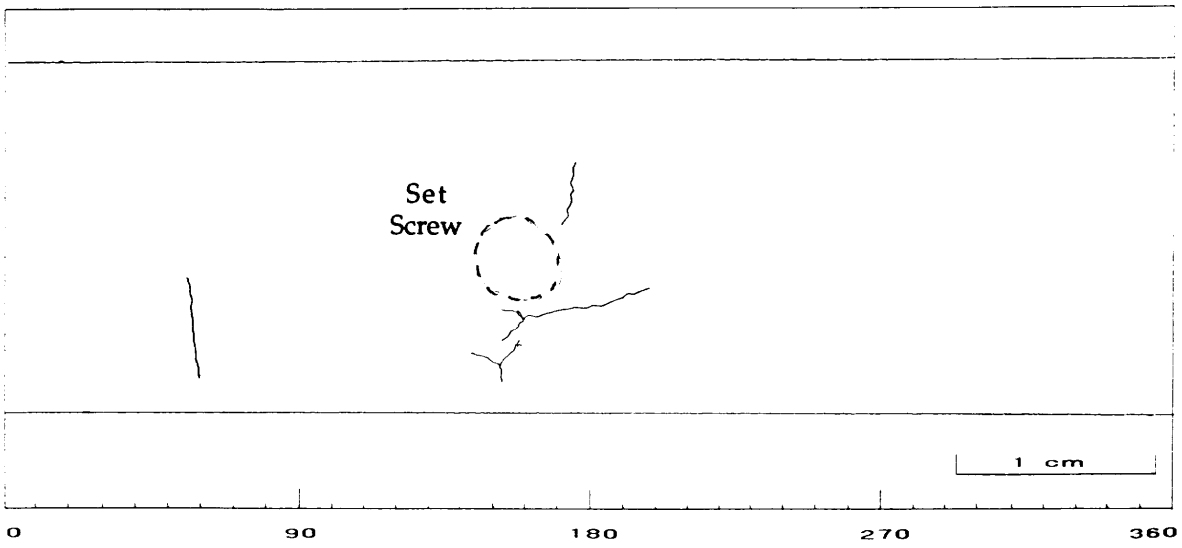

Figure D-40
Exterior Surface Replication Map of Intersection 15-15-4-3b (After bulging)

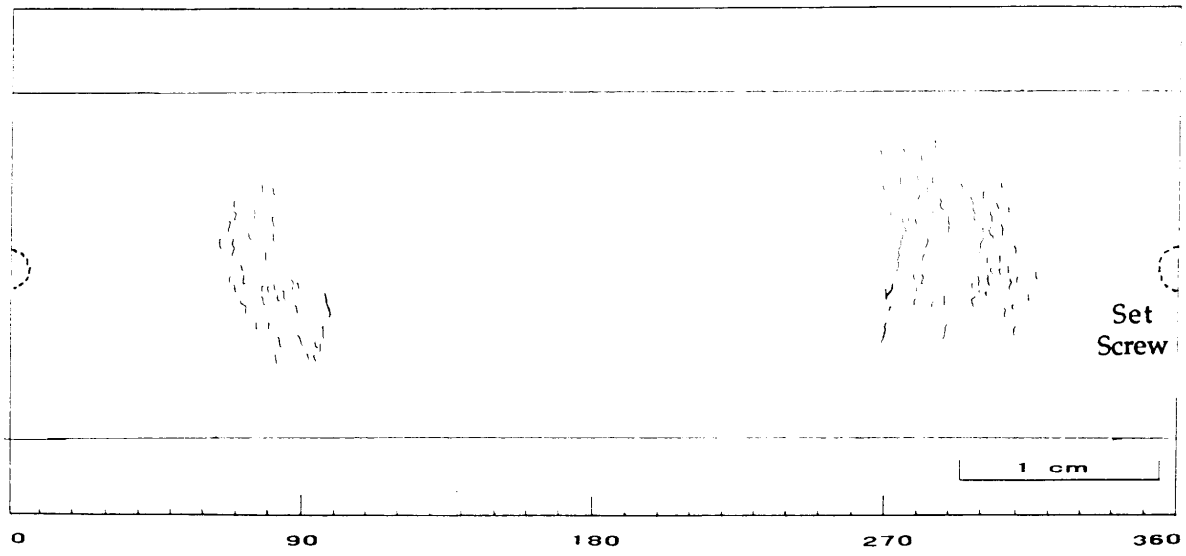

Figure D-41
Exterior Surface Replication Map of Intersection 16-14-1-1 (After bulging)

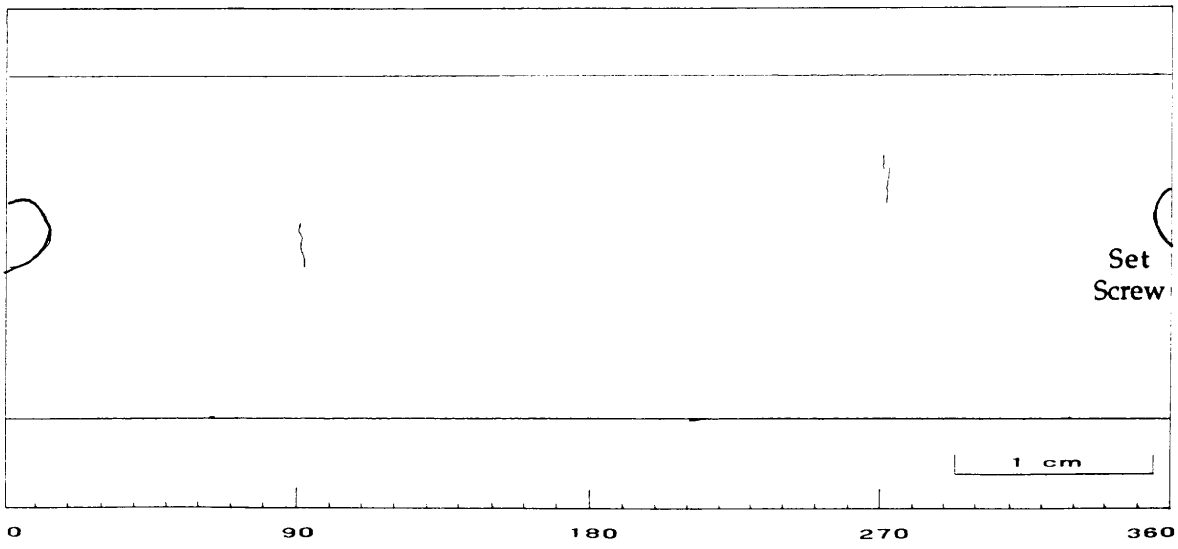

Figure D-42
Exterior Surface Replication Map of Intersection 16-14-2-2 (After bulging)

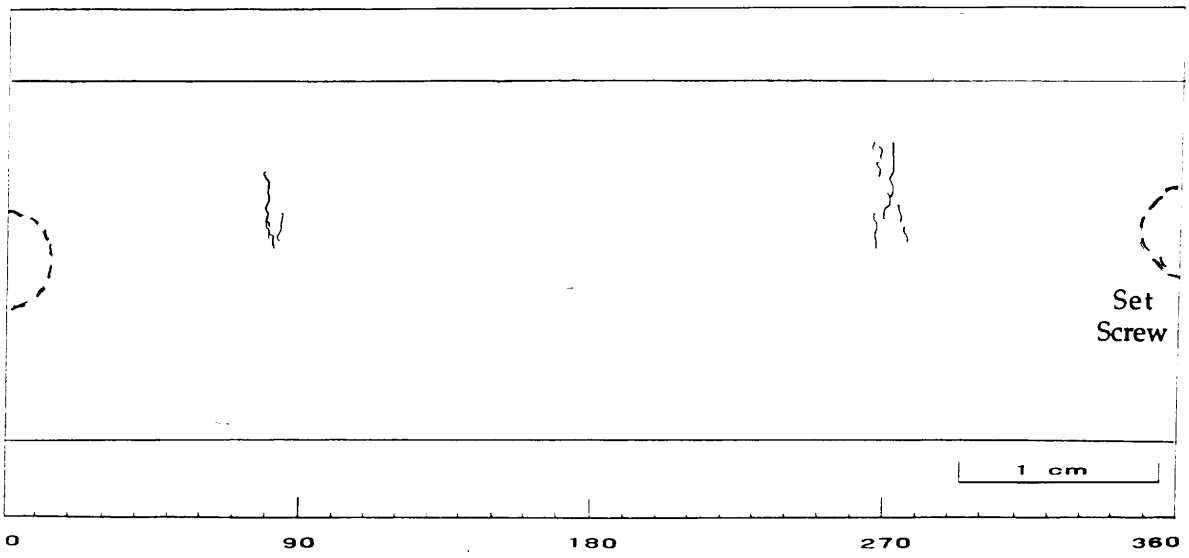

Figure D-43
Exterior Surface Replication Map of Intersection 16-14-4-1 (After bulging)

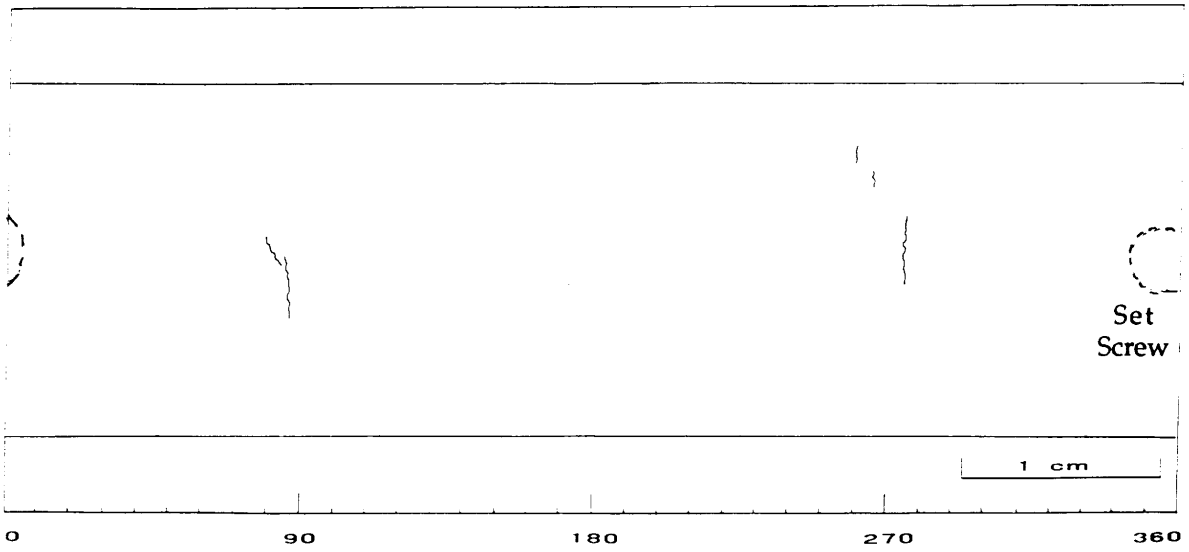

Figure D-44
Exterior Surface Replication Map of Intersection 16-14-4-2 (After bulging)

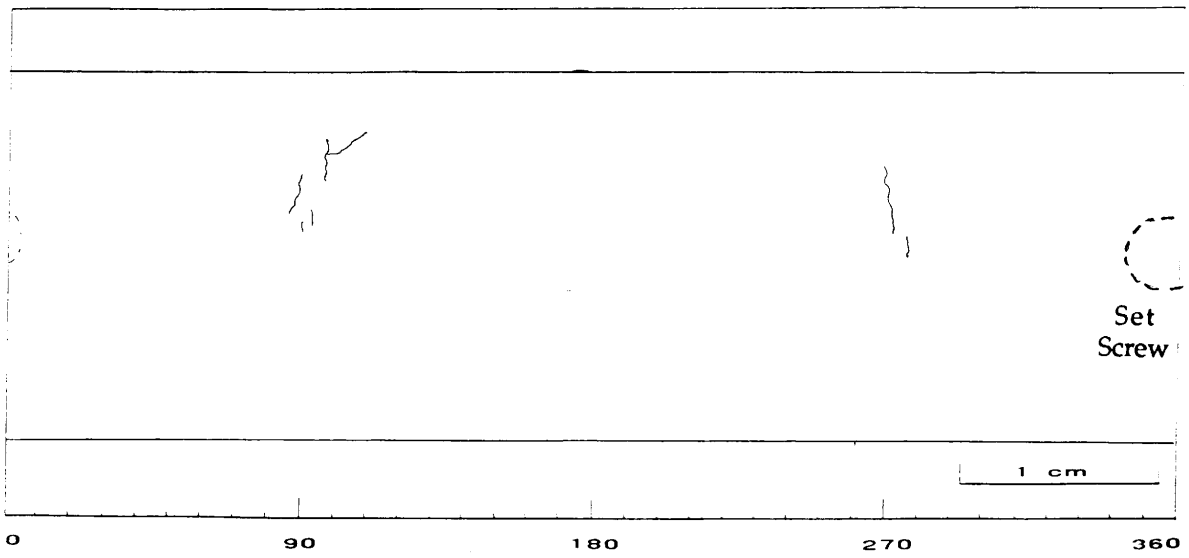

Figure D-45
Exterior Surface Replication Map of Intersection 16-14-4-3 (After bulging)

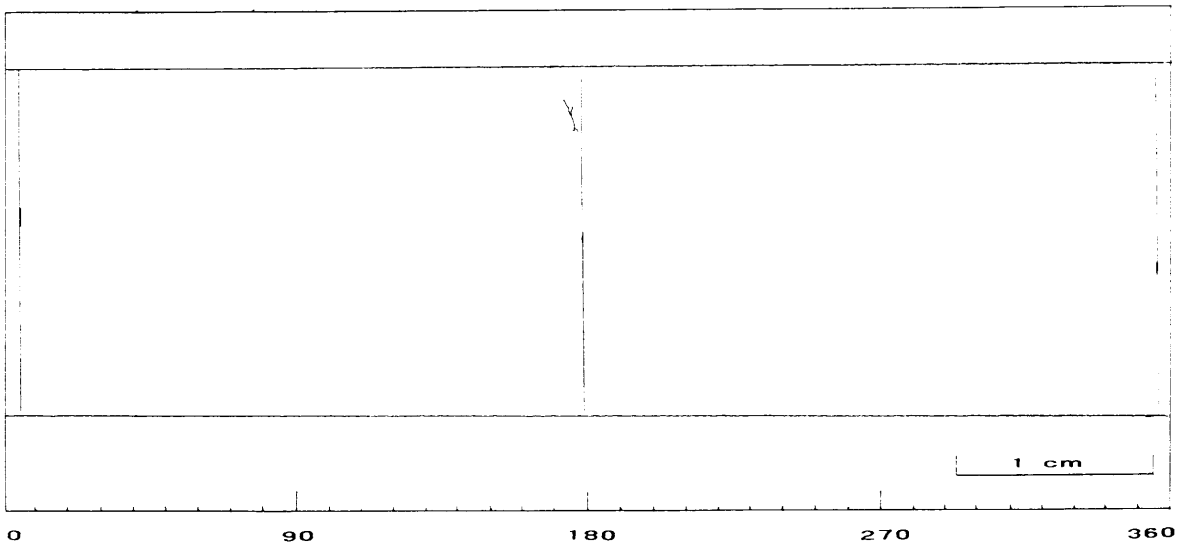

Figure D-46
Exterior Surface Replication Map of Intersection 16-15-2-2 (After bulging)

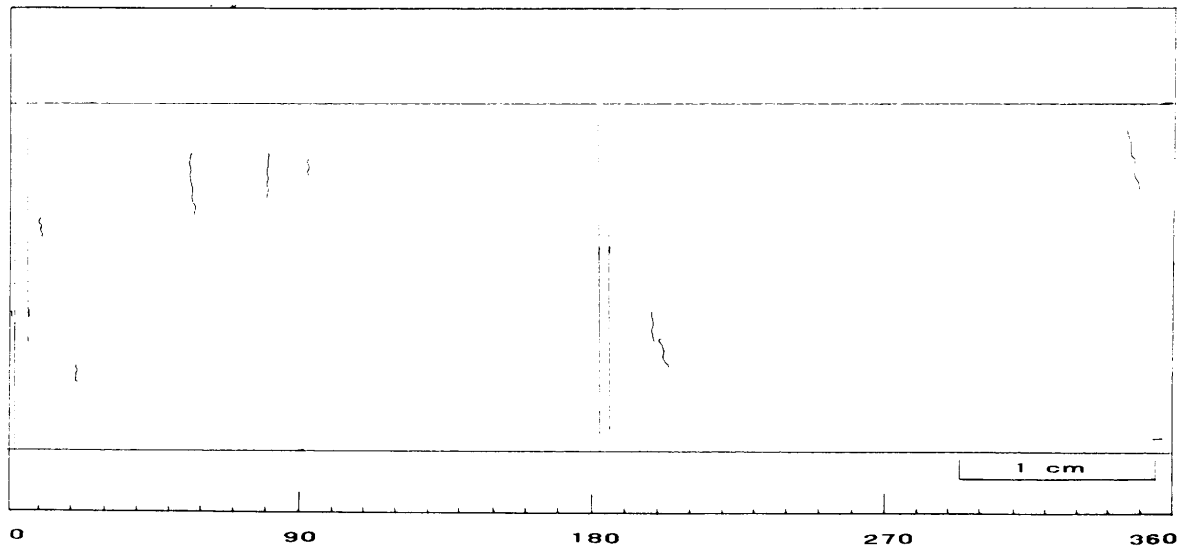

Figure D-47
Exterior Surface Replication Map of Intersection 16-15-2-3 (After bulging)

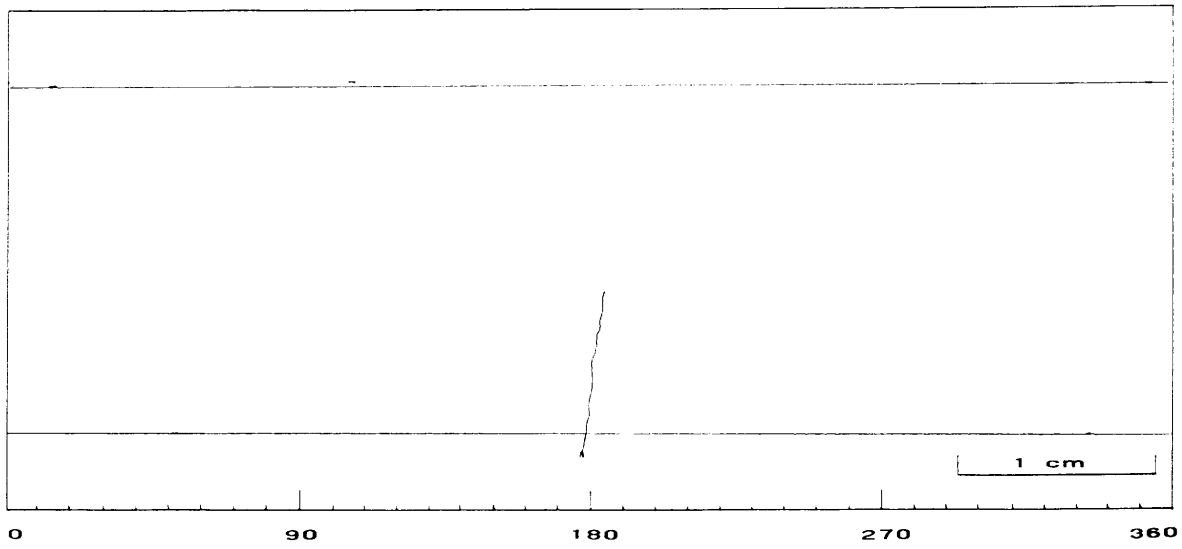

Figure D-48
Exterior Surface Replication Map of Intersection 16-16-1-1 (After bulging)

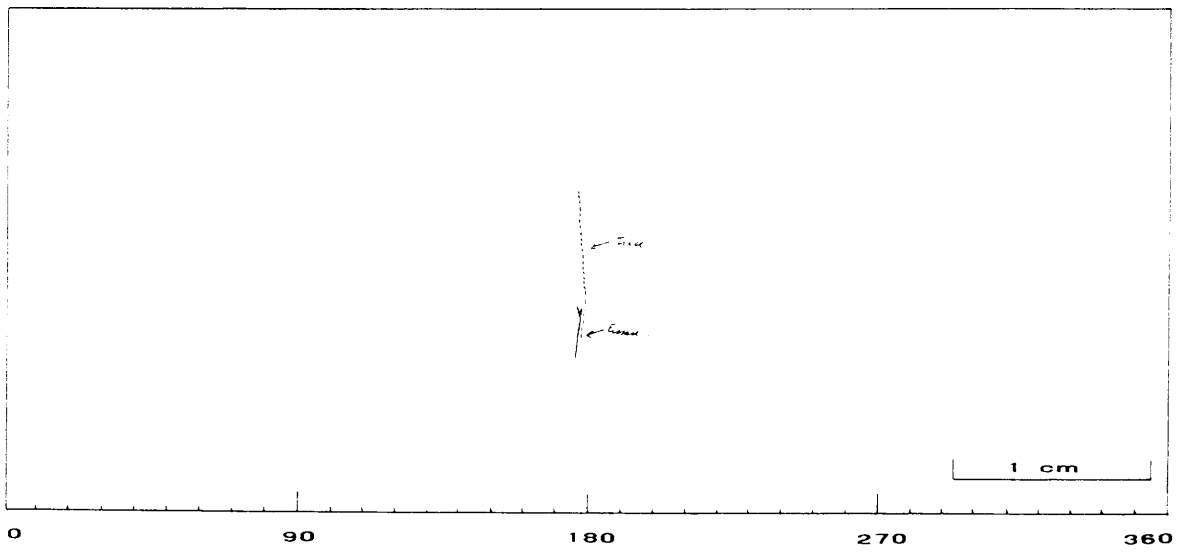

Figure D-49
Exterior Surface Replication Map of Intersection 16-16-2-3 (After bulging)

WARNING: This Document contains information classified under U.S. Export Control regulations as restricted from export outside the United States. You are under an obligation to ensure that you have a legal right to obtain access to this information and to ensure that you obtain an export license prior to any re-export of this information. Special restrictions apply to access by anyone that is not a United States citizen or a Permanent United States resident. For further information regarding your obligations, please see the information contained below in the section titled "Export Control Restrictions."

Export Control Restrictions

Access to and use of EPRI Intellectual Property is granted with the specific understanding and requirement that responsibility for ensuring full compliance with all applicable U.S. and foreign export laws and regulations is being undertaken by you and your company. This includes an obligation to ensure that any individual receiving access hereunder who is not a U.S. citizen or permanent U.S. resident is permitted access under applicable U.S. and foreign export laws and regulations. In the event you are uncertain whether you or your company may lawfully obtain access to this EPRI Intellectual Property, you acknowledge that it is your obligation to consult with your company's legal counsel to determine whether this access is lawful. Although EPRI may make available on a case by case basis an informal assessment of the applicable U.S. export classification for specific EPRI Intellectual Property, you and your company acknowledge that this assessment is solely for informational purposes and not for reliance purposes. You and your company acknowledge that it is still the obligation of you and your company to make your own assessment of the applicable U.S. export classification and ensure compliance accordingly. You and your company understand and acknowledge your obligations to make a prompt report to EPRI and the appropriate authorities regarding any access to or use of EPRI Intellectual Property hereunder that may be in violation of applicable U.S. or foreign export laws or regulations.

About EPRI

EPRI creates science and technology solutions for the global energy and energy services industry. U.S. electric utilities established the Electric Power Research Institute in 1973 as a nonprofit research consortium for the benefit of utility members, their customers, and society. Now known simply as EPRI, the company provides a wide range of innovative products and services to more than 1000 energy-related organizations in 40 countries. EPRI's multidisciplinary team of scientists and engineers draws on a worldwide network of technical and business expertise to help solve today's toughest energy and environmental problems.

EPRI. Electrify the World

SINGLE USER LICENSE AGREEMENT

THIS IS A LEGALLY BINDING AGREEMENT BETWEEN YOU AND THE ELECTRIC POWER RESEARCH INSTITUTE, INC. (EPRI). PLEASE READ IT CAREFULLY BEFORE REMOVING THE WRAPPING MATERIAL.

BY OPENING THIS SEALED PACKAGE YOU ARE AGREEING TO THE TERMS OF THIS AGREEMENT. IF YOU DO NOT AGREE TO THE TERMS OF THIS AGREEMENT, PROMPTLY RETURN THE UNOPENED PACKAGE TO EPRI AND THE PURCHASE PRICE WILL BE REFUNDED.

1. GRANT OF LICENSE

EPRI grants you the nonexclusive and nontransferable right during the term of this agreement to use this package only for your own benefit and the benefit of your organization. This means that the following may use this package: (I) your company (at any site owned or operated by your company); (II) its subsidiaries or other related entities; and (III) a consultant to your company or related entities, if the consultant has entered into a contract agreeing not to disclose the package outside of its organization or to use the package for its own benefit or the benefit of any party other than your company.

This shrink-wrap license agreement is subordinate to the terms of the Master Utility License Agreement between most U.S. EPRI member utilities and EPRI. Any EPRI member utility that does not have a Master Utility License Agreement may get one on request.

2. COPYRIGHT

This package, including the information contained in it, is either licensed to EPRI or owned by EPRI and is protected by United States and international copyright laws. You may not, without the prior written permission of EPRI, reproduce, translate or modify this package, in any form, in whole or in part, or prepare any derivative work based on this package.

3. RESTRICTIONS

You may not rent, lease, license, disclose or give this package to any person or organization, or use the information contained in this package, for the benefit of any third party or for any purpose other than as specified above unless such use is with the prior written permission of EPRI. You agree to take all reasonable steps to prevent unauthorized disclosure or use of this package. Except as specified above, this agreement does not grant you any right to patents, copyrights, trade secrets, trade names, trademarks or any other intellectual property, rights or licenses in respect of this package.

4. TERM AND TERMINATION

This license and this agreement are effective until terminated. You may terminate them at any time by destroying this package. EPRI has the right to terminate the license and this agreement immediately if you fail to comply with any term or condition of this agreement. Upon any termination you may destroy this package, but all obligations of nondisclosure will remain in effect.

5. DISCLAIMER OF WARRANTIES AND LIMITATION OF LIABILITIES

NEITHER EPRI, ANY MEMBER OF EPRI, ANY COSPONSOR, NOR ANY PERSON OR ORGANIZATION ACTING ON BEHALF OF ANY OF THEM:

(A) MAKES ANY WARRANTY OR REPRESENTATION WHATSOEVER, EXPRESS OR IMPLIED, (I) WITH RESPECT TO THE USE OF ANY INFORMATION, APPARATUS, METHOD, PROCESS OR SIMILAR ITEM DISCLOSED IN THIS PACKAGE, INCLUDING MERCHANTABILITY AND FITNESS FOR A PARTICULAR PURPOSE, OR (II) THAT SUCH USE DOES NOT INFRINGE ON OR INTERFERE WITH PRIVATELY OWNED RIGHTS, INCLUDING ANY PARTY'S INTELLECTUAL PROPERTY, OR (III) THAT THIS PACKAGE IS SUITABLE TO ANY PARTICULAR USER'S CIRCUMSTANCE; OR

(B) ASSUMES RESPONSIBILITY FOR ANY DAMAGES OR OTHER LIABILITY WHATSOEVER (INCLUDING ANY CONSEQUENTIAL DAMAGES, EVEN IF EPRI OR ANY EPRI REPRESENTATIVE HAS BEEN ADVISED OF THE POSSIBILITY OF SUCH DAMAGES) RESULTING FROM YOUR SELECTION OR USE OF THIS PACKAGE OR ANY INFORMATION, APPARATUS, METHOD, PROCESS OR SIMILAR ITEM DISCLOSED IN THIS PACKAGE.

6. EXPORT

The laws and regulations of the United States restrict the export and re-export of any portion of this package, and you agree not to export or re-export this package or any related technical data in any form without the appropriate United States and foreign government approvals.

7. CHOICE OF LAW

This agreement will be governed by the laws of the State of California as applied to transactions taking place entirely in California between California residents.

8. INTEGRATION

You have read and understand this agreement, and acknowledge that it is the final, complete and exclusive agreement between you and EPRI concerning its subject matter, superseding any prior related understanding or agreement. No waiver, variation or different terms of this agreement will be enforceable against EPRI unless EPRI gives its prior written consent, signed by an officer of EPRI.

Programs:

Nuclear Power

TR-106212-V3

EPRI • 3412 Hillview Avenue, Palo Alto, California 94304 • PO Box 10412, Palo Alto, California 94303 • USA
800.313.3774 • 650.855.2121 • askepri@epri.com • www.epri.com